Bifurcation Analysis of Regulatory Modules in Cell Biology

DISSERTATION

zur Erlangung des akademischen Grades
doctor rerum naturalium
(Dr. rer. nat.)
im Fach Biophysik

eingereicht an der
Mathematisch-Naturwissenschaftlichen Fakultät I
Humboldt-Universität zu Berlin

von
Herr Dipl.-Phys. Maciej J. Swat
geboren am 03.07.1967 in Wrocław/Polen

Präsident der Humboldt-Universität zu Berlin:
Prof. Dr. Jürgen Mlynek

Dekan der Mathematisch-Naturwissenschaftlichen Fakultät I:
Prof. Thomas Buckhout, PhD

Gutachter:

1. Prof. Dr. Hanspeter Herzel
2. Priv.-Doz. Dr. Andreas Deutsch
3. Prof. Dr. Thomas Bley

eingereicht am:	19.Mai 2005
Tag der mündlichen Prüfung:	3.November 2005

Abstract

The thesis emphasizes the importance of small modules as key components of biological networks. Especially, those which perform positive feedbacks seem to be involved in a number of regulatory units. Processes like gene regulation, differentiation and homeostasis often require autoregulation. Therefore, detailed knowledge of dynamics of small modules becomes nowadays an important subject of study.

We analyze two biological systems: one regarding cell cycle regulation and one immunological example related to T-cell activation. Their underlying networks can be dissected into subunits with well defined functions. These modules decide about the behavior of the global network. In other words, they have decision taking function, which is inherited by the whole system.

Stimulated by the cell cycle model and its interesting dynamics resulting from coupled modules, we analyzed the switching issue separately. Serial coupling of positive feedback circuits provides astonishing possibilities to construct systems with multiple stable steady states.

Even though, in current stage, no exact experimental proof of all hypotheses is possible, one important observation can be made. Common structures and mechanisms found in different biological systems allow to classify biological systems with respect to their structural similarities.

Keywords:
cell cycle, G1/S-Transition, bifurcation theory, feedback loop

Zusammenfassung

Das Kernstück der vorliegenden Arbeit ist die Betonung von kleinen Modulen als Schlüsselkomponenten von biologischen Netzwerken. Unter den zahlreichen möglichen Modulen scheinen besondere diejenigen interessant zu sein, welche die Rückkopplungen realisieren und in regulatorischen Einheiten auftreten. Prozesse wie Genregulation, Differentiation oder Homeostasis benötigen häufig Autoregulation. Auf Grund dessen ist die detaillierte Kenntnis der dynamischen Eigenschaften von kleinen Modulen von größerem Interesse.

Es werden zwei biologische Systeme analysiert. Das erste beschäftigst sich mit dem Zellzyklus, das zweite Beispiel kommt aus der Immunologie und betrifft die Aktivierung von T-Zellen. Beide Modelle, d.h. ihre zugrundeliegende Netzwerke, lassen sich in Untereinheiten mit wohldefinierten Funktionen zerlegen. Diese Module entscheiden über das Verhalten des gesamten Netzwerkes. Mit anderen Worten, die von den Modulen getroffenen Entscheidungen, werden von dem gesamten System übernommen.

Bei der Analyse des Modells zum Zellzyklus wurde eine interessante Eigenschaft von gekoppelten Modulen deutlich, die wir dann getrennt behandelt haben. Seriell geschaltete Module mit positiver Rückkopplung liefern überraschende Konstruktionsmöglichkeiten für Systeme mit mehreren stabilen Gleichgewichtslagen.

Obwohl nicht alle hier aufgestellten Hypothesen derzeit experimentell überprüfbar sind, es kann eine wichtige Aussage getroffen werden. Übereinstimmende Strukturen und Mechanismen, die in verschiedenen biologischen Systemen vorkommen, bieten uns die Möglichkeit einer Klassifizierung von biologischen Systemen bezüglich ihrer strukturellen Ähnlichkeiten.

Schlagwörter:
Zellzyklus, G1/S-Übergang, Bifurkationstheorie, Rückkopplungsschleife

Contents

List of Figures

List of Tables

Introduction

The thesis emphasizes the importance of small regulatory modules and their connections as key components of biological networks. Especially those, which realize feedbacks seem to be involved in a number of important regulatory units. Processes like gene regulation, differentiation and homeostasis often require autoregulation.

One of the pioneering works on this topics is a paper by Monod and Jacob, published over 40 years ago, in which six regulatory and differentiation systems have been analyzed [Monod and Jacob, 1961]. All these examples contain a positive feedback loop in form of a double inhibition. At this time however,

> "... the study either from the genetic or from the biochemical point of view has not attained a state which would allow any detailed comparison of theory and experiment.... The greatest obstacle is the impossibility of performing genetical analysis, without which there is no hope of ever dissecting the mechanisms of differentiation."

The huge progress in experimental techniques in biotechnology and molecular biology in recent years makes at least some dreams of understanding of cellular systems true. Although we are still far from being able to construct biological networks on demand, first successes in this field make hope for the future [Gardner et al., 2000, Isaacs et al., 2003]. Now we can make, to some extent, quantitative predictions about behavior of biological networks and test them.

However, there is a need to develop simplifying higher level models and to find general principles behind those networks [Hartwell et al., 1999, Fraser and Harland, 2000, Isaacs et al., 2003, Kobayashi et al., 2004]. First, we have to understand the functionality of individual modules, then we can move on to complicated systems. In the face of the complexity, as found in nature, intuition can be misleading and high-throughput simulations do not uncover underlying mechanisms. The search for such "decision taking modules" will be one of the greatest challenges in biology.

This thesis focuses on these ideas. Two different systems are discussed, where positive feedbacks and their coupling explain the dynamical structure. In the following we give a short overview about the thesis.

Chapter 1: Mammalian Cell Cycle

The goal of the mammalian mitotic cell cycle is the proliferation, i.e. duplication and partition of chromosomes between two daughter cells. The

process can be divided in four phases: mitosis (M), synthesis (S) and two gap phases (G1 and G2). They are characterized by cyclicly expressed proteins and named cyclins. Their partners, cyclin dependent kinases, are the functional units indispensable for the cell cycle progression. In this chapter we describe those proteins and their regulation occurring in higher eukaryotes and compare them to the yeast cell cycle machinery.

Chapter 2: G1/S Transition in Focus

Now we concentrate our attention on the phase transition between G1 and S phase. The latter one is the phase when the chromosomes are duplicated and therefore crucial for a successful division. Although hundreds of genes are involved in each phase, there are players of special importance. For the G1/S transition such players are: the transcriptor factor E2F and its counterpart Retinoblastoma, pRB, a tumor suppressor. Interesting for the theoretical model on G1/S transition is the occurrence of two binding sites in the E2F1 promoter, the prominent agent of the whole E2F family, which lends credibility to the cooperativity assumption. Among the huge number of E2F target genes is also the pRB gene, whose product inhibits E2F via protein–protein interaction. We discuss the resulting activation/inhibition relationship. Finally, we concentrate on the G1 checkpoint, the restriction point and the growth factor dependence of the cell cycle.

Chapter 3: Nonlinear Dynamics

Nonlinear dynamics tools have become standard in the analysis of biochemical systems. Onsets of oscillations, threshold phenomena and phase transitions may be characterized in an elegant way by bifurcations. The transcritical and saddle node bifurcations will play major roles in our theoretical models. Under certain conditions steady state problems can be illustrated as algebraic surfaces defined by polynomials. Some of such surfaces can be transformed into normal forms, called catastrophes. These exciting geometrical structures describe for example discontinuous transitions between different steady states. Basic catastrophes for parameter spaces with dimension less then five are classified.

Chapter 4: Autocatalytical Reactions and Bistability

This chapter gives an overview about autocatalytical systems found in biological regulatory networks. Simple positive, negative or double negative feedback circuits are present in nature and they excite the scientific community since the mid of the last century. We sketch the major acquisitions in

this field. It turns out that basal protein expression is essential to observe switching behavior, together with cooperativity. A class of autocatalytical functions is discussed from the modeler point of view. Different dynamics showed by those functions correspond to specific types of bifurcation. At the end of the chapter we sketch the connection between two simple autocatalytical systems and catastrophic surfaces.

Chapter 5: Coupling of Modules

Single modules are interesting from a theoretical point of view, but they are meaningless for biological purposes without a cellular environment. Although the analysis of coupled modules was stimulated by our findings in the G1/S model, it also provides new possibilities for modeling of related processes like cell differentiation. In this way one can construct systems with almost an arbitrary number of stable steady states. These problems are often reducible to a polynomial roots search. Moreover, very powerful switches can be constructed with coupled autocatalytical feedback loops, characterized by nearly perfectly separated on and off states.

Chapter 6: Mathematical Model of the G1/S Transition

In the main chapter of this thesis a mathematical model for G1/S transition in mammalian cells is proposed. The huge number of participating proteins has been reduced to a handy set still capable to cover the most important features of the phenomenon. We use the results from previous chapters about positive feedbacks and their serial connections. The Cyclin D/cdk4,6 activation module and E2F1/pRB antagonistic doublet and their coupling fit in this scenario. Finally the G1/S phase transition is characterized. Additional feedback due to a E2F1 binding site in the promoter of transcription factor family, AP-1, is analyzed showing surprising effects on the whole system. Finally, ongoing experiments and their preliminary results are discussed.

Chapter 7: Model of Vav Truncation and Caspase Activation

Rising interest in theoretical investigations led to a interesting cooperation with an experimental lab and work on an immunological system. The activation of T-cells is connected with cytoskeleton remodeling. The presented mathematical model involves a signal transducer, Vav1, in its full length and truncated form, actin filaments and caspase 3. The protein in focus, Vav1, leads in its short form to caspase activation and apoptosis. The decision whether or not this will happen is dependent on an extrinsic caspase path-

way activation. We show in a reduced model that there is a threshold for this reaction and define it using bifurcation theory.

From the analysis done in previous chapters it turns out, that crucial features of the analyzed systems are encoded in small modules. Their dynamics is often based on positive and negative feedbacks. In the last chapter we discuss which conclusions can be drawn. Especially necessary model extension to more realistic networks and applications in pharmaceutical research is in focus.

In this thesis we use the ordinary differential equations to describe the dynamics of the analyzed systems. This approach has been applied in countless examples to analyze pathways and networks in molecular cell biology, metabolic regulation, signal transduction etc. Beside this well known method there exists a number of other approaches, such as: directed graphs, Bayesian networks, Boolean networks and their generalizations, partial differential equations, qualitative differential equations, stochastic master equations, rule-based formalisms and Petri nets [de Jong, 2002]. Recently, algorithms for symbolic model checking of biochemical networks has been developed. An example of such formal methods is a biochemical abstract machine defined by Fages et al. [2004], used for validation of MAPK pathway components.

All these methods are or will be in use as tools of systems biology in e.g. cancer research. Pharmaceutical and biotech companies develop drugs against cancer based on mathematical models. The hope is to speed up and lower the costs of the development process of new drugs.

Part I

Biological Background and Methods

Chapter 1

Mammalian Cell Cycle

1.1 Introduction

Cell growth is controlled by an orderly sequence of events termed the mitotic cell cycle. Each stage of the cycle is characterized by an expression of a set of proteins and protein complexes required to progress through the phases of the cycle.

To some extend, the cell cycle of mammals shares a lot of common features with cell cycle of other eukaryotes. However, as we may expect, it is the most complex of them all. Kohn [1998] compiled a so called 'Kohn map' which best exemplifies in a graphical way the intricacy of the system. This chapter gives a short introduction into the topic. We also point out the main discrepancies between the mammalian and the yeast cell cycle, which is also a subject of intensive studies.

The science community works more than 100 years on the cell cycle related problems. Nevertheless, it seems that we are still at the beginning of its full understanding.

1.2 Phases and checkpoints

The eukaryotic cell cycle is usually divided into four phases ($\rightarrow$G1 $\rightarrow$S $\rightarrow$G2 $\rightarrow$M $\rightarrow$): S-phase (Synthesis – DNA replication), M-phase (Mitosis – chromosome separation) and two gaps between them, G1 and G2. In the time during G_1 and G_2 phases, cells prepare for the next phase, synthesizing needed proteins and increasing their mass. Two points during the loop are of particular importance, the so called checkpoints; one before the G1/S and the other before the G2/M transition. The checkpoints block the entry to the next stage if the previous step has not been completed, or if the signal is insuf-

ficient to progress. When cells are not cycling because of lack of nutrients, differentiation, anti-mitotic factors or contact inhibition, they usually enter a resting state, called also quiescence or G_0.

1.3 Cyclins and cyclin-dependent kinases

The regulation of the cell cycle progression is executed by evolutionary conserved serine/threonine protein kinases, called cyclin–dependent kinases (cdk) [Massague, 2004, Ekholm-Reed, 2004]. Cdks were first identified by genetic analysis of the cell cycle in yeast and via the analysis of M phase in frog and early embryos. The catalytically inactive cdk subunit creates complex with a regulatory subunit, a cyclin. Cyclins were so named because of their fluctuating levels through the cell cycle. The presence of a 100 amino acid sequence, the "cyclin box", defines a protein as a cyclin family member.

Cyclins were initially discovered in clam and sea urchin embryos where they were found to accumulate during interphase, and to be degraded later in mitosis. Via homology search, Cyclin A and B were the first identified human cyclins [Pines and Hunter, 1989]. The G1 cyclins type D and E were found after screening of human cDNA libraries for counterparts of related yeast sequences.

Cyclin/cdk complexes control events that drive the transitions between cell cycle phases by phosphorylation of specific substrates. (Table 1.1 gives an overview of different cyclins and their various functions.) The cyclins integrate information flow from outside the cell to drive G1-phase progression and initiate chromosome replication in response to mitogenic signals [Bielinsky and Gerbi, 2001, Sherr and Roberts, 2004, Kastan and Bartek, 2004]. More precisely, e.g. the D-type cyclins (D1, D2, and D3) and their catalytic partners cdk4 and cdk6 act early in G1 phase. Mitogen-induced signal transduction pathways promote the activation of Cyclin D/cdk4,6 complexes at many levels, including gene transcription, Cyclin D translation and stability and assembly of D cyclins with their cdk partners.

Cyclin E and Cyclin A are E2F-responsive genes, and their synthesis increases after phosphorylation of Retinoblastoma (pRB) protein by the D-cyclin-dependent kinases. Cyclin E/cdk2 complexes participate in further phosphorylation of pRB constituting another E2F1 related positive feedback. Cyclin A/cdk2 complexes in turn, close the G1/S transition and E2F1 activity by phosphorylation of DP1, a regulatory unit of the E2F1/DP1 complexes. These facts exemplify very clearly the importance and role of feedbacks. There is no complex network without such control mechanism.

From the point of view of a G1/S model, recent discovery of a new cyclin,

Cyclins	**A**ssociated cdk	**F**unction
A	cdk1(cdc2), cdk2	S phase entry and transition anchorage-dependent growth
B1, B2	cdk1	G2 exit, mitosis
C	cdk8	transcriptional regulation G0-to-S phase transition
D1, D2, D3	cdk4, cdk6	G0-to-S phase transition
E	cdk2	G1-to-S phase transition
F	?	G2-to-M phase transition
G1, G2	cdk5	DNA damage response
H	cdk7	cdk activation transcriptional regulation DNA repair
I	?	expressed constantly during cell cycle
K	?	transcriptional regulation cdk activation
T1, T2	cdk9	transcriptional regulation

Table 1.1: Mammalian cyclins with their cdk partners, from [Johnson and Walker, 1999]. Eleven classes have been identified so far. In three cases the associated cdk has not been specified.

Cyclin C, makes the story even more complex [Sage, 2004, Ren and Rollins, 2004]. Cyclin C/cdk3 is required for the exit from G_0, what was shown in the cell line 3T3, of murine fibroblasts. Suppression of Cyclin C delayed serum-induced S phase entry by 8 hours. This finding suggests that there are (possibly) three stages in the phosphorylation of pRB: between G_0 and early G_1, between early G_1 and late G_1 and finally at transition from late G_1 to S phase done by Cyclin C/cdk3, Cyclin D/cdk4,6 and Cyclin E/cdk2, respectively.

Beside having the precise knowledge about the functions of all cyclins and cdks, one has to be careful when making general statements about the role and importance of these complexes. Recent Cdk and cyclin knockouts in the mouse show that the functions of G1 cell cycle regulatory genes are often essential only in specific cell types [Pagano and Jackson, 2004]. This underlines our limited understanding of tissue-specific expression, redundancy, and compensating mechanisms in the Cyclin/cdk network.

1.4 Cdk inhibitors

CDK inhibitors (CDKI) are regulators of cyclin-dependent kinases. Three classes of CDKIs have been established: INK4 proteins (inhibitors of cdk4), Cip/Kip family and pocket proteins. The last group, pocket proteins, will be described in detail in the next chapter. INK4 have the ability to inhibit the catalytic subunits of cdk4 and cdk6, but not other cdks or cyclins. The group contains four such proteins; $p15^{INK4b}$, $p16^{INK4a}$, $p18^{INK4c}$, $p19^{INK4d}$. The second group, Cip/Kip, includes $p21^{Cip1}$, $p27^{Kip1}$ and $p57^{Kip2}$. In contrast to the selective binding of the first group, they are able to bind both to cyclin and cdk subunits.

$p27^{Kip1}$ will play a role in the G1/S transition, as it inhibits the Cyclin E/cdk2 complex during G_0 and G_1. The inhibitor is phosphorylated by Cyclin E/cdk2 itself and targeted to degradation. The phosphorylation and degradation of $p27^{Kip1}$ is believed to function as positive feedback loop to rapidly facilitate S phase entry.

1.5 Comparison with the yeast cell cycle

Important aspects about the mammalian cell cycle are the differences and similarities in the network topology in comparison with other organisms.

We start with the differences regarding the main regulatory unit in the cell cycle, the cyclin/cdk complex. As shown in the table 1.2, the most striking difference is that in yeast only one cdk unit, cdk1, is enough for a sufficient control of the cell cycle. It forms complexes with different substrate specificities. From the point of view of a modeling scientist it is a very helpful property. Very detailed models have been developed for yeast. Their results can be given in form of a bifurcation diagram of this component. This is clearly not possible for systems where there is no core unit, which is active through one whole cycle.

Moreover, the mass of the nucleus is used as the control parameter of cell division. It is widely believed that cell-size checkpoints help to coordinate cell growth and cell-cycle progression, so that proliferating eukaryotic cells maintain their size. There is a strong evidence for such size checkpoints in yeasts, which maintain a constant cell-size distribution as they proliferate, even though large yeast cells grow faster than small yeast cells [Conlon and Raff, 2003]. It has been shown that proliferating rat Schwann cells do not require a cell-size checkpoint to maintain a constant cell-size distribution. Unlike yeasts, large and small Schwann cells grow at the same rate, which depends on the concentration of extracellular growth factors.

Species		**G**1	**G**1/S	**S**	**M**
Yeast	cyclin	Puc1	Puc1, Cig1	Cig2, Cig1	Cdc13
	cdk	Cdk1	Cdk1	Cdk1	Cdk1
Human	cyclin	Cyclin D1,2,3	Cyclin E	Cyclin A1,2	Cyclin B1,2
	cdk	Cdk4,6	Cdk2	Cdk2,1	Cdk1

Table 1.2: Yeast (*S.*pombe)–human comparison. In both cases there exists a number of different cyclins. However, in yeast, only one cdk unit is sufficient for a full control of the cell cycle.

Fortunately there are also similarities between mammalian and yeast cell cycles. The most important of them have been discovered only recently. Initiation of the budding yeast cell cycle follows an induction of G1 cdk activity that activates a pair of heterodimeric transcription factors, SBF and MBF. The two last are transcription complexes, which have similar function to those of E2F proteins in higher eukaryotes. The timed regulation expression of these genes results in cell cycle progression and DNA synthesis [Hateboer et al., 1998].

As we have seen earlier, pRB and related proteins block transcriptional activation of genes critical to initiation of the mammalian cell cycle and suppress undesired cell division. The mechanisms controlling this response are generally conserved from humans to yeast, but no negative regulator like pRB has been found in yeast. The experiments revealed that Whi5, a negative regulator and inhibitor of G1/S transcription acting upstream of SBF, appears to play the role of pRB in preventing unwanted cell cycle entry in budding yeast [Sherr and Roberts, 2004, Costanzo et al., 2004, de Bruin et al., 2004, Schaefer and Breeden, 2004].

The presented results extend the parallels between yeast and metazoans at the initiation of the cell cycle. Whi5 and the pRB-like proteins show remarkable similarities regarding their activity as repressors and in the regulation of that activity by Cdk-dependent phosphorylation. However, like the activators of transcription, there is no primary sequence homology between Whi5 and pRB. Rather, these parallels serve as an exquisite example of convergent evolution.

Chapter 2

G1/S Transition in Focus

Introduction

One of the major topics in this dissertation are modules governing the G1/S transition. Therefore, we want to describe the phenomenon in detail. Two phases during which DNA replication is prepared for and occurs are termed presynthetic (G1) and synthetic (S), respectively. A process of DNA replication requires a large number of protein factors. Additionally, for the new DNA to fold in chromatin, *d*e nuovo histons synthesis is needed. Genes for the proteins and protein complexes required for the processes are mainly expressed in the S phase. Many of them are transcription targets of the E2F family. Therefore, members of transcription factor family E2F, with their heterodimeric partners, DP1-3, will be in focus of this chapter.

2.1 E2F transcription factor family

Cell cycle progression depends on the execution of a regulatory cascade of gene expression, driven by E2F/DP transcription factors (TF), which are in turn regulated by the products of some of these genes. That E2F factors are potent regulators of cell-cycle checkpoints in mammalian cells is supported by experiments demonstrating that ectopic expression of individual E2F family members is sufficient to modulate cell proliferation and apoptosis. It was shown that deregulation of E2F activity results in the loss of particular checkpoint controls, which leads cells to malignant conversion.

The E2F transcription factor was originally identified as a cellular component that could bind to and activate the adenoviral E2 gene promoter [Kovesdi et al., 1986].

The factor, named E2F, is a complex of DNA binding heterodimers con-

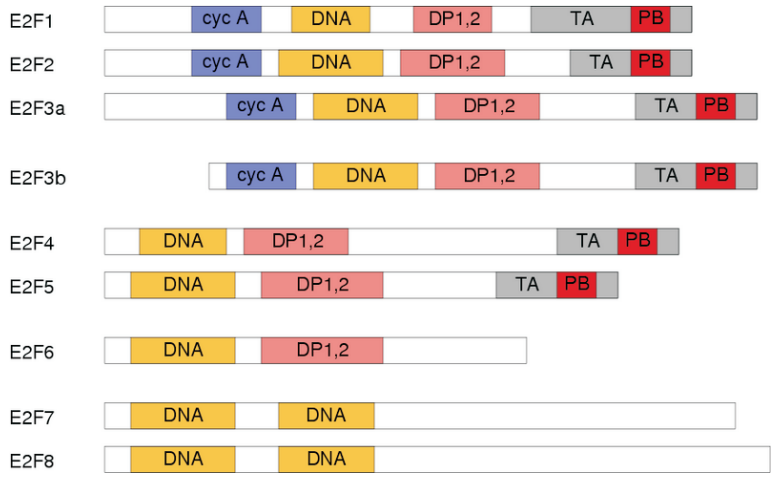

Figure 2.1: E2F transcription family domains. The E2F1–E2F6 proteins contain one DNA-binding domain, *DNA*, and a domain for dimerization with DP, *DP1,2*. Sequences for transcriptional activation, *TA*, and pocket protein binding, *PB*, are present only in E2F1–E2F5. E2F1, E2F2, E2F3a and E2F3b share a cyclin-A-binding domain, *cyc A*, that is absent in E2F4 and E2F5. E2F7 (E2F7a and E2F7b) diverge further from E2F–E2F5 and do not contain a *DP1,2* but they contain two *DNA* domains. (Based on [Bracken et al., 2004]).

taining one E2F subunit and one DP subunit. These subunits are encoded by two gene families: the E2F family includes seven characterized members, E2F1 through E2F7 and family of E2F heterodimeric partners DP1-3. E2F6 act mainly as transcriptional activators or repressors. The recently discovered member [Di Stefano et al., 2003, de Bruin et al., 2003], repressor E2F7, has been identified as an E2F target gene that is induced in S phase.

The E2F1–E2F6 proteins contain one DNA-binding domain (*DNA*) and a domain for dimerization with DP (*DP1,2*). Sequences for transcriptional activation (*TA*) and pocket protein binding (*PB*) are present only in E2F1–E2F5, see Fig.2.1. E2F1, E2F2, E2F3a and E2F3b share a cyclin-A-binding domain (*cyc A*) that is absent in E2F4 and E2F5. The sixth member, E2F6, is different. It carries a DNA-binding, but not a transcriptional activation domain. E2F7 (E2F7a and E2F7b) diverge further from E2F1–E2F5 and do not contain a *DP1,2* but they contain two *DNA* domains required for binding to the E2F DNA-binding consensus sites.

The first six E2F family members require heterodimerization with DP

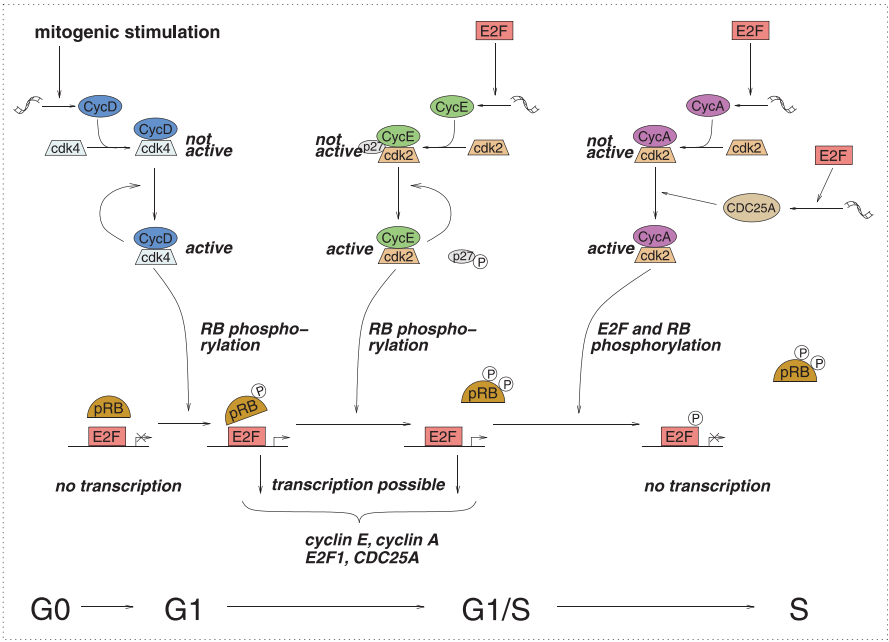

Figure 2.2: G1/S transition. After growth factor stimulation Cyclin D is expressed and binds with cdk4 and cdk6. Due to an autocatalytic activation via CAK, Cyclin D/cdk4,6 is now able to phosphorylation of pRB. This marks the start of the expression of E2F1 regulated genes (among others: Cyclin E and Cyclin A genes) and entry of the S phase. Second step of the phosphorylation is done by Cyclin E/cdk2, which constitutes one of the E2F1 positive feedbacks. Finally, a negative feedback, i.e. the deactivation of E2F1 by Cyclin A/cdk2 closes the G1/S transition.

proteins DP1 or DP2 to be functional [Dyson, 1998]. DP-1 is a ubiquitously expressed phosphoprotein that is structurally related to E2F. DP3 is a splice variant of DP2.

The levels of E2F1–E2F3 increase at the G1/S transition. E2F target genes are transactivated by E2F1–E2F3 in late G1 and S and are essential for cellular proliferation [Wu et al., 2001]. Experiments have shown that E2F1 mediates growth factor-initiated signal transduction [Li et al., 1994] and that it alone can promote S-phase entry of quiescent fibroblasts [Zetterberg et al., 1995, Harbour and Dean, 2000a,b]. From now on we shall concentrate on that first factor, E2F1, as a representative for the activators in the E2F family. It is a well conserved as Tab.2.1 shows.

Species	**H**omology [%]	**L**ength
A. thaliana	34.27	241 aa
C. elegans	36.05	159 aa
D. melanogaster	38.10	227 aa
H. sapiens	99.31	437 aa
M. musculus	85.06	435 aa
R. norvegicus	34.89	304 aa

Table 2.1: Table shows the E2F1 protein homology.

2.1.1 E2F1 promoter

The promoter sequence of E2F1 gene is very GC rich. Between -176 and +98 relative to the transcription starting site, the GC content is equal to 74%. It does not contain TATA box 30 bp upstream of the initiation site but it contains potential binding sites for several TFs: CAAT box, GC box, AP-2, CRE, YY1 and Adf-1.

Sequence analysis revealed two sets of overlapping E2F-binding sites, TTT(C/G)GCGC(C/G), located between -12 and -40 relative to the transcription initiation site [Hsiao et al., 1994, Furukawa et al., 1999]. These sites bind cellular E2F1 and an E2F1 promoter fragment can be activated up to 100-fold by coexpression of E2F proteins. Moreover, it has been shown, that the activity of an E2F1 promoter fragment increases approximately 80-fold at the G1/S-phase boundary. Hence, E2F1 is its own transcription factor [Johnson et al., 1994]. An example of such an autocatalytical positive feedback loop of an transcription factor is shown in Fig.2.3. Mutation experiments show that the expression rate is much higher when two binding boxes are present; measurements were done 12 hours after serum stimulation. The fold induction was 84% for -176/+98 and 42 % for -176/+36 promoter fragment. The fold induction was reduced to 9% in case when one site was mutated and to 5% when both sites were deleted.

Other experiments proved the hypothesis, that E2F1 appears to be regulated at the level of transcription, and this regulation is due to, at least in part, binding of one or more E2F family members to the E2F1 promoter [Neuman et al., 1994, Johnson et al., 1994, Dynlacht, 1997, Furukawa et al., 1999]. These results are confirmed by the observation that E2F1 mRNA is low in serum-starved cells and increases at the G1/S-phase boundary in a protein synthesis-dependent manner [Slansky et al., 1993].

The presence of two binding sites and the presented mutation experiments results give rise to a cooperativity hypothesis. When we define the

mathematical model, the cooperativity will be expressed in terms of a highly nonlinear function of Hill type.

2.1.2 E2F transcription targets

E2F activity controls the transcription of a group of genes that encode proteins important for cell cycle progression. There is no doubt that the transcription factor family E2F is indispensable and essential for the cell cycle. Bracken et al. [2004] compiled a list of 130 E2F target genes. They have been identified via gene array analysis of cells overexpressing E2Fs or indicated by mutations of E2F binding sites. The Table 2.2 gives an overview of the most important E2F target genes based on different experimental studies [Lavia and Jansen-Durr, 1999, DeGregori, 2002, Bracken et al., 2004].

Class	**T**arget gene
Cell cycle	CCNA1,2, CCND1,2, CDK2, MYB
	E2F1,2,3, TFDP1, CDC25A
Negative regulators	E2F7, RB1, TP107, TP21
Checkpoints	TP53, BRCA1,2, BUB1
Apoptosis	TP73, APAF1, CASP3,7,8, MAP3K5,14
Nucleotide synthesis	thymidine kinase (tk), thymidylate synthase (ts)
	DHFR
DNA repair	BARD1, RAD51, UNG1,2
DNA replication	PCNA, histone H2A, DNA polα and δ,
	RPA1,2,3, CDC6, MCM2,3,4,5,6,7

Table 2.2: The table shows E2F driven promoters. Bracken et al. [2004] compiled recently a list of 130 E2F target genes which enlarges previous compilations [Lavia and Jansen-Durr, 1999, DeGregori, 2002].

2.2 Pocket proteins

E2F transcription factors associate with and are regulated by all three members of the pocket protein family: pRB, p107 and p130 [Dyson, 1998, Li et al., 1993, Hannon et al., 1993, Ewen et al., 1991]. E2F is a critical target of the action of pRB as a growth suppressor. The interaction of pRB with E2F results in an inhibition of E2F transcriptional activity and directly correlates with the ability of pRB to arrest cell growth in G1 phase.

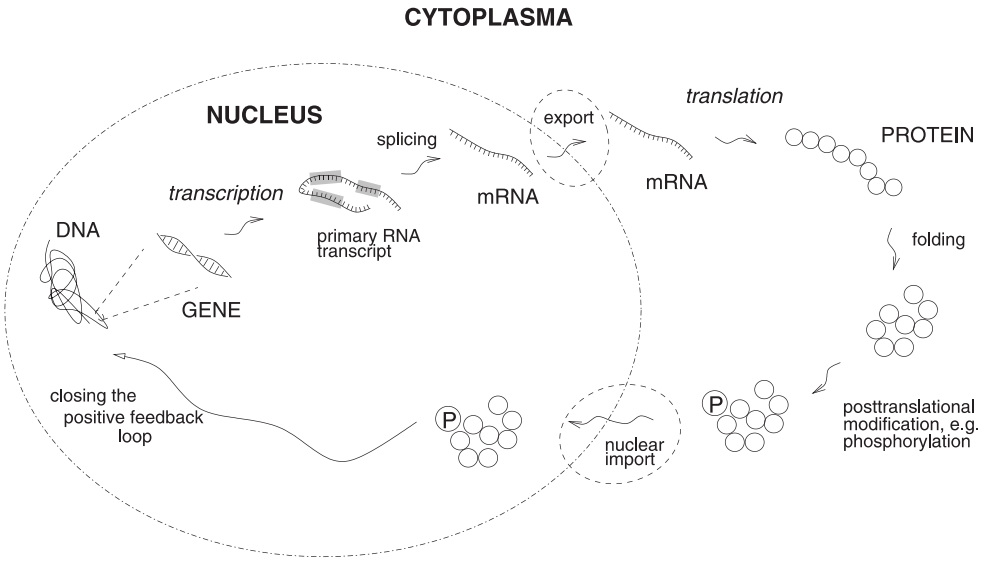

Figure 2.3: Autocatalytical loop containing transcription and translation processes.

pRB as the only pocket protein is able to block the activity of E2F1 when it is not or hypophosphorylated. This phosphorylation status of pRB is regulated by cyclin/cdk complexes. pRB contains at least 16 cdk phosphorylation consensus sequences, some of which are successively phosphorylated by cyclin D/Cdk4 and cyclin E/Cdk2 complexes in G1 phase [Coqueret, 2002].

The retinoblastoma gene, Rb, was identified as the first tumor suppressor. It was thought initially to be involved only in a rare pediatric eye tumor, retinoblastoma. Nowadays it is considered to play a fundamental role in cellular regulation and its mutations are observed in different tumor cell types [Harbour and Dean, 2000a].

The protein, pRB, contains several functional domains. Two domains, A and B, are highly conserved from humans to plants. They interact with each other along an extended interdomain interface to form the central pocket [Chow and Dean, 1996], which is critical to the tumor suppressor function of pRB. The pocket is disrupted by naturally occurring mutations and by most tumor-derived mutations [Harbour and Dean, 2000a].

Due to the similarities between E2F1, E2F2 and E2F3, we will use in the following only the first one, E2F1. We will write E2F1, thought it is only active as a transcription factor when bound to DP1.

2.3 Retinoblastoma – E2F1 connection

As mentioned previously, pRB inhibits E2F1 activity by binding to it and represses transcription by blocking the activity of surrounding enhancers on the promoter. The active repression by pRB is related, at least in part, to the recruitment of pocket binding corepressors, like the chromatin remodeling enzymes [Weintraub et al., 1992, Harbour and Dean, 2000a]. Modification of chromatin structure, involving E2F1 and pRB, is an important mechanism for regulation of gene transcription. Histone acetyltransferase (HAT) activity associated with E2F1 can promote binding of E2F1 to the promoter and it can inhibit nucleosome formation. In this way further access of transcription factors to the promoter is possible. In contrast, HDAC recruited by pRB–E2F1 complexes appears to promote nucleosome assembly on the promoter, blocking access to transcriptional machinery [Martinez-Balbas et al., 2000, Zhang and Dean, 2001, Johnstone, 2002].

Interestingly, pRB is also a target gene of an E2F1. When E2F1/DP1–pRB complex is build, an autorepression of the Rb promoter by pRB is apparent, i.e. pRB inhibits its own activator. This negative feedback has been confirmed in a transient assay [Lavia and Jansen-Durr, 1999].

The arising double activator and double inhibitor system, E2F1–pRB, can be considered as the core module which governs the G1/S transition. It has the ability to define a sharp transition, e.g. in form of a toggle switch. It has been shown that binding of pRB to E2F1 depends on the phosphorylation state of pRB. The phosphorylation state, as we know from the previous chapter, changes during progression trough the cell cycle. E2F1 alternates between active and non-active state depending on the phosphorylation state of pRB.

Surprisingly, after sequential phosphorylation of pRb by Cyclin D/cdk4,6 and Cyclin E/cdk2, E2F1 itself is also phosphorylated by cyclin D/cdk 4,6 complex. It increases the stability of E2F1 and prevents its binding to pRB irrespectively of its phosphorylation status. This ensures the availability of free E2F1 at the G1/S transition point [Mundle and Saberwal, 2003].

2.4 Checkpoints

Human cells are continuously exposed to external agents (e.g. reactive chemicals or UV light) and to internal agents, such as tobacco carcinogens, dietary factors, infectious agents and sex hormones. These factors can induce cell stress. Eukaryotic cells evolved a machinery with a series of surveillance pathways, called cell cycle checkpoints [Jones and Kazlauskas, 2001a,b].

During the first gap phase, G1, cells prepare for the process of DNA replication. They integrate mitogenic and growth inhibitory signals and make the decision to proceed, pause, or even exit the cell cycle. An important checkpoint in G1 has been identified in both yeast and mammalian cells. In yeast it is called START, in mammalian cells the restriction point(R). This is the point at which the cell stops to divide, when extracellular conditions are unfavorable. This is the case when cell is starved of essential growth factors or if protein synthesis is inhibited. The exact position of R in G_1 is different for various organisms and cell lines. However, in mouse and human cells, R was found to occur always between 3 to 4 hours after the end of mitosis [Zetterberg et al., 1995]. Some cells enter S phase immediately after passage through R, while others may spend up to 20 hours in G1. This suggests that beside R point passage, other regulatory events must be completed.

Another type of checkpoint is connected to various genetic alterations, which eventually would lead to cell death or malignant cell growth. If, for example, cells have damaged or unreplicated DNA, the cell will arrest at such checkpoint and try to repair it. In case when the damages are to serious, the checkpoint will induce apoptosis, the programmed cell death [Blagosklonny and Pardee, 2002].

2.5 Growth factor coupling

The whole cell cycle machinery, involving E2F TFs, pocket proteins and cyclin/cdk complexes, would be useless without stimulation from the extracellular matrix. Growth factors and sufficient nutrition are indispensable for successful cell proliferation. The activity of transcription factor E2F1 is only possible when its inhibitor, pRB, is phosphorylated. This is done in the first step by Cyclin D/cdk4,6 complex, which is a growth factor sensor.

Cyclin D gene, CCND1,2, is stimulated by a transcription factor family, AP–1 [Chang et al., 2003]. Activating protein (AP-1) transcription factors consist of homodimers and heterodimers of that belong to the Jun (c-Jun, v-Jun, JunB, JunD) and Fos (c-Fos, v-Fos, FosB, Fra1, Fra2) subfamilies. Fos proteins cannot form stable homodimers with itself, but they can mediate gene expression by forming heterodimers with various Jun proteins. Among all these possible connections, a heterodimer of c-Jun with c-Fos is a very stable and transcriptionally active complex.

c-Jun is phosphorylated in the cytoplasm by the last player of Raf/ MEK/ ERK pathway. After that it is translocated to the nucleus, where it binds with c-Fos.

Conclusions

The known facts for the G1/S transition in mammalian cells have been compiled to a coherent picture. Many of them, like E2F target genes expression and pRB phosphorylation, come from experiments with synchronized cell cultures. Such experiments use different synchronization methods like serum starvation, contact inhibition, the double-thymidine block or batch synchronization methods. They are supposed to synchronize a whole cell culture in certain state. However, there are some arguments against the common assumption about the successful synchronization [Cooper, 2003, 2004]. The author presents the problem using a 'Gedanken experiment', showing that experiments using whole-culture treatments are not suitable for cell-cycle analysis because these methods do not produce a synchronized culture.

Despite the experimental difficulties, cell cycle research will remain major topic in future. One of the main reasons is that alteration in components of the cell cycle machinery and checkpoint signaling pathways occur in the majority of human tumors, Tab.2.3. This finding underscores how important is the maintenance of cell cycle control in the prevention of human cancer.

Gene/Protein	**C**heckpoint	**T**umors associated with mutations **o**r altered expression
Bub1	Spindel	Colorectal carcinomas
Cdc25A	G1/S	Carcinomas of breast, lung, head and neck, and lymphoma
Cdk4,6	G1/S	Wide array of cancers
Chk1	Spindel	Colorectal and endometrial carcinomas
Cyclin D1	G1/S	Wide array of cancers
Cyclin D2	G1/S	Lymphoma and carcinomas of the colon, tesis and ovary
Cyclin E	G1/S	Wide array of cancers
MDM2	G1/S	Soft tissue tumors, osteosarcomas
$p16^{INK4a}$, $p27^{KIP1}$	G1/S	Wide array of cancers
p53	G1/S & G2/M	Wide array of cancers
pRB	G1/S	Wide array of cancers

Table 2.3: Mutations of cell cycle checkpoints regulators in human tumors. Only alterations that are present in $>10\%$ of primary tumors are represented.

Chapter 3

Nonlinear Dynamics

3.1 Introduction

The study of modules dynamics requires an appropriate framework. Usually, complex network behavior can be characterized through steady states of its dynamical system. Bifurcation diagrams illustrate changes in the number of fixed points and in their stability type as function of a control parameter. In this chapter we want to characterize such bifurcation points, called nonhyperbolic equilibrium points, where the vector field is structurally unstable. One can also plot a two-dimensional bifurcation diagram if the steady states of a system depend on two parameters.

In some special cases, there exist a polynomial form of the steady state problem. With a bit of luck such steady state polynomial can be, using an appropriate coordinate transformation, converted into a normal form of a catastrophic surface. This geometrical structures characterize noncontinuous transitions between different steady states.

In this chapter we follow the monographs by Jetschke [1989] and Perko [1993]. The nonlinear theory should only be sketched briefly, pointing to the most important results, required in this thesis.

3.2 Bifurcations at nonhyperbolic equilibrium points

The aim of this section is to define normal forms for the most frequently occurring bifurcations: saddle node and transcritical bifurcations, which emerge when changes in a parameter occur.

We want to analyze nonlinear systems of the form

$$\dot{x} = f(x). \tag{3.1}$$

The qualitative behavior of (3.1) will change as we change the vector field f. If the qualitative behavior remains the same for all nearby vector fields, then the system (3.1) or the vector field f is said to be structurally stable. The exact definition is given by

Definition 1 *Let E be an open subset of $\mathbb{R}^n$. A vector field $f \in C^1(E)$ is said to be **s**tructurally stable if there is an $\epsilon > 0$ such that for all $g \in C^1(E)$ with*

$$\|f - g\|_1 < \epsilon$$

f and g are topologically equivalent on E; i.e. there is a homeomorphism $H : E \to E$ which maps trajectories of (3.1) onto trajectories of

$$\dot{x} = g(x) \tag{3.2}$$

*and preserves their orientation by time. In this case, we also say that the dynamical system (3.1) is **s**tructurally stable.*

Specifically, we want to determine their equilibrium points and to describe the behavior near its equilibrium points. The Hartman-Grobman Theorem shows that close to a hyperbolic equilibrium point x_0, the nonlinear system (3.1), has the same qualitative structure as the linear system

$$\dot{x} = Ax, \tag{3.3}$$

with the matrix $A = \mathrm{D}f(x_0)$. The linear function $Ax = \mathrm{D}f(x_0)x$ is called the **l**inear part of f at x_0.

Definition 2 *A point $x_0 \in \mathbb{R}^n$ is called an **e**quilibrium point or **c**ritical point of (3.1) if $f(x_0) = 0$. An equilibrium point x_0 is called a **h**yperbolic equilibrium point if none of the eigenvalues of the matrix $\mathrm{D}f(x_0)$ have zero real part. The linear system (3.3) with the matrix $A = \mathrm{D}f(x_0)$ is called the **l**inearization of (3.1) at x_0.*

Further, we are interested in the qualitative behavior of the solution set of the system

$$\dot{x} = f(x, \mu), \tag{3.4}$$

where the vector field f depends on a parameter $\mu \in \mathbb{R}$. Qualitative changes in the solutions occur as the vector field f passes through a bifurcation as the

parameter μ varies through a bifurcation value μ_0. A value μ_0 of parameter μ in equation (3.4) for which the C^1–vector field $f(x, \mu_0)$ is not structurally stable is called a **b**ifurcation point. In the following we analyze bifurcations at nonhyperbolic equilibrium points. Such changes emerge if a real eigenvalue or a pair of complex conjugated eigenvalues crosses the imaginary axis. The following theorem states four associated bifurcations, from which the first two will be discussed in detail.

Theorem 1 *By changing a one-dimensional parameter μ in a differential equation, four bifurcation types can occur in the following normal forms:*

1. *saddle node bifurcation:* $\dot{x} = \mu - x^2$,
2. *transcritical bifurcation:* $\dot{x} = \mu x - x^2$,
3. *pitchfork bifurcation:* $\dot{x} = \mu x - x^3$,
4. *Hopf bifurcation:* $\dot{x} = \mu x - y - x(x^2 + y^2)$, $\dot{y} = x - \mu y - y(x^2 + y^2)$.

The fixed points $x = x(\mu)$ of eq.(3.4), which can be also written as $\mu = \mu(x)$, fulfill the algebraic equation

$$f(x, \mu(x)) = 0. \tag{3.5}$$

In the following, we call $\mu_0 = \mu(x_0)$ the critical value of the parameter, for which x_0

$$f(x_0, \mu_0), \tag{3.6}$$

has the nonhyperbolic equilibrium point x_0. After twice total differentiation of (3.5) we get

$$f_x(x, \mu(x)) + f_\mu(x, \mu(x)) \cdot \mu'(x) = 0, \tag{3.7}$$
$$f_{xx} + 2f_{x\mu}\, \mu'(x) + f_{\mu\mu}\, (\mu'(x))^2 + f_\mu \cdot \mu''(x) = 0. \tag{3.8}$$

Case 1

Let $f_\mu(x_0, \mu_0) \neq 0$. Due to the implicit function theorem, there exists a function $\mu = \mu(x)$, for which it follows from (3.7) and (3.8):

$$\mu'(x_0) = 0, \quad \mu''(x_0) = -(f_{xx}/f_\mu)(x_0, \mu_0). \tag{3.9}$$

If we assume that $f_{xx}(x_0, \mu_0) \neq 0$ then $\mu''(x_0) \neq 0$ follows. It means that there is a regular inversion at the point (x_0, μ_0) and that the graph of $\mu = \mu(x)$ is tangent to the straight line $\mu = \mu_0$. Therefore one calls it the **t**angent

bifurcation. It can be transformed with appropriate choice of coordinates to the normal form 1, Theorem 1. From

$$f_x(x_0, \mu_0) = -f_\mu(x_0, \mu_0)\ \mu'(x_0) \tag{3.10}$$

and because $\mu'(x)$ changes its sign in x_0, one can follow that one of the branches is stable and the other unstable. Due to this fact one calls it the **s**addle-node bifurcation.

Case 2

For $f_\mu(x_0, \mu_0) = 0$ there is a **s**ingular point of the surface $f(x, \mu) = 0$. From (3.8) we get

$$f_{xx}(x_0, \mu_0) + 2f_{x\mu}(x_0, \mu_0) \cdot \mu'(x_0) + f_{\mu\mu}(x_0, \mu_0) \cdot (\mu'(x_0))^2 = 0 \tag{3.11}$$

or, for relation $x = x(\mu)$,

$$f_{xx}(x_0, \mu_0) \cdot (x'(\mu_0))^2 + 2f_{x\mu}(x_0, \mu_0) \cdot x'(\mu_0) + f_{\mu\mu}(x_0, \mu_0) = 0. \tag{3.12}$$

(3.11) and (3.12) can be seen as quadratic equations in $\mu'(x_0)$ or $x'(\mu_0)$, respectively. Let D be defined as

$$D := (f_{x\mu}(x_0, \mu_0))^2 - (f_{xx} \cdot f_{\mu\mu})(x_0, \mu_0) = 0. \tag{3.13}$$

If the inequality $D < 0$ holds then (3.11) and (3.11) have no real solution for $\mu'(x_0)$ or $x'(\mu_0)$. There exists an **i**solated point, i.e. $f(x, \mu)$ has in (x_0, μ_0) a local extreme with $f(x_0, \mu_0) = 0$. For $D = 0$ a double root exists, which means that two solution branches are tangent to each other at (x_0, μ_0). For the case $D > 0$ two curves cross each other and the following case is interesting

Case 2a

If additionally $f_{xx}(x_0, \mu_0) \neq 0$ holds then from equation (3.11) we get both roots:

$$x'_{1,2}(\mu) = (f_{x\mu} \cdot f_{xx})(x_0, \mu_0) \pm \sqrt{D/\big(f_{xx}(x_0, \mu_0)\big)^2}. \tag{3.14}$$

Two branches of fixed points $x = x_1(\mu)$, $x = x_2(\mu)$ go through (x_0, μ_0) and cross with the calculated slops $x'_{1,2}(\mu)$. In case when $f_{\mu\mu}(x_0, \mu_0) \neq 0$, the branches can be written in the form $\mu_1(x)$ and $\mu_2(x)$.

The point (x_0, μ_0) is a **d**ouble point, at which the **t**ranscritical bifurcation appears with the normal form 2, th.1. The stability of these two branches changes in the bifurcation point as one can recognize from 3.10 or from $f_{x\mu} = -f_{\mu\mu} \cdot \mu'$. Therefore, the phenomenon is called the **s**tability exchange.

3.3 Catastrophes

Under certain circumstances two or more saddle nodes can appear in a dynamical system. The simplest case of two connected tangential bifurcations emerges in a single autocatalytical feedback loop, see discussion in chapter 4. Such phenomenon is called **b**istability, i.e. the coexistence of two stable and one unstable steady states. A hysteresis-like curve is a cut through the steady state surface. Only for few cases such an algebraic surface can be calculated analytically.

For the purpose of later applications, feedback loops and their coupling (chapter 4 and 5), only steady states surfaces as polynomials will be important. Fortunately, there is a beautiful mathematical theory describing, geometrically speaking, foldings of algebraic surfaces defined by polynomials. **C**atastrophe theory [Poston and Stewart, 1978, Jetschke, 1989] was founded by Thom (1972) and has been applied in various fields of sciences. In general the aim of the catastrophe theory is a description of noncontinuous processes which take place in physics or biology.

The catastrophe theory applies to gradient systems, defined by

$$\dot{x} = -\mathrm{grad}_x V(x,\mu), \quad x \in X = \mathbb{R}^n, \quad \mu \in C = \mathbb{R}^m, \tag{3.15}$$

for which complete description of their potential bifurcations is possible. In the following the potential function $V(x,\mu),\ x \in X,\ \mu \in C$ is a smooth function of x and μ.

The **s**et of stationary points of V is given by

$$M := \big\{(x,\mu) \in X \times C \ \big|\ \partial V(x,\mu)/\partial x_i = 0,\ i = 1,\ldots,n\big\}. \tag{3.16}$$

The points, given by the set

$$K := \big\{(x,\mu) \in M \ \big|\ \det\big((\partial^2 V(x,\mu)/\partial x_i^2 x_j^2)_{i,j=1}^n\big) = 0\big\}, \tag{3.17}$$

are called **s**ingularities of M or the **c**atastrophic set. Its projection in the parameter space

$$B := \{\mu \in C \mid \exists x \in X \ \text{ with } \ (x,\mu) \in M\} \tag{3.18}$$

is called the **b**ifurcation set.

The following Thom's theorem states that there are very few different types of catastrophe curve in the lower dimensions. For only one control parameter and one variable there is only one shape of catastrophic jump - the fold. In case of two control parameters and two variables there are only two shapes, the fold and the cusp. For parameter space of five dimensions or more, there is no classification.

Theorem 2 (Thom) *Let C be a four-dimensional parameter space, let X be a finite dimensional state space and let V be parameterized through C, a smooth function on X. Let M be the set of stationary points of V. Then, M is a smooth hyperplane in $X \times C$. Moreover the following seven elementary catastrophes are the sole singularity types of M:*

Name	dim X	dim C	**N**ormal form of V
Fold	≥ 1	1	$x^3/3 + ux$
Cusp	≥ 1	2	$x^4/4 + (u/2)x^2 + vx$
Swallowtail	≥ 1	3	$x^5/5 + (u/3)x^3 + (v/2)x^2 + wx$
Butterfly	≥ 1	4	$x^6/6 + (t/4)x^4 + (u/3)x^3$ $+(v/2)x^2 + wx$
hyperbolic umbilic	≥ 2	3	$x^3 + y^3 + wxy - ux - vy$
elliptic umbilic	≥ 2	3	$x^3 - xy^2 + w(x^2 + y^2) - ux - vy$
parabolic umbilic	≥ 2	4	$x^2y + y^4 + tx^2 + wy^2 - ux - vy$

Part II

Results

Chapter 4

Autocatalytical Reactions and Bistability

Summary

Autocatalytical feedback loops are omnipresent in biological systems. It is also one of the most popular keywords in the literature, either experimental and theoretical, and has a long history. It started with the influential paper by Monod and Jacob over 40 years ago [Monod and Jacob, 1961], in which the authors analyzed six regulatory and differentiation systems. Each of them was built out of components known from studies of gene regulation in eukaryotes, and each was a variation of a double-negative feedback loop.

The present chapter gives at the beginning an overview of autocatalytical systems discovered or constructed in a biological context and/or analyzed theoretically. We then take basal expression into account, which is responsible for interesting changes in the module dynamics. In parallel we assume autocatalysis with and without cooperativity and get in this way different behavior in positive feedback systems. There are three types of such mixed systems: those with no bifurcation, further ones with transcritical and finally with saddle node bifurcations. At the end the obvious connection between autocatalytical systems with basal expression and cooperativity and the catastrophic cusp surface is discussed. The steady state polynomial of a double-negative feedback loop has also a surprisingly rich geometrical structure.

4.1 Introduction

Autocatalytical reactions are omnipresent in nature. A number of well studied examples of such circuits has been published, either on the level of molecular reactions, protein-protein interactions or gene regulation. Positive circuits are involved in many processes showing hysteresis or memory [Demongeot et al., 2000], they are indispensable in cell differentiation [Monod and Jacob, 1961], immunology [Staudt, 2004] and in general in biology as an all-or-none response or a "flip-flop" switch [Iglesias and Levchenko, 2002]. They occur in signal transduction pathways [Ferrell, 1998, Ferrell and Xiong, 2001, Blüthgen and Herzel, 2003], circadian clocks [Gonze et al., 2002, Becker-Weimann et al., 2004] and many other systems.

Lee et al. [2002] used the genome-wide location data of yeast to identify six regulatory network motifs: autoregulation, multicomponent loops, feed-forward loops, single-input, multi-input, and regulator chain. An autoregulation motif was defined by the authors as one consisting of a regulator that binds to the promoter region of its own gene. 10 autoregulation motifs were identified with genome-wide location data for 106 regulators (P value threshold 0.001), suggesting that about 10% of yeast genes encoding regulators are auto-regulated. Moreover, taking into account less stringent P value threshold, the data indicate that most (52% to 74%) prokaryotic genes encoding transcriptional regulators are auto-regulated [Shen-Orr et al., 2002, Thieffry et al., 1998].

The all-or-non response of a module or network to an input signal has gained more and more attention in recent years. Bistability is a phenomenon closely related to autoregulatory loops. This elegant and well defined feature exemplifies a coexistence of two stable steady states and the discontinuous transitions from one state to the other [Angeli et al., 2004]. Although the subject of this chapter is primarily positive feedbacks and their coupling, negative circuits are also of interest. Beside their ability to produce oscillations, appropriate coupling of such negative circuits, e.g. in form of a mutual inhibitor module, provides a bistable system response, i.e. a discontinuous amplification of an input signal [Gardner et al., 2000].

Positive feedbacks

Ferrell [2002] describes in his review inalienability of positive feedbacks for bistability. Simple positive feedback, double negative feedback, auto-catalysis or an equivalent does not guarantee however that a system will be bistable. A bistable system must also possess some type of non-linearity within the feedback circuit, which may come from a cooperative-like answer of an circuit

element to its regulators.

There have been many attempts to study the behavior of autocatalytical loops and their influence on networks in which they are incorporated. Bagowski and Ferrell [2001] presented a model of the JNK cascade. The responses of JNK to both physiological stimulus (progesterone) and a pathological stress (hyperosmolar sorbitol) in Xenopus oocytes were found to be essentially all-or-none.

Hofer et al. [2002] analyzed the positive feedback loop occurring in GATA-3 imprinting. However, autoregulation is only the necessary condition to achieve multistability. Cooperativity, which provides the nonlinearity, is essential for the bistable response in this system. The processes of transcription and translation are very complex and are composed of steps including splicing, nuclear export and several post-translational modifications, to name only the most important. Hofer et al. [2002] showed that these multiple and complicated tasks combined with cooperativity can be expressed under the steady state by the simple equation:

$$\alpha + k_G \frac{G_n^2}{(1+G_n)^2} = \kappa\, G_n \tag{4.1}$$

with G_n the transcriptionally active form of the GATA-3 in nucleus, α the basal activation rate, k_G the rate constant of GATA-3 activation, and the effective lose rate constant κ. The solutions of the resulting steady state polynomial provide the required bistability.

Isaacs and colleagues [Hasty et al., 2000, 2001, Isaacs et al., 2003] provided, using an integrated approach, an example for a positive feedback system in *E.*coli with temperature as a control parameter. In a number of papers deterministic and stochastic approaches for the description of such a simple system are discussed [Becskei and Serrano, 2000, Gardner et al., 2000, Walczak et al., 2005]. In accordance with the prediction of the theoretical model, temperature-induced protein destabilization led to the existence of two expression states, thus elucidating the distinguishing characteristic of bistability of this autoregulatory network architecture. One interesting conclusion made in these papers is that one needs to characterize quantitatively the functionality of individual modules in order to understand how sets of modules interact in large-scale networks.

Positive feedbacks in form of double inhibitor systems are also wide spread in molecular systems. One possibility has already been shown in the historical paper by the Nobel prize winners Monod and Jacob [Monod and Jacob, 1961]. It consists of two enzyme pathways, as reproduced in Fig.4.1. The end product of the first pathway, d, inhibits the other pathway by inhibiting enzyme E_1'. Conversely, the end-product of the second pathway, δ, inhibits

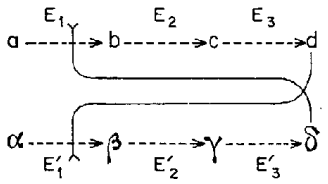

FIGURE 1. Model I. The reactions along the two pathways a → b → c → d, and α → β → γ → δ, are catalyzed by enzymes E_1, E_2, E_3 and E_1', E_2', E_3'. Enzyme F_1 is inhibited by δ, the product of the other pathway. Conversely, enzyme E_1' is inhibited by metabolite d, produced by the first pathway.

Figure 4.1: Historical double inhibitor module analyzed by Monod and Jacob, [Monod and Jacob, 1961]. The pathways end products inhibit respectively the opposite chain.

the first pathway by inhibiting E_1. Temporary changes in the concentrations of the pathways end products can swing the circuits towards one of two possible stable steady states.

The second variant is a module where two gene repressors inhibit each other's expression. Such circuit has the useful property that a perturbation of one of the regulators can push the system towards one of the two stable states. Gardner et al. [2000] analyzed both theoretically and experimentally such toggle-switch in *E.coli*. Two genes with repressible promoters placed in this purposely constructed plasmid were stimulated by two different transient chemicals. Each promoter was inhibited by the repressor transcribed by the opposing promoter. The mutual inhibition in this system provides a positive feedback loop. A simple deterministic model based on Hill function [Cherry and Adler, 2000] explains the bistable features of the system. The model preserves the two most fundamental aspects of the network: cooperative repression of constitutively transcribed promoters and degradation/dilution of the repressors.

Yet another example is the recent published double-negative circuit occurring in the B-cell differentiation [Fujita et al., 2004, Staudt, 2004]. BCL-6 and Blimp-1 are two gene repressors which inhibit each other. As explained, before transient changes in activity of either repressor can push a cell towards one or the other differentiation state.

Recent results of an experiment with a so called "programmable cell" [Kobayashi et al., 2004, Kramer et al., 2003, Weber and Fussenegger, 2002] illustrate in an impressive manner how such biological hardware can be constructed and used. The paper of the Boston group of J.J.Collins [Kobayashi

et al., 2004] describes how to create cells with programmable behaviors. A toggle switch has been constructed in *E.*coli and coupled with signaling pathways. In the next step, different strains with such constructs have been obtained, each of them detecting certain stimuli like e.g. DNA damage and responding to it in a well defined way.

Positive feedback are in general thought to be inherently unstable [Sauro and Kholodenko, 2004]. However, under certain conditions they produce bistability which is obviously of great importance in biological systems and makes them so popular. Interestingly, systems are imaginable in which positive feedback can be stabilizing [Cinquin and Demongeot, 2002]. Two examples are presented in that paper, one artificial and one with a straightforward biological interpretation. It describes the gene expression and autoregulation through the expressed mRNA and protein.

Negative feedbacks

Negative feedbacks are also very important in biological systems, since they occur probably even more often than their positive counterparts. It has been discovered that negative feedbacks play a role in generating oscillations. Examples of such systems are the circadian clock [Gonze et al., 2002, Becker-Weimann et al., 2004], mitotic oscillations and oscillation in the MAP-kinase cascade [Kholodenko, 2000].

Another role is making a system robust against alteration of its parameters. Experimental evidence of the stabilizing influence of negative loops on gene networks has been shown to be in agreement with results gained from numerical simulations [Becskei and Serrano, 2000, Gardner and Collins, 2000]. The designed and constructed simple gene circuits consisting of a regulator and transcriptional repressor modules in *E.*coli showed the gain of stability produced by the negative feedback.

A digital pacemaker consisting of the tumor suppressor p53 and its transcriptional target and negative regulator Mdm2 has been analyzed by Lahav et al. [2004]. As shown in an ordinary differential equation model and measured in the lab, under certain circumstances, oscillations in p53 and Mdm2 protein levels can emerge in response to a stress signal like DNA damage. A further conclusion is that the negative feedback loop generates a 'digital' clock that releases well-timed quanta of p53 until damage is repaired or the cell dies.

However, besides these examples, it has been demonstrated that negative feedbacks can be destabilizing for some systems [Cinquin and Demongeot, 2002]. The authors present an example, in which negative feedback can lead to exponentially growing oscillations, a source of instability. Recapitulat-

ing, there are diverse application of negative and positive feedbacks. Both negative and positive circuits can play a stabilizing or destabilizing role in biological systems and networks.

4.2 Positive feedbacks – mathematical formulation

As emphasized before, the main focus of this chapter is on positive feedbacks. One reason is their appearance in biological systems studied here. It is one of the simplest units commonly used in transcriptional regulatory network architecture, or network motifs.

The other reason we care so much about positive feedbacks is due to their ability to produce, under some conditions, all-or-non responses which appear repeatedly in biological networks and signaling pathways mentioned in the previous section.

The question of how to put gene expression into a mathematical formula was first addressed in the 1960's. Griffith was one of the first who established the mathematical foundations of cellular control processes like gene expression [Griffith, 1968b,a]. He considered the induction of activity in a gene by the protein for which it codes, or by the metabolic product of that protein, which constitutes a classical positive feedback circuit. Basically, his original approach remained nowadays unchanged. In the most general non-dimensional form with three variables it reads:

$$\frac{dM}{dt} = \frac{B^n}{1+B^n} - \phi_M M \tag{4.2}$$

$$\frac{dP}{dt} = M - \phi_p P \tag{4.3}$$

$$\frac{dB}{dt} = P - \phi_b B \tag{4.4}$$

It has been shown that the qualitative behavior of the system is similar in one, two and three-variable cases, with mRNA as first variable M, the protein P as the second and a metabolite B as third variable. In all cases, because of the assumption of linear production and degradation processes of M and P, the stationary states are given by the roots of the equation

$$\alpha\, x^{n+1} - x^n + \beta\, x = 0, \qquad \alpha, \beta \in \mathbb{R}^+ \backslash \{0\}, \tag{4.5}$$

where x stands for M, P or B, respectively. This equation always has a zero root and according to the Descartes' rule of sign (see Appendix B) at most two more or zero real positive roots (see analysis below, Sec.4.2.1).

The analysis done by Griffith and Höfer shows that the detailedness of applied equation systems does not essentially change the behavior and prediction abilities of such autocatalytical gene expression models. As far as all processes beside transcription factor binding are described using linear kinetics, it does not matter how many steps the model contains. The bistable response of the system is encoded in the sigmoidal gene transcription function. Other examples can be found of textbooks about biological modeling and nonlinear dynamics by Strogatz [2001], Murray [1993], Edelstein-Keshet [1988], Heinrich and Schuster [1996] and Goldbeter [1996].

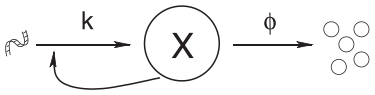

Figure 4.2: Autocatalytic module: expression (gene transcription and translation) of the protein x is reduced to one step. The protein degradation ϕ is assumed to be linear (4.6).

In order to include a possibly basal gene expression at negligible activator concentration, we modify slightly the one variable equation by adding a constant [Smolen et al., 1998, Fall et al., 2002]. Another reason was to get a compact and handy formula for the process. The differential equation for the autocatalytical function with this extension reads

$$\frac{dx}{dt} = f(x), \qquad f(x) = \underbrace{k\,\frac{a + x^n}{b + x^n}}_{production} - \underbrace{\phi\, x}_{degradation} \tag{4.6}$$

with $n \in \mathbb{N};\ a, b, k, \phi \in \mathbb{R}^+;\ a < b$. This can be seen as follows. From the differential equation, e.g. [Smolen et al., 1998],

$$\frac{dx}{dt} = \alpha + k\,\frac{x^n}{\beta + x^n} - \phi\, x = \frac{\alpha\,\beta + \alpha\, x^n + k\, x^n}{\beta + x^n} - \phi\, x = f(x) - \phi\, x$$

it follows for the production function

$$\Rightarrow f(x) = \frac{\alpha\,\beta + (\alpha + k)\, x^n}{\beta + x^n} = (\alpha + k)\,\frac{\frac{\alpha\beta}{\alpha+k} + x^n}{\beta + x^n}.$$

Assuming $\alpha \ll k$ we get the desired equation (4.6).
The steady state polynomial now reads

$$\phi\, x^{n+1} - k\, x^n + b\phi\, x - a\, k = 0, \qquad a, b, k, \phi \in \mathbb{R}^+ \backslash \{0\}. \tag{4.7}$$

In the following we discuss two possible qualitative types of behavior of this simple system. The variation of the parameter k, which represents the production rate of the protein x, leads to bifurcations. Two different kinds of bifurcation are encoded in this simple equation, depending whether or not the cooperativity in gene expression is taken into account.

4.2.1 Case I – no cooperativity

For the choice $n = 1$ and $a = 0$ the autocatalytic system shows a transcritical bifurcation. It can be easily seen by analyzing the system in steady state, e.g. assuming that $f(x) = 0$. The bifurcation plot depicts an exchange of stability between two steady states which meet at the bifurcation point (TC), Fig.4.3B. Until the critical value, k^{tr}, of the control parameter the system is captured in the stable zero steady state. This kind of bifurcation is often used to describe threshold phenomena, for example, in physics [Strogatz, 2001] or in biological applications [Aguda, 1999].

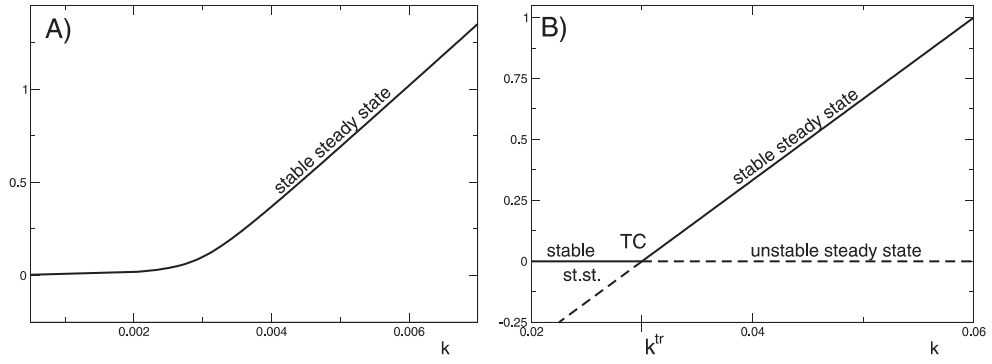

Figure 4.3: Bifurcation plots of the system $\frac{dx}{dt} = k\,\frac{a+x}{b+x} - \phi\,x$. A) $a \neq 0$ with $a = 0.01, b = 1$ and $\phi = 0.003$. B) $a = 0$ with $b = 1$ and $\phi = 0.03$: the threshold point is located at $k^{tr} = b\,\phi$. This and all others bifurcation diagrams have been done using XPPAUT tool, Ermentrout [1998].

One may wonder why in the first case the transcritical bifurcation occurs only for $a = 0$, $n = 1$. Figure 4.3A shows the situation if $a \neq 0$. There is only one steady state and no bifurcation regardless of the value of the control parameter.

One possibility to explain these differences is via rewriting the steady state polynomial in a normal form. This can be easily done in both cases.

For the case when $a = 0$ the steady state polynomial reads

$$k\,x - \phi\,x\,(b + x) = 0$$

which reduces to the normal form of transcritical bifurcation, Sec.3.2:

$$\mu\,x - x^2 = 0 \tag{4.8}$$

with $\mu := \frac{k - b\,\phi}{\phi} = 0$. The bifurcation point occurs when $\mu = 0$, i.e. at $k^{tr} = b\,\phi$ (Fig.4.3 B).

For the case $a \neq 0$ the steady state polynomial reads

$$a\,k + (k - \phi)\,x - \phi\,x^2 = 0$$

with the roots

$$x_{1/2} = \frac{k - b\,\phi \pm \sqrt{4\,a\,k\,\phi + (k - b\,\phi)^2}}{2\,\phi}$$

A coordinate transformation $\hat{x} = x + x_{1/2}$ provides the required normal form like equation

$$\hat{\mu}\,\hat{x} - \hat{x}^2 = 0 \tag{4.9}$$

with $\hat{\mu} = \frac{\sqrt{4\,a\,k\,\phi + (k - b\,\phi)^2}}{\phi}$.

However, the difference in comparison to (4.8) is that $\hat{\mu} \neq 0$ for $a, b, k, \phi \in \mathbb{R}^+\backslash\{0\}$. This explains why there is no bifurcation for the case $a \neq 0$, Fig.4.3 A.

A threshold defined by the transcritical bifurcation (i.e. when $a = 0$) has also been used to describe biochemical reactions. It has been shown [Aguda, 1999] how to define cell cycle checkpoints in terms of transcritical bifurcation. It occurs, for example, in coupled phosphorylation-dephosphorylation cycle sets with positive feedbacks.

4.2.2 Case II – cooperative kinetics

A simple extension is to assume higher order dynamics which occurs e.g. in case of cooperativity. Therefore, for $n > 1$ and $a \neq 0$, bistability and hysteresis can be observed. For certain values of a parameter, two stable steady states coexist and are separated by an unstable one.
For the case $n = 2$ the steady state polynomial reads

$$\phi\,x^3 - k\,x^2 + b\phi\,x - ak = 0; \qquad a, b, k, \phi \in \mathbb{R}^+\backslash\{0\} \tag{4.10}$$

The increase of the control parameter k causes initially a continuous increase of the steady state. At the saddle node bifurcation point (SN) the unstable and one stable steady state vanish. The system jumps to the only possible high stable steady state. In order to return to the initial steady state the control parameter has to be decreased. In this case, one would complete the hysteresis as shown in Fig.4.4A. Although theoretically easy to construct, the experimental realization and proof even for simplest systems which are supposed to accomplish bistability might be very challenging. One of the newest examples of an experimentally tested bistable autocatalytical system was simulated and measured by Isaacs [Isaacs et al., 2003].

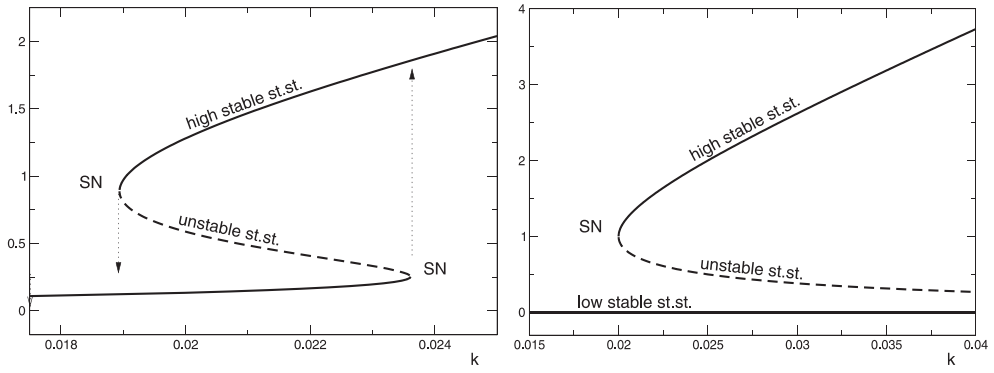

Figure 4.4: Bifurcation plot of the autocatalytical system with: A) basal transcription: $dx/dt = k\,(a+x^n)/(b+x^n) - \phi\,x$ for $a = 0.05$, $b = 1$, $\phi = 0.01$ and $n = 2$, B) without basal transcription i.e. for $a = 0$, $b = 1$, $n > 1$ and $\phi = 0.01$. In contrast to case A) there is no saddle-node bifurcation, i.e. no transition from the low to the middle steady state. Both steady states meet for $k \to \infty$.

As the following analysis shows the basal transcription, e.g. due to extrinsic stimulation, is indispensable for switching from the low to the high steady state. We plotted the bifurcation curves of the autocatalytical system without basal transcription but still assumed cooperativity i.e. $dx/dt = k\,x^n/(b+x^n) - \phi\,x$ with $n > 1$, Fig.4.4B. As one can see the outcome is qualitatively different. The reason can be explained by calculation of the roots of the steady state polynomial:

$$x_1 = 0; \qquad x_{2,3} = \frac{k \pm \sqrt{k^2 - 4\,b\,\phi^2}}{2\phi}$$

While x_1 does not change, letting $k \to \infty$ which means $k - \sqrt{k^2 - 4\,b\,\phi^2} \to 0$ we get the other solutions $x_2 \to 0$ and $x_3 \to \infty$. This explains the existence

of only one saddle node in the bifurcation curve, Fig.4.4B.

The whole purpose of this section was the detailed analysis of possible steady state structure arising from the basic equation 4.6. We use it later to describe autocatalytical modules and their coupling and in the G1/S transition model. Also, the results can be helpful in modeling of positive circuits with certain desired behavior. As discussed above, threshold phenomena and discontinuous changes are encoded in this simple module.

4.3 Positive feedback and cusp catastrophe

For the special case $n = 2$, even more insights in the solution structure of this simple system are immediately clear. The steady-state assumption $f(x) = 0$ leads to the cubic polynomial:

$$\phi\, x^3 - k\, x^2 + b\, \phi\, x - a\, k = 0 \tag{4.11}$$

Applying the Descartes' rule of sign (the necessary condition) we conclude the existence of maximum one or three real positive roots of the polynomial which is equal to the number of physically reasonable steady-states. The sufficient condition for the existence of three different roots is that:

$$D := \beta^2 - 3\alpha\, \gamma > 0 \qquad \text{and} \qquad -A - B < \sigma < -A + B$$

with $\alpha = \phi$, $\beta = -k$, $\gamma = b\, \phi$, $\sigma = -a\, k$, $A = \frac{2\,\beta^3}{27\,\alpha^2} - \frac{\beta\,\gamma}{3\,\alpha}$, $B = \frac{2\,D^{3/2}}{27\,\alpha^2}$.

The steady-state surface with $y = b$ and $z = k$ which can be written as function $f(x, y, z)$

$$f(x, y, z) = \phi\, x^3 - x^2\, z + \phi\, x\, y - a\, z \tag{4.12}$$

is a cubic algebraic surface of surface order 3.

One can show that the steady-state surface can be transformed into a cusp manifold applying a simple coordinate transformation which will be sketched in the following. Consider the steady-state surface (4.11) as cubic polynomial:

$$f(x, \beta) = x^3 + \beta_2\, x^2 + \beta_1\, x + \beta_0 = 0 \tag{4.13}$$

with $\beta_0 = -ak/\phi$, $\beta_1 = k$ and $\beta_2 = -k/\phi$. It is the normal form of an equation of the third degree. It can be reduced to the form

$$f(x', \rho) = (x')^3 + \rho_1\, x' + \rho_0 = 0. \tag{4.14}$$

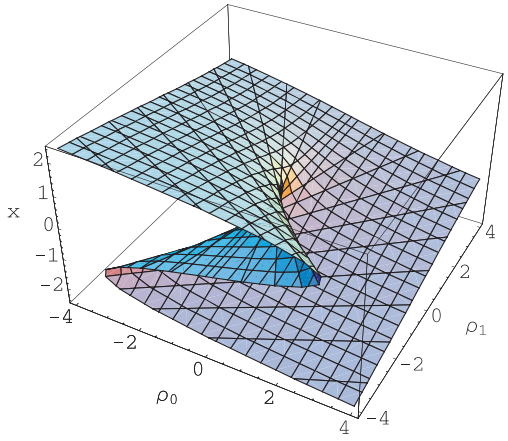

Figure 4.5: Plot of the steady state surface as cusp manifold $f(x', \rho) = (x')^3 + \rho_1 x' + \rho_0 = 0$.

using the following transformation [Poston and Stewart, 1978, Jetschke, 1989]:

$$\begin{aligned} x' &= x + (\beta_2/3) \\ \rho_1 &= \beta_1 - 3(\beta_2/3) \\ \rho_0 &= \beta_0 - \beta_1(\beta_2/3) + 2(\beta_2/3)^3. \end{aligned} \tag{4.15}$$

The equation (4.14) is called the reduced form of (4.13). For each solution of x' of the reduced form, $x = x' - (\beta_2/3)$ is the solution of the normal form. In the special case $a \neq 0$ and $n = 2$ the steady-state surface eq.(4.11) for the solution space of the autocatalytical feedback problem is equal to the cusp manifold, shown in Fig.4.5 and given by the reduced form (4.14).

The reduction transformation (4.15), by which the number of parameter is reduced by one, is not just an elegant way to visualize the problem in terms of the cusp catastrophe. It allows an analysis of the whole parameter space ρ_0–ρ_1 with respect to the existence of subspaces having zero, one, two or three steady states respectively. The detailed analysis of this beautiful geometrical problem can be found in a number of textbooks about catastrophe theory [Poston and Stewart, 1978, Jetschke, 1989].

4.4 Double inhibition and butterfly catastrophe

Surprisingly, another important module whose behavior is governed by a positive feedback can be characterized by an elementary catastrophe. Mutually

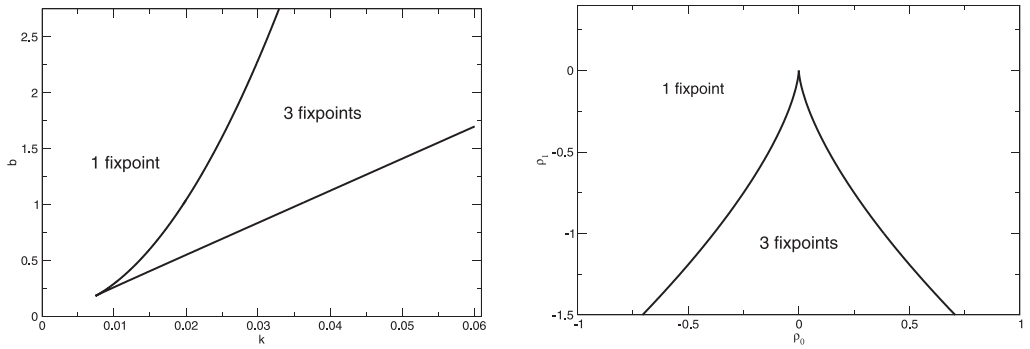

Figure 4.6: Two-dimensional bifurcation plots for the autocatalytical module (left), Eq.4.11, and its reduced form (right), the cusp manifold, Eq.4.14 shown in Fig.4.5.

double inhibition module (DI) which realizes a bistable toggle switch is usually defined using Hill-type functions [Cherry and Adler, 2000, Gardner et al., 2000]:

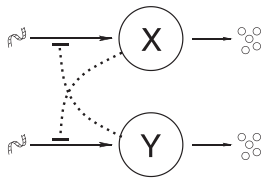

$$\frac{dx}{dt} = k_x \frac{1}{1+y^\alpha} - \phi_x\, x \tag{4.16}$$

$$\frac{dy}{dt} = k_y \frac{1}{1+x^\beta} - \phi_y\, y \tag{4.17}$$

Table 4.1: Schema of the double inhibition module and defining differential equations.

The concentration of repressor X is denoted by x and k_x stands for its effective rate of synthesis. Analogues meaning have y and k_y for the repressor Y. α is the cooperativity of repression of promoter Y and β is the cooperativity of repression of promoter X. The form of the double inhibition module equations preserves the two important aspects of the network: cooperative repression of transcribed promoters, and linear degradation of the repressors.

We calculate for $\alpha = \beta = 2$ the steady state polynomial for y:

$$P_{DI}(y) = k_y\phi_y + \frac{-k_x^2\phi_y - \phi_x^2\phi_y}{\phi_1^2\phi_y}\, y + \frac{2k_y}{\phi_y}\, y^2 - 2\, y^3 + \frac{k_y}{\phi_y}\, y^4 - y^5, \tag{4.18}$$

The polynomial is of the form $E - D\, y + C\, y^2 - B\, y^3 + A\, y^4 - y^5$ with real positive coefficients $A = \frac{k_y}{\phi_y}, B = 2, C = \frac{2k_y}{\phi_y}, D = \frac{k_x^2\phi_y + \phi_x^2\phi_y}{\phi_1^2\phi_y}, E = k_y\phi_y$. Using

the coordinate transformation $y = z - A/5$ we get:

$$\hat{P}_{DI}(z) = E + D\Big(\frac{A}{5}+z\Big) + C\Big(\frac{A}{5}+z\Big)^2 + B\Big(\frac{A}{5}+z\Big)^3 + A\Big(\frac{A}{5}+z\Big)^4 + \Big(\frac{A}{5}+z\Big)^5$$

and finally

$$\begin{aligned}\hat{P}_{DI}(z) &= \frac{4A^5}{3125} - \frac{A^3B}{125} + \frac{A^2C}{25} - \frac{AD}{5} + E + \Big(-\frac{3A^4}{125} + \frac{3A^2B}{25} - \frac{2AC}{5} + D\Big)z \\ &\quad + \Big(\frac{4A^3}{25} - \frac{3AB}{5} + C\Big)z^2 + \Big(-\frac{2A^2}{5} + B\Big)z^3 + z^5.\end{aligned}$$

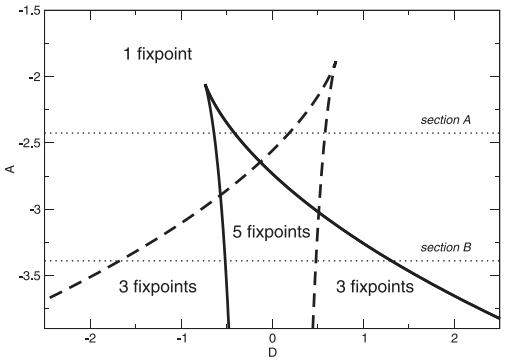

Figure 4.7: Two dimensional bifurcation diagram for the double inhibitor module.

After inserting original coefficients it reads:

$$P_{DI}(z) = V + Uz + Tz^2 + Sz^3 + z^5 \tag{4.19}$$

with

$$\begin{aligned}S &= -2 - \frac{2k_y^2}{5\phi_y^2}, \quad T = \frac{4\,k_y^3}{25\,\phi_y^3} + \frac{16\,k_y}{5\,\phi_y}, \\ U &= -\frac{3\,k_y^4}{125\,\phi_y^4} - \frac{26\,k_y^2}{25\,\phi_y^2} + \frac{-k_x^2\,\phi_y - \phi_x^2\,\phi_y}{\phi_x^2\,\phi_y}, \\ V &= \frac{4k_y^5}{3125\,\phi_y^5} + \frac{12\,k_y^3}{125\,\phi_y^3} + \frac{k_y}{\phi_y} - \frac{k_y(-k_x^2\,\phi_y - \phi_x^2\,\phi_y)}{5\,\phi_x^2\,\phi_y^2}.\end{aligned}$$

The difference between (4.18) and (4.19) is the missing 4th degree term in the latter one. The resulting polynomial (4.19) is the normal form of the butterfly catastrophe, as defined in Section 3.3, with the independent coefficients S, T, U, V.

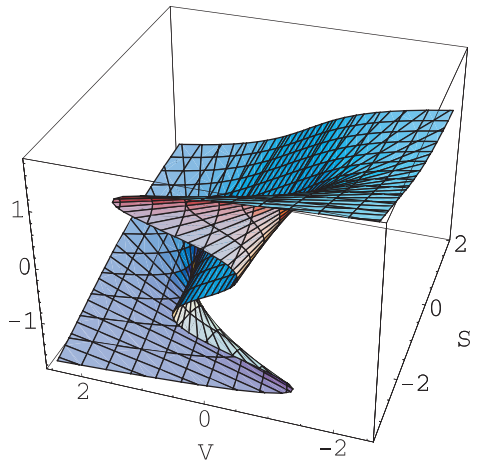

Figure 4.8: Steady state surface of the double inhibitor module is a "butterfly" manifold $P_{DI}(z) = V + Uz + Tz^2 + Sz^3 + z^5 = 0$.

4.5 Conclusions

The first half of this chapter was devoted to the rich history of feedback research in biological sciences with focus on positive autocatalytic reactions. Meanwhile a lot is known about this interesting mechanism and some of these circuit systems have been realized in experiments. One of their most important features is the possibility to construct a discontinuous hysteresis-like transition between two stable steady states. We discussed further in detail the importance of basal expression and cooperativity in feedback systems. Systems without these properties show a threshold mechanism in form of transcritical bifurcation. Finally, we demonstrated with two examples that some autocatalytical loops have an geometrical representation in form of a catastrophic surface.

Chapter 5

Coupling of Modules

Summary

Single isolated modules, like those described in previous chapter, do not exist in nature. They are of significant importance for a regulatory process only if they appear coupled in larger networks. In this chapter we analyze features of serially coupled autocatalytical circuits, described in previous chapter. The discussion was on the one side stimulated by suggestions and ideas from immunology, where a simple serial connection of multiple autocatalytical units was proposed as a cell differentiation mechanism. On the other side, our own observations related to the cell cycle gave reason to study this topic more carefully. Positive feedbacks can serve as checkpoint and phase transition engines.

The main focus lies therefore on the number of stable steady states in a given system. Fortunately, in our examples it is always possible to formulate the problem as polynomial in one variable. It means that the problem merely reduces to finding roots of polynomials.

Another advantage of coupled positive feedbacks lies in their ability of creating of powerful toggle switches, defined by steep transitions between extremal stable steady states.

5.1 Introduction

The idea of dissecting big networks into functional subunits, called the bottom-up approach, is very popular in different scientific areas [Hartwell et al., 1999]. Nature developed different organs in living organisms, each of them having a specific function, being coupled and indispensable for the whole organism. Social and political systems are based on the existence of different special-

ized groups. Engineering systems like electrical control units are basically a combination of sub-modules with clearly defined tasks. There is no doubt that modularization is essential for complex organisms and systems.

5.2 First examples

As discussed in chapter 6 about a G1/S model, even small networks are separable in modules. Each of them has its own function. The first module describes the activation reaction of the Cyclin D/cdk4,6 complex, the second the phase transition. They are defined in terms of transcritical or saddle node bifurcation, respectively. Motivated by this observation we analyzed

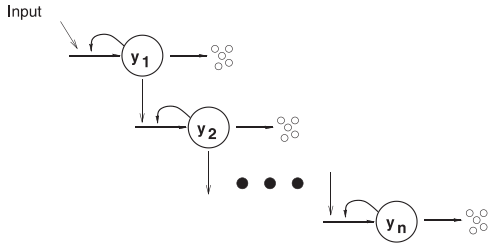

Figure 5.1: A n-element chain of serial connected autocatalytical feedback loops

the features of such positive feedback chains. Besides our G1/S transition model, other examples for such connected circuits exist. Thomas [1998] raised the possibility of such constructs in the context of cell differentiation. As discussed in chapter 4, bistable module governing the B-cell differentiation has been discovered. This and many other examples prove the biological relevance of bistable modules. In contrast, Thomas postulates an easy way to produce multiple cell types by a serial connection of n regulatory genes, each of which exerts a positive control on its own expression. For proper parameter values, each of these genes would be switched on or off independently of the others, so that such a system could define up to 2^n possible cell types, each characterized by the lasting presence or absence of the proteins whose synthesis is regulated by these n genes.

More recently, Tyson and Novak [Tyson et al., 2001] defined the whole yeast cell cycle as a very complex bifurcation diagram of the cdc2/cdc13 dimer activity, an indicator of the state of the control system. The transitions from G1 to S/G2/M and from S/G2 to M are defined as bistable switches.

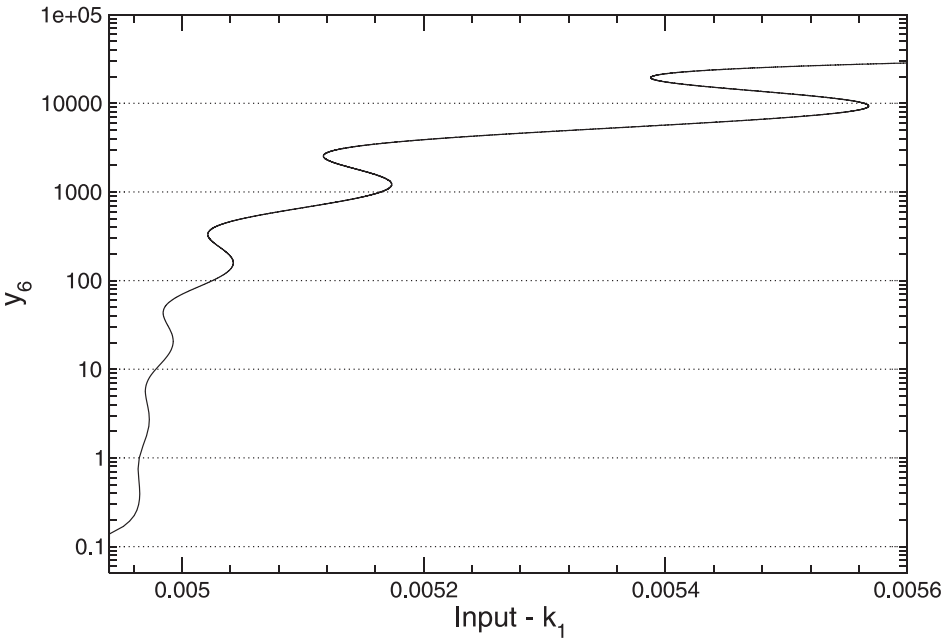

Figure 5.2: Bifurcation diagram of six serially coupled autocatalytical feedback circuits, defined analog to system eqs.(5.1) – (5.3). For certain parameter values seven stable steady states are possible. Each of the saddle node pairs corresponds to one autocatalytical loop. Theoretically, up to 3^6 steady states are possible, see explanation in text.

A straightforward generalization of the above examples and direct implementation of the ideas of Thomas [1998] is illustrated in the following n-element chain of autocatalytical circuits, Fig.5.2, :

$$\frac{dy_1}{dt} = k_1 \frac{a_1 + y_1^2}{b_1 + y_1^2} - \phi_1 y_1 \tag{5.1}$$

$$\frac{dy_2}{dt} = k_2 y_1 \frac{a_2 + y_2^2}{b_2 + y_2^2} - \phi_2 y_2 \tag{5.2}$$

$$\cdots$$

$$\frac{dy_n}{dt} = k_n y_{n-1} \frac{a_n + y_n^2}{b_n + y_n^2} - \phi_n y_n \tag{5.3}$$

The search for the steady states gets very hard, even for small n. As in the example of one autoregulatory module the steady state assumption $F(\underline{y}) = 0$ leads to a polynomial in y_n. For a degree of polynomial larger than

4 there exists no analytical solution for the roots. It means that even for $n = 2$ only numerical solutions are possible as the steady state polynomial of such 2-element chain is of degree 9, as the following discussion shows.

5.3 Double feedback loop

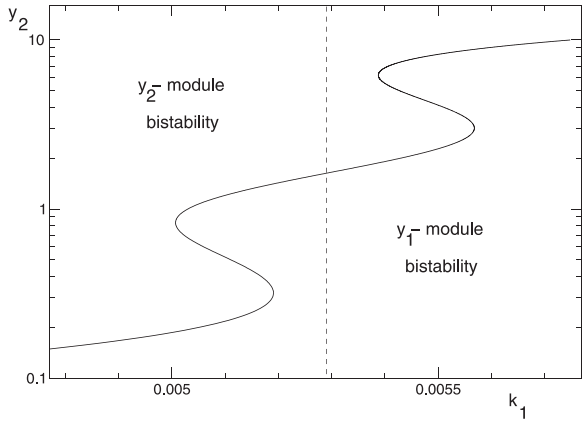

Figure 5.3: Bifurcation diagram for the double feedback module defined by equation system (5.1)–(5.2). The first bistability occurs due to the second module y_2 and the second due to the first y_1 module.

In this section we will discuss a simple module with only two feedback loops. We assume in the following that there is no conservation of the concentrations for both coupled species y_1 and y_2. Identical systems with conservation leads, as will be discussed later, to different results. Lets consider the following description of the 2-element chain described in the equations (5.1) and (5.2).

Such formulation leads for certain values of parameters to the following qualitative picture. Each of the loops result in one bistability. In contrast to the order of loops in the chain, the order of responding bistabilities is reversed, Fig.5.3. Moreover, for a certain range of parameters, the second y_2 module produces bistability while the first y_1 does not. This stimulated the following analysis, which aim was to construct a logical biochemical device. In such a system we should be able to switch singular modules on or off.

If we vary certain parameters of singular modules in such serial connected system, the existence of different numbers and combinations of steady states is, in fact, possible. It can be realized, if we can control behavior of singular

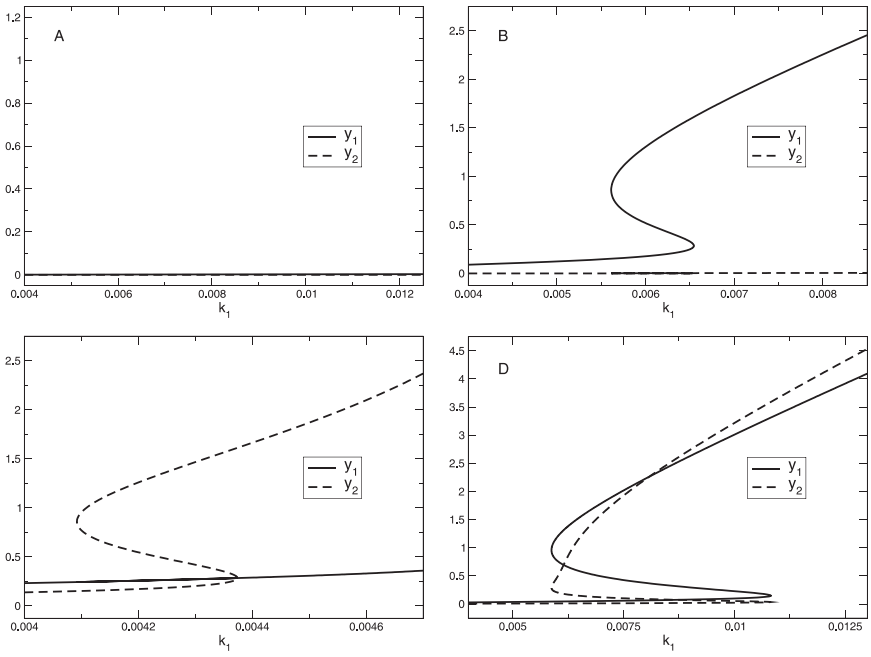

Figure 5.4: Double autocatalytical logic circuit (5.1)–(5.2) with four different 'on' (1) and 'off' (0) combinations. Figures A-D illustrate 0/0, 1/0, 0/1 and 1/1 states respectively. Each of them is achievable by suitable basal expression and degradation rates of responding module element. The parameter values were as follow: $k_2 = 0.023$. A: $a_1 = 0.16$, $a_2 = 0.15$, $\phi_1 = 0.6$, $\phi_2 = 0.1$; B: $a_1 = 0.06$, $a_2 = 0.03$, $\phi_1 = 0.003$, $\phi_2 = 0.3$; C: $a_1 = 0.13$, $a_2 = 0.06$, $\phi_1 = 0.003$, $\phi_2 = 0.003$; D: $a_1 = 0.02$, $a_2 = 0.2$, $\phi_1 = 0.003$, $\phi_2 = 0.02$.

modules by changing their basal expression and degradation rates. With the two feedback loop circuit we are then able to achieve up to 2^2 combinations of steady states y_1 and y_2, illustrated in (Fig.5.4 A-D). The steady state are either off (0) or on (1). This is valid for the simplest case when each loop produces one bistability, defined by eqs. (5.1)–(5.2). We have seen before that in the general case in a two circuits chain up to nine steady states are possible. In this case a n element chain can have up to 2^n steady states, exactly as much as postulated by Thomas [Thomas, 1998] in his model of cell differentiation.

As mentioned above, even a simple two modules system has a surprisingly rich structure and possesses up to 9 steady states. This can be seen after a simple algebraic calculation. We solve the second equation with respect to y_1

and insert it into the first equation. The steady-state polynomial then reads:

$$P_{StSt}^{[9]} = A_0 - A_1 y_2 + A_2 y_2^2 - A_3 y_2^3 + A_4 y_2^4 - A_5 y_2^5 + A_6 y_2^6 - A_7 y_2^7 + A_8 y_2^8 - A_9 y_2^9 \tag{5.4}$$

with the following coefficients $A_n \in \mathbb{R}^+$, $n = 0, \ldots, 9$:

$$\begin{aligned}
A_0 &= a_1 a_2^3 k_1 k_2^3 \\
A_1 &= a_2^2 b_1 b_2 k_2^2 \phi_1 \phi_2 \\
A_2 &= a_2 b_2^2 k_1 k_2 \phi_2^2 + 3 a_1 k_1 k_2^3 a_2^2 \\
A_3 &= a_2^2 b_1 k_2^2 \phi_1 \phi_2 + 2 a_2 b_1 b_2 k_2^2 \phi_1 \phi_2 + b_2^3 \phi_1 \phi_2^3 \\
A_4 &= 2 a_2 b_2 k_1 k_2 \phi_2^2 + b_2^2 k_1 k_2 \phi_2^2 + 3 a_1 a_2 k_1 k_2^3 \\
A_5 &= 2 a_2 b_1 k_2^2 \phi_1 \phi_2 + b_1 b_2 k_2^2 \phi_1 \phi_2 + 3 b_2^2 \phi_1 \phi_2^3 \\
A_6 &= a_2 k_1 k_2 \phi_2^2 + 2 b_2 k_1 k_2 \phi_2^2 + a_1 k_1 k_2^3 \\
A_7 &= b_1 k_2^2 \phi_1 \phi_2 + 3 b_2 \phi_1 \phi_2^3 \\
A_8 &= k_1 k_2 \phi_2^2 \\
A_9 &= \phi_1 \phi_2^3.
\end{aligned}$$

The sign of the coefficients A_i in the resulting polynomial are alternating. Therefore, following the sign rule of Descartes, which is the necessary condition for the existence of the roots of a polynomial, up to nine real positive roots, i.e. up to nine steady states are possible. Unfortunately, there are no analytical methods to derive any sufficient conditions for the existence of a certain number of roots for such a high degree polynomial. However, we can browse through the parameter space to find the interesting parameter sets. In such a way we found a small parameter set corresponding to nine steady states as shown in Fig.5.5. (The Figure was done based on a Matlab script provided by Samuel Bernard.) The calculation was preformed for the special case when $a_2 = 0.005$, $b_1 = b_2 = 1$, $k_2 = 5$ and $\phi_1 = \phi_2 = 1$. a_1 and k_1 were varied between $0.04 - 0.12$ and $1.6 - 2.5$, respectively.

Analog analysis could be done for a higher number of coupled loops. Consequentially, the three autocatalytic loops module is of the degree 27:

$$P_{StSt}^{[27]}(y_3) = A_0 - A_1 y_3 + A_2 y_3^2 - \cdots + A_{26} y_3^{26} - A_{27} y_3^{27}, \quad A_n \in \mathbb{R}^+. \tag{5.5}$$

We print the impressive polynomial in the Appendix C. As in the previous case the signs of the polynomial are alternating, which means that up to 27 steady states of the state variable y_3 are possible.

On the basis of this observations we can derive a rule for the maximal number of steady state in a positive feedback loop: The degree of the resulting steady state polynomial increases according to 3^n, where n is the number of serial connected feedback circuits. The number of steady states is due to

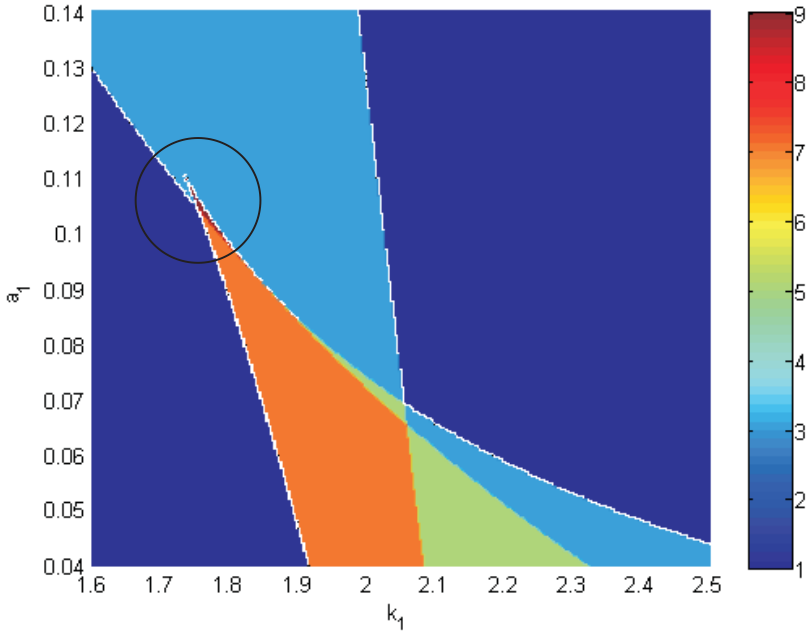

Figure 5.5: Two parameter bifurcation diagram for the double feedback module. Different colors depict different numbers of real positive polynomial roots (see color bar on the right hand side). For a subset of parameters a_1 and k_1 we found nine real positive roots of the polynomial (5.4), i.e. nine stable steady states of the module (dark red triangle-like region inside the circle).

alternating polynomial coefficients signs equal n, $n-2$, ... (according to the Descartes' Rule of Signs, Appendix B).

5.4 Feedback circuits with mass conservation

So far we assumed that each element of the circuit is produced due to the stimulus of the upstream element. However, frequently the total concentrations of entities in signaling cascades are conserved. En example is the MAPK kinase pathway, in which each pathway level consists of inactive and active components. The transition between the two forms happens due to the influence of enzymes such as kinases and phosphatases. Thus, we want to analyze such a system with conserved entities.

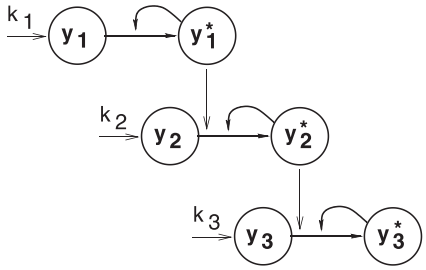

Figure 5.6: Three serial coupled feedback circuits. The preservation of the total concentration of y_i and y_i^*, $i = 1 \ldots 3$, is assumed.

The equation system reads now:

$$\begin{aligned}
\frac{dy_1}{dt} &= k_1 - k_1\, y_1\, \frac{a_1 + (y_1^\star)^2}{b_1 + (y_1^\star)^2} - \phi_1\, y_1 \\
\frac{dy_1^\star}{dt} &= k_1\, y_1\, \frac{a_1 + (y_1^\star)^2}{b_1 + (y_1^\star)^2} - \phi_1\, y_1^\star \\
\frac{dy_2}{dt} &= k_2 - k_2\, y_1\, y_2\, \frac{a_2 + (y_2^\star)^2}{b_2 + (y_2^\star)^2} - \phi_2\, y_2 \\
\frac{dy_2^\star}{dt} &= k_2\, y_1\, y_2\, \frac{a_2 + (y_2^\star)^2}{b_2 + (y_2^\star)^2} - \phi_2\, y_2^\star \\
\frac{dy_3}{dt} &= k_3 - k_3\, y_2\, y_3\, \frac{a_3 + (y_3^\star)^2}{b_3 + (y_3^\star)^2} - \phi_3\, y_3 \\
\frac{dy_3^\star}{dt} &= k_3\, y_2\, y_3\, \frac{a_3 + (y_3^\star)^2}{b_3 + (y_3^\star)^2} - \phi_3\, y_3^\star
\end{aligned}$$

with $y_1 + y_1^\star = 1$, $y_2 + y_2^\star = 1$ und $y_3 + y_3^\star = 1$.

The system reduces therefore to:

$$\frac{dy_1^\star}{dt} = k_1\,(1 - y_1^\star)\, \frac{a_1 + (y_1^\star)^2}{b_1 + (y_1^\star)^2} - \phi_1\, y_1^\star \tag{5.6}$$

$$\frac{dy_2^\star}{dt} = k_2\, y_1^\star\,(1 - y_2^\star)\, \frac{a_2 + (y_2^\star)^2}{b_2 + (y_2^\star)^2} - \phi_2\, y_2^\star \tag{5.7}$$

$$\frac{dy_3^\star}{dt} = k_3\, y_2^\star\,(1 - y_3^\star)\, \frac{a_3 + (y_3^\star)^2}{b_3 + (y_3^\star)^2} - \phi_3\, y_3^\star \tag{5.8}$$

The conservation assumption provides new insight into possible applications of serial connected feedback loops. The comparison of two bifurcation

curves for y_1 and y_2 in Fig.5.7 points to interesting features of the system described by equations (5.6)–(5.8). The first one, illustrated in Fig.5.7, shows the first y_1 and third y_3 module element and omits the second for clarity. Each of them exhibits one or multiple bistabilities, as expected. However, more important is that the first saddle node bifurcation of y_3 happens earlier, for the stimulus equal 0.0023, than the saddle node bifurcation of y_1, which is nearly switched off until 0.0033. In other words, the last submodule achieves the maximum activity while the first one is still far from being switched on.

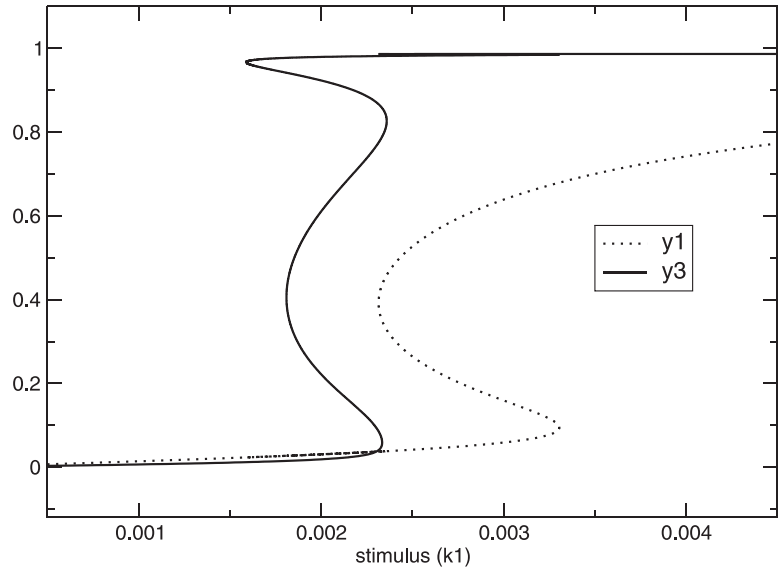

Figure 5.7: Bifurcation diagram of the last of three serial connected feedback loops system, Eqs. (5.6)–(5.8). Interestingly, the full activation of the third submodule described by y_3 appears through a much smaller input signal than the activation of the first submodule y_1.

Yet another characteristic appears useful for practical reasons, not only for biological systems. For the appropriate set of parameters, we constructed a real two level system for the last module (Fig.5.8), i.e. y_3 is fully activated or it remains off. The third submodule, in this case together with the first one, gets switched on, at SN_f, for the stimulus equal 0.035 and can be switched off, at SN_b, if the stimulus is decreased to approx. 0.014. The rectangle-like arms of the hysteresis, i.e. the lowest and the highest steady states, can be approximated we high precision with step functions. In this way the transitions from a low to high state and from high to low state are separated over a large stimulus values range.

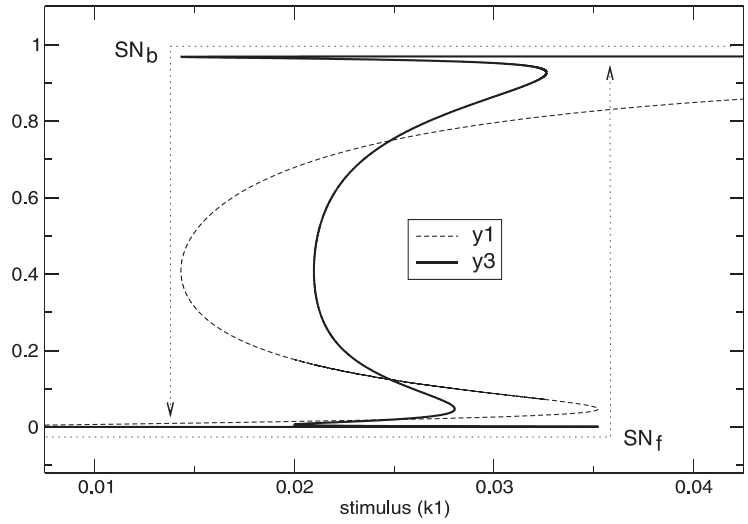

Figure 5.8: The perfect switch. Bifurcation diagram of serial connected feedback loops system with three modules, Eqs.(5.6)–(5.8). Shown are the first, y_1, and the third, y_3, component. The highest and lowest stable steady states of y_3 constitute nearly an ideal switch as function of the stimulus, k_1. In contrast to smooth and round hysteresis arms of y_1, the extreme arms of y_3 are almost horizontal. The step function fits best the y_3-transitions at saddle nodes in forward and backward directions, marked by SN_f and SN_b respectively. Moreover, the transitions from low to high state and vice versa are clearly separated from each other on large stimulus interval.

5.5 Conclusions

Coupled autocatalytical circuits offer new possibilities for modern bioengineering. Moreover, they could help to understand interesting problems like realization of memory modules or efficient signal amplification in biological pathways.

However, experimental realization of coupled modules and the proof of the multiple steady states in such systems will be very difficult. Even simplest single autocatalytical circuits are hard to design and to measure, as the experiments done by Isaacs et al. [2003] show. Major progress requires therefore development and improvement in experimental techniques.

Chapter 6

Model of the G1/S Transition

Summary

Mathematical models of the cell cycle can contribute to an understanding of its basic mechanisms. Modern simulation tools make the analysis of key components and their interactions very effective. This paper focuses on the role of small modules and feedbacks in the gene protein network governing the G1/S transition in mammalian cells. Mutations in this network may lead to uncontrolled cell proliferation. Bifurcation analysis helps to identify the key components of this extremely complex interaction network.

We identify various positive and negative feedback loops in the network controlling the G1/S transition. It is shown that the positive feedback regulation of E2F1 and a double activator inhibitor module can lead to bistability. Extensions of the core module preserve the essential features such as bistability. The complete model exhibits a transcritical bifurcation in addition to bistability. We relate these bifurcations to the Cyclin D activation process and the G1/S phase transition point. Thus, core modules can explain major features of the complex G1/S network and have a robust decision taking function.

6.1 Introduction

There is a number of models on the mammalian G1/S transition, [Novak and Tyson, 2004, Kohn, 1998, Hatzimanikatis et al., 1999, Obeyesekere et al., 1995, 1997, Thron, 1997, Aguda and Tang, 1999, Aguda, 2001, Qu et al., 2003, 2004]. However, one aspect of the G1/S transition remains unanswered. As previously mentioned, large networks, such the one governing the G1/S transition, can be dissected into submodules with well defined functions.

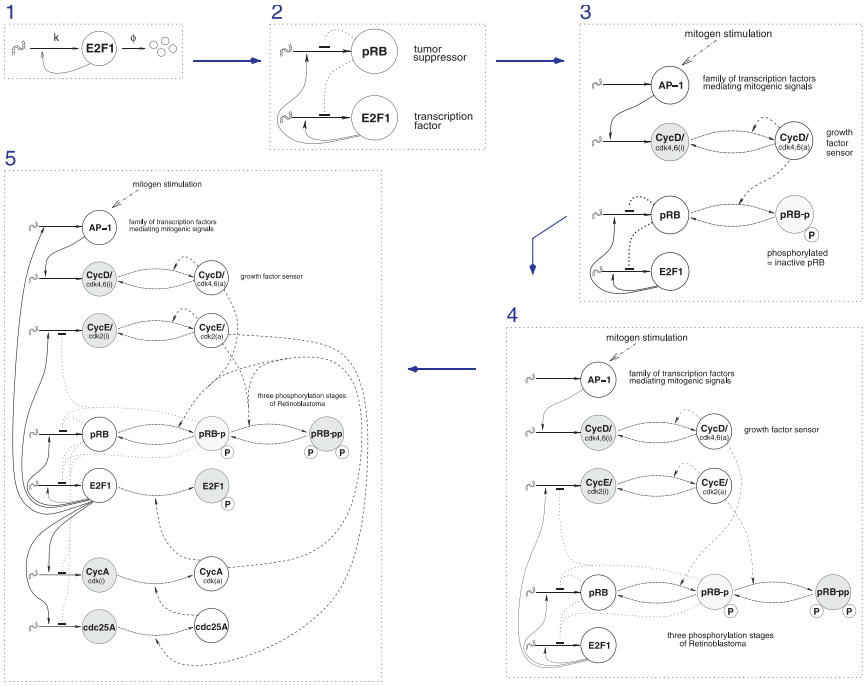

Figure 6.1: Model evolution: from modules to network. We start with a simple autocatalytical E2F1-circuit, couple it with Retinoblastoma, pRB, and get the double activator / double inhibitor module. After that we take the Cyclin D/cdk4,6 activation module into account and yet another pRB phosphorylation complex, Cyclin E/cdk2. The resulting G1/S network can be further enlarged with Cyclin A/cdk2 which shuts down E2F1 via phosphorylation.

Starting with a core module of a network, adding other modules and connecting them together results in a desired system covering the whole functionality. To understand how sets of modules interact in large-scale networks, one needs to decode the quantitative and qualitative role of individual submodules [Isaacs et al., 2003].

As discussed in the introductory biological chapter 1, gene-protein networks governing cell cycle phase transitions are highly complex systems. Whitfield and collegues [Whitfield et al., 2002] performed measurements of gene expression during cell cycle in the HeLa cell line and determined more than 850 periodic genes. 211 genes of these have been assigned as regulated during the G1/S transition. For the purpose of a precise mathematical model,

a simplification and reduction to a reasonable dimension is needed. The current model is based on a simple model proposed by [Kel, 2000], which was based on the common knowledge known about the mammalian cell cycle. We enlarged it and performed detailed bifurcation analysis of the whole system and its subsystems [Swat et al., 2004].

Subsystems containing two or three proteins have well established functions. The first module is responsible for the activation of the growth sensor protein – Cyclin D in complex with cdk4 and cdk6. The second module models the phase transition. We analyzed whether the behavior of the subsystems changed when coupled together and connected with the remaining network elements. As the strong simplified model covers most of the features occurring during G1/S transition, observed in large numbers of different cell types and tissues, we call it the minimal model of the G1/S transition.

More general observation arising from our results is that networks possibly contain decision-taking subunits. Their behavior dominates the whole network in which they are embedded, meaning a qualitative robustness of the dynamics of crucial modules built-in in larger networks.

6.2 Double activator/double inhibitor module

The discussion regarding autocatalytical feedbacks theory (Sec. 4.2) is essential to the dynamics of proteins which activate their own transcription. This model applies to one of the most important protein complexes in the mammalian cells - the E2F1/DP dimer, Sec.2.3. Therefore, the following kinetic equation adapted to this case reads (Sec.4.2, eq.4.6):

$$\frac{d}{dt}[E2F1] = k\frac{a^2 + [E2F1]^2}{K_m^2 + [E2F1]^2} - \phi_{E2F1}\,[E2F1]$$

where [E2F1] stands for the E2F/DP dimers.

As analyzed before, within a certain range of a bifurcation parameter three steady states coexist, whereas outside of this interval only a single steady state exists. This implies that slow varying parameters can induce a sudden jump from low to high concentrations of the transcription factor E2F1.

Interestingly, E2F1 is also a transcription factor for its inhibitor, pRB. This tumor suppressor binds to the E2F/DP complex and causes inhibition of E2F1-induced transcription by masking its activation domain. The knock down of pRB in Hela cells [Whitfield et al., 2002] leads to an extremely fast

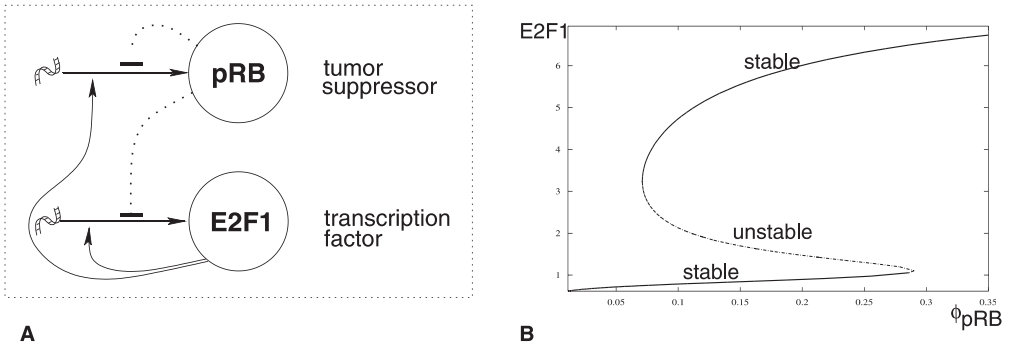

Figure 6.2: **A**) Core double activator/double inhibitor module (DADI) containing the tumor suppressor retinoblastoma pRB and the transcription factor E2F1. **B**) Bifurcation diagram for E2F1; increase of a control parameter, here the degradation rate ϕ_{pRB}, forces the system to jump from a low to a high stable steady state.

proliferation. This underlines the central relevance of the E2F-pRB dynamics for cell cycle progression. Therefore, as a next step of the model development, we consider the coupling with pRB, a major control element at the G1/S transition, governed by phase specific pRB phosphorylation [Sherr and Roberts, 1995]. Since E2F1 is a transcription factor of pRB and E2F1 itself, we find a double inhibition and a double activation (the DA/DI module). The following equations describe such a module (see Fig.6.2):

$$\frac{d}{dt}[pRB] = k_1 \frac{[E2F1]}{K_{m1} + [E2F1]} \frac{J_{11}}{J_{11} + [pRB]} - \phi_{pRB}\,[pRB] \tag{6.1}$$

$$\frac{d}{dt}[E2F1] = k_{ext} + k_2 \frac{a^2 + [E2F1]^2}{K_{m2}^2 + [E2F1]^2} \frac{J_{12}}{J_{12} + [pRB]} - \phi_{E2F1}\,[E2F1] \tag{6.2}$$

In the differential equation for E2F1 an additional constant k_{ext} appears. It is known that other E2F-family members such as E2F2 and E2F3 can stimulate the expression E2F1. The inclusion of the extrinsic expression k_{ext} helps us to omit E2F2 and E2F3 and to restrict the model to pRB and E2F1. The qualitative picture and dynamics will remain the same.

The module (Fig.6.2 A) shows the desired bistability: E2F1 switches pRB off, and jumps to a higher concentration (Fig.6.2 B). The double inhibitor-activator module constitutes a key element of the G1/S network. As a bifurcation parameter we considered the degradation rate of pRB. Different values for the degradation rate of retinoblastoma ϕ_{pRB} result in a shift in position of the pRB nullclines, Fig.6.3. This yields different numbers of cross-points

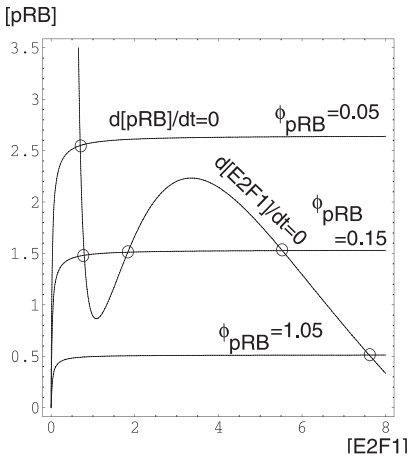

Figure 6.3: The figure shows nullclines of Retinoblastoma and E2F1 and their intersections, which mark steady states of the DA/DI module. See explanation in text.

with the E2F1 nullcline.

If either growth or proliferation signals are present in the cell environment, the expression of a growth factor sensor Cyclin D begins. The cyclin-dependent kinases cdk4,6 as active subunits start to phosphorylate the tumor suppressor pRB. As mentioned above, the duration and strength of the mitogenic signal are the crucial parameters in the stimulation phase. For a sufficient mitogenic signal, phosphorylation of pRB exceeds its dephosphorylation rate, and hence the amount of a phosphorylated less active pRB increases. The E2F/DP transcription complex is released and can activate its targets.

6.3 Cyclin D activation module and growth factors

Consequently, we enlarged the pRB-E2F1 key-module by a Cyclin D activation module. The expression of Cyclin D is the very end of signaling cascades required to conduct growth signals from the extracellular space to the nucleus. First, an external signal has to be received by the cell membrane receptors, which further activates e.g. the Ras/Raf/MEK/ERK pathway [Chang et al., 2003]. ERK activates a transcription factor, c-Jun, which forms complexes with Fos-proteins, called AP-1. In this way, transcription factor AP-1 induces

the G1/S transition (see Fig.6.4).

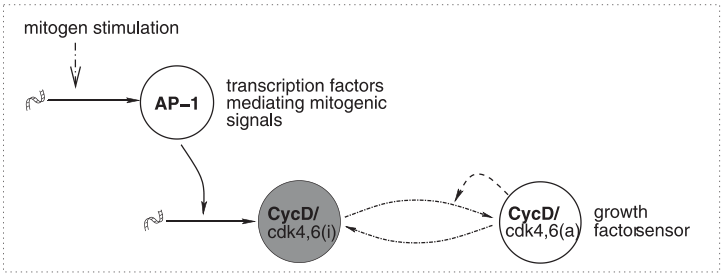

Figure 6.4: Cyclin D/cdk4,6 activation module. Mitogenic stimulation signals are transfered via the MAPK pathway through the cytoplasm to the nucleus where the transcription factor AP-1 induces Cyclin D expression.

The differential equations for this module read:

$$\begin{aligned}
\frac{d}{dt}[CycD_i] &= k_3[AP1] + k_{43}[CycD_a] - k_{34}[CycD_i]\,\frac{[CycD_a]}{K_{m4}+[CycD_a]} \\
&\quad - \phi_{_{CycD_i}}[CycD_i] \qquad (6.3)\\
\frac{d}{dt}[CycD_a] &= k_{34}[CycD_i]\,\frac{[CycD_a]}{K_{m4}+[CycD_a]} - k_{43}[CycD_a] \\
&\quad - \phi_{_{CycD_a}}[CycD_a] \qquad (6.4)\\
\frac{d}{dt}[AP\text{–}1] &= F_m - \phi_{_{AP-1}}[AP\text{–}1] \qquad (6.5)
\end{aligned}$$

with $[CycD_i]$ and $[CycD_a]$ for inactive or active Cyclin D/cdk4,6 complex, respectively. $[AP\text{–}1]$ stands for the transcription factor family AP-1, F_m for the strength of the mitogenic stimulation signal.

The activation of Cyclin D/cdk4,6 is reduced to one step. As discussed in the introductory biological chapter 1, the phosphatase CDC25A is necessary for this activation reaction. Due to the fact that it is activated by Cyclin D/cdk4,6, the autocatalytical loop omitting CDC25A is assumed for simplicity. Even though the structure of the equations is a bit more complicated and the deactivation reaction of Cyclin D is included, the feedback of the Cyclin determines the behavior of the module. The steady state assumption provides the solution with respect to the active form of Cyclin D/cdk4,6:

$$\begin{aligned}
&\mu\,[CycD_a] - [CycD_a]^2 = 0 \qquad (6.6)\\
\text{with} \quad &\mu = \frac{F_m k_3 k_{34} - k_{43}K_{m4}\phi_3\phi_5 - K_{m4}\phi_3\phi_4\phi_5}{k_{43}\phi_3\phi_5 + k_{34}\phi_4\phi_5 + \phi_3\phi_4\phi_5}
\end{aligned}$$

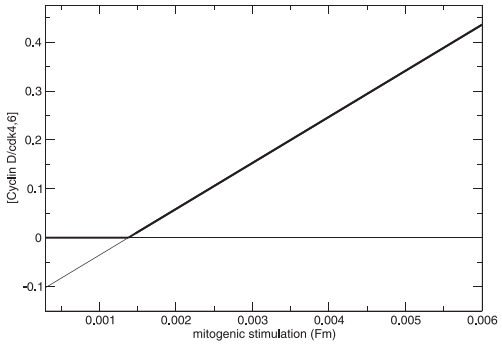

Figure 6.5: Bifurcation diagram of the activation of Cyclin D/cdk4,6 complex. The threshold for activation is marked by the bifurcation point.

It is the expected normal form of a transcritical bifurcation, see equation (4.8), defining the process of Cyclin D activation in dependence of mitogenic stimulation. The bifurcation point is located at

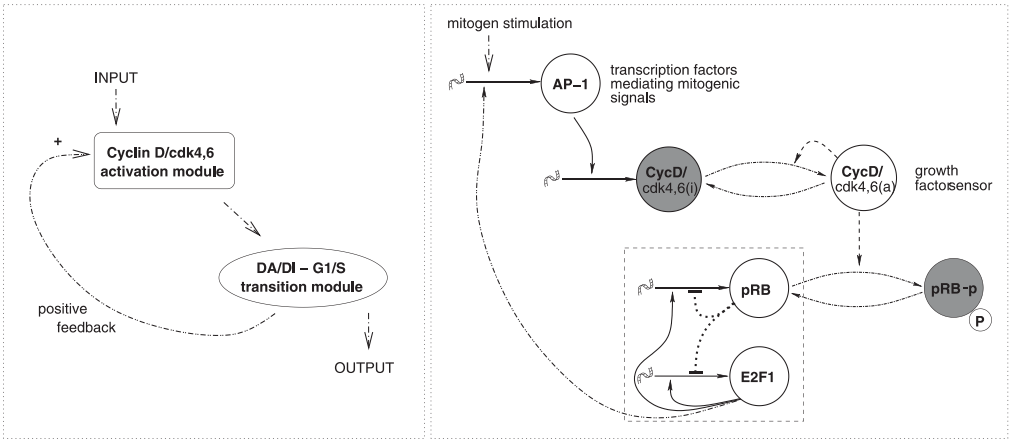

Figure 6.6: Coupling of Cyclin D/cdk4,6 activation module and the double activator/double inhibitor module.

$$F_{m_{TC}} = \frac{K_{m4}\phi_3\phi_5(k_{43} - \phi_4)}{k_3 k_{34}}. \tag{6.7}$$

We are now able to couple the modules and extend the model by the simple wiring of the two small modules (Fig.6.6). The strength of the mitogenic stimulation F_m is now the bifurcation parameter for the joined system. Moreover, we introduce a phosphorylated Retinoblastoma form $\mathrm{pRB_p}$ which

is inactive from the point of view of E2F1 inhibition. The deactivation reaction of Retinoblastoma is achieved by the active Cyclin D/cdk4,6 complex. It is further known that the promoter of the AP-1 transcriptor family contains binding E2F1 sites, giving another positive feedback in the network. Its significance will be discussed later.

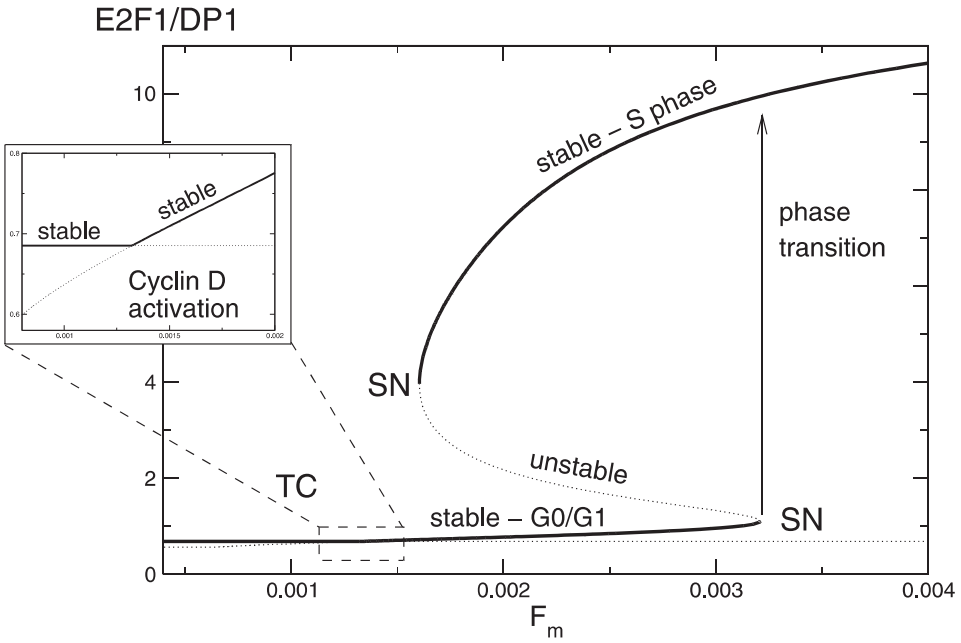

Figure 6.7: Bifurcation diagram of G1/S transition. Transcritical and saddle node bifurcations are shown. The strength of the mitogenic stimulation F_m is the bifurcation parameter.

Next we discuss the bifurcations due to the variation of F_m. Suppose the cell rests in the G0 phase. Until a critical value $F_{m_{crit}}$ of stimulation, there should be no progress in the cell cycle as observed in experiments. In other words, we expect an existence of a threshold value for mitogenic growth and proliferation signals. This is indeed what results from the simulation (see Fig.6.7). A transcritical bifurcation is observed around $F_m = 0.0057$. The stable steady state loses its stability and an unstable one becomes stable. The definition of a restriction point between mid and late G1 as the point of no return does not fully apply to the described situation. The decrease of the control parameter does not lock the non-zero steady state. Therefore, the bifurcation point will be referred to as Cyclin D/cdk4,6 activation threshold.

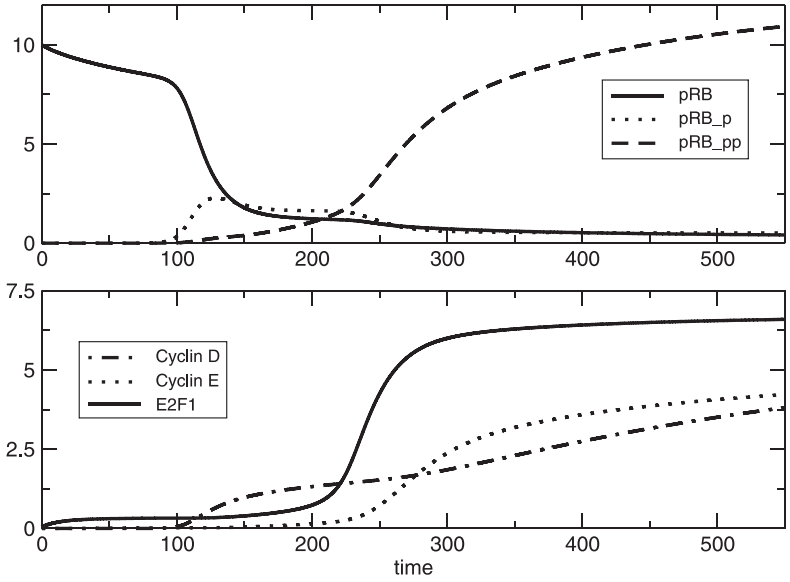

Figure 6.8: Time course of computed protein concentrations for the full G1/S transition model. The applied mitogenic stimulus was sufficient to overcome the saddle node point threshold and was chosen as $F_m = 0.0074$.

A further increase of the stimulation parameter F_m leads to a saddle node bifurcation around $F_m = 0.0074$. This saddle node bifurcation represents the G1/S phase transition associated with a sudden jump of the high E2F/DP complex concentration. Fig.6.8 illustrates the time course as an output from a simulation after a stepwise increase of F_m. The switching behavior of the two antagonists E2F/DP and pRB is apparent.

6.4 Further phosphorylation of Retinoblastoma

In yeast, the G1/S transition is a multi-step process, [Deshaies and Ferrell, 2001, Ferrell, 2001]. The shift from G1 to S phase is blocked by the protein Sic1, which must be phosphorylated at least six times by the Cdc28–Cln complex before it can bind to the Cdc4 protein, be tagged with ubiquitin groups, and destroyed. The process is precisely timed so that the S phase does not happen too early.

Constant		**V**alue
pRB expression	k_1, K_{m1}	1,0.5
pRB inhibition	J_{11}, J_{61}	0.5, 5
pRB (de)phosphorylation	k_{61}, k_{16}	0.3, 0.4
pRB degradation	$\phi_{_{pRB}}$	0.005
$E2F1$ extrinsic production	k_{ext}	0.05
$E2F1$ basal expression	a	0.04
$E2F1$ expression	k_2, K_{m2}	1.6, 4
$E2F1$ inhibition	J_{12}, J_{62}	5, 8
$E2F1$ degradation	$\phi_{_{E2F1}}$	0.1
$CycD_i$ expression	k_3	0.05
$CycD_i$ degradation	$\phi_{_{CycD_i}}$	0.023
$CycD_a$ (de)activation	k_{43}, k_{34}, K_{m4}	0.01, 0.04, 0.3
$CycD_a$ degradation	$\phi_{_{CycD_a}}$	0.03
mitogenic stimulation	F_m	0.001-0.01
AP–1 (de)activation	J_{15}, J_{65}, k_{25}	5, 6, 0.9
AP–1 degradation	$\phi_{_{AP-1}}$	0.01
pRB_p (de)phosphorylation	k_{76}, k_{67}	0.1, 0.7
pRB_{pp} degradation	$\phi_{_{pRB_{pp}}}$	0.04
$CycE_i$ degradation	$\phi_{_{pRB_{pp}}}$	0.04
$CycE_i$ expression	k_{28}	0.06
$CycE_i$ inhibition	J_{18}, J_{68}	0.6, 0.6
$CycE_i$ degradation	$\phi_{_{pRB_{pp}}}$	0.04
$CycE_a$ (de)activation	k_{98}, k_{89}, K_{m9}	0.01, 0.07, 0.005
$CycE_a$ degradation	$\phi_{_{CycE_i}}$	0.05

Table 6.1: The table of parameters of the G1/S model. They were chosen in such a way, that the simulation results reflect the experimentally known features.

$$
\begin{aligned}
\frac{d}{dt}[pRB] &= k_1 \frac{[E2F1]}{K_{m1}+[E2F1]} \frac{J_{11}}{J_{11}+[pRB]} \frac{J_{61}}{J_{61}+[pRB_p]} \\
&\quad - k_{16}[pRB][CycD_a] + k_{61}[pRB_p] - \phi_{_{pRB}}[pRB] \\
\frac{d}{dt}[E2F1] &= k_{ext} + k_2 \frac{a^2+[E2F1]^2}{K_{m2}^2+[E2F1]^2} \frac{J_{12}}{J_{12}+[pRB]} \frac{J_{62}}{J_{62}+[pRB_p]} \\
&\quad - \phi_{_{E2F1}}[E2F1] \\
\frac{d}{dt}[CycD_i] &= k_3[AP1] + k_{43}[CycD_a] - k_{34}[CycD_i] \frac{[CycD_a]}{K_{m4}+[CycD_a]} \\
&\quad - \phi_{_{CycD_i}}[CycD_i] \\
\frac{d}{dt}[CycD_a] &= k_{34}[CycD_i] \frac{[CycD_a]}{K_{m4}+[CycD_a]} - k_{43}[CycD_a] \\
&\quad - \phi_{_{CycD_a}}[CycD_a] \\
\frac{d}{dt}[AP\text{–}1] &= F_m + k_{25}[E2F1] \frac{J_{15}}{J_{15}+[pRB]} \frac{J_{65}}{J_{65}+[pRB_p]} \\
&\quad - \phi_{_{AP\text{–}1}}[AP\text{–}1] \\
\frac{d}{dt}[pRB_p] &= k_{16}[pRB][CycD_a] - k_{61}[pRB_p] - k_{67}[pRB_p][CycE_a] \\
&\quad + k_{76}[pRB_{pp}] - \phi_{_{pRB_p}}[pRB_p] \\
\frac{d}{dt}[pRB_{pp}] &= k_{67}[pRB_p][CycE_a] - k_{76}[pRB_{pp}] - \phi_{_{pRB_{pp}}}[pRB_{pp}] \\
\frac{d}{dt}[CycE_i] &= k_{28}[E2F1] \frac{J_{18}}{J_{18}+[pRB]} \frac{J_{68}}{J_{68}+[pRB_p]} + k_{98}[CycE_a] \\
&\quad - k_{89}[CycE_i] \frac{[CycE_a]}{K_{m9}+[CycE_a]} - \phi_{_{CycE_i}}[CycE_i] \\
\frac{d}{dt}[CycE_a] &= k_{89}[CycE_i] \frac{[CycE_a]}{K_{m9}+[CycE_a]} - k_{98}[CycE_a] \\
&\quad - \phi_{_{CycE_a}}[CycE_a]
\end{aligned}
$$

Table 6.2: The complete ordinary differential equation system for the G1/S model.

The pocket protein and tumor suppressor Retinoblastoma has 16 known phosphorylation sites. We assume now, for simplicity, only one new phosphorylation stage of pRB, the hyper-phosphorylated form pRB_{pp} (Tab.6.2). The phosphorylated form pRB_p is assumed to be the active suppressor of E2F1/DP1, however, with lower efficiency. The first step in the inactivation of pRB is the phosphorylation of Retinoblastoma by Cyclin D/cdk4,6 due to mitogenic signals. The E2F1/DP related expression of Cyclin E constitutes another positive feedback loop.

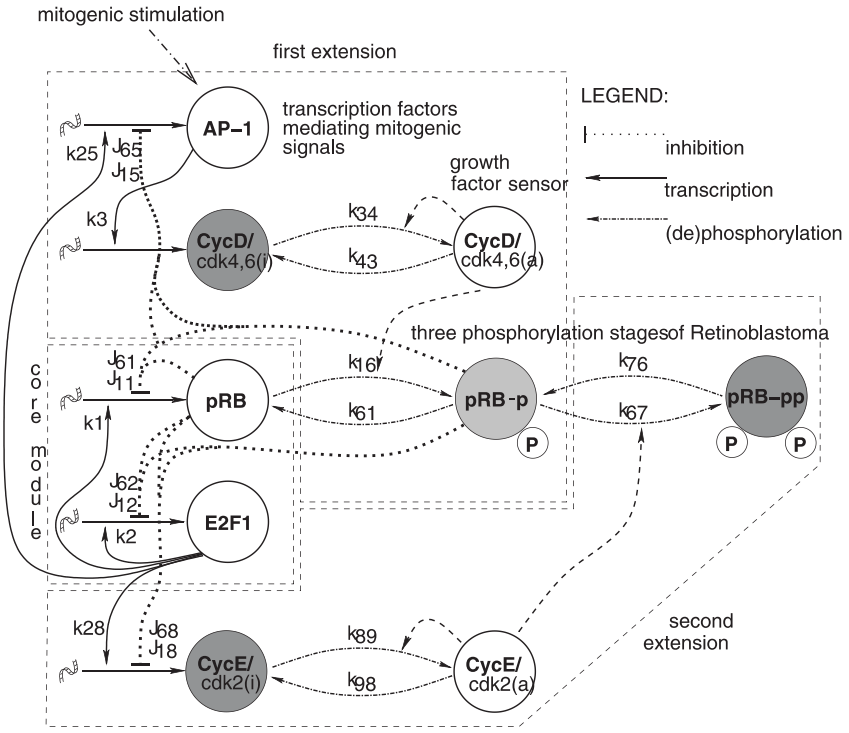

Figure 6.9: The complete schema of the G1/S model. Transition from G0/G1- to S-phase stays under the control and influence of growth factors. The phase-dependent phosphorylation of pRB and E2F1/DP1 is carried out successively by the complexes of cyclins D,E and cyclin-dependent kinases cdk4,6 and cdk2, respectively.

The kinase cdk2, activated by binding with Cyclin E, is responsible for further phosphorylation of pRB. During the activation process, an autocatalytic feedback via phosphorylation of the Cyclin E/cdk2 inhibitor p27 is needed. This is implicitly considered in the present model: the inhibitor

p27 does not appear as a separate variable. We again apply the bifurcation analysis and get the same dynamics as in Fig.6.7. The qualitative behavior of the system remains the same. We observe network robustness regarding the bifurcation scenario: a transcritical bifurcation is followed by bistability.

For the full system with 9 variables, Tab.6.2, 37 parameters were chosen to reflect the experimentally known features, Tab.6.1.

6.5 The influence of feedbacks

Finally, the influence of particular positive feedbacks will be discussed. First we assume different values for the constant K_{m4}, which expresses variable kinetics of the autocatalytic feedback loop of Cyclin D/cdk4,6. For decreasing K_{m4}, representing an enlargement of the positive feedback by more effective substrate binding, the bifurcation thresholds are reduced drastically (Fig.6.10, upper graph). The whole branch with all characteristic points such as saddle nodes and the transcritical bifurcation point is moved. The result confirms the biological observations, that insufficient mitogenic stimulation delays the entry into the cell cycle. This example also illustrates that positive feedbacks can control cell proliferation effectively.

As discussed by [Kel, 2000] E2F1 binding sites are present in the promoter of AP-1. This regulation constitutes another positive feedback (Tab.6.2, rate constant k_{25}). Interestingly, the transcritical bifurcation, i.e. the Cyclin D/cdk4,6 activation is not influenced by this feedback (Fig.6.10, lower graph).

However, the typical S-shape of the bifurcation branch becomes more pronounced. For a strong positive feedback, even with a zero stimulation, two stable steady states exist. This implies irreversibility of the G1/S transition: If E2F1 has reached a high concentration, a removal of the mitogenic signal cannot lead to a return to the G1 phase.

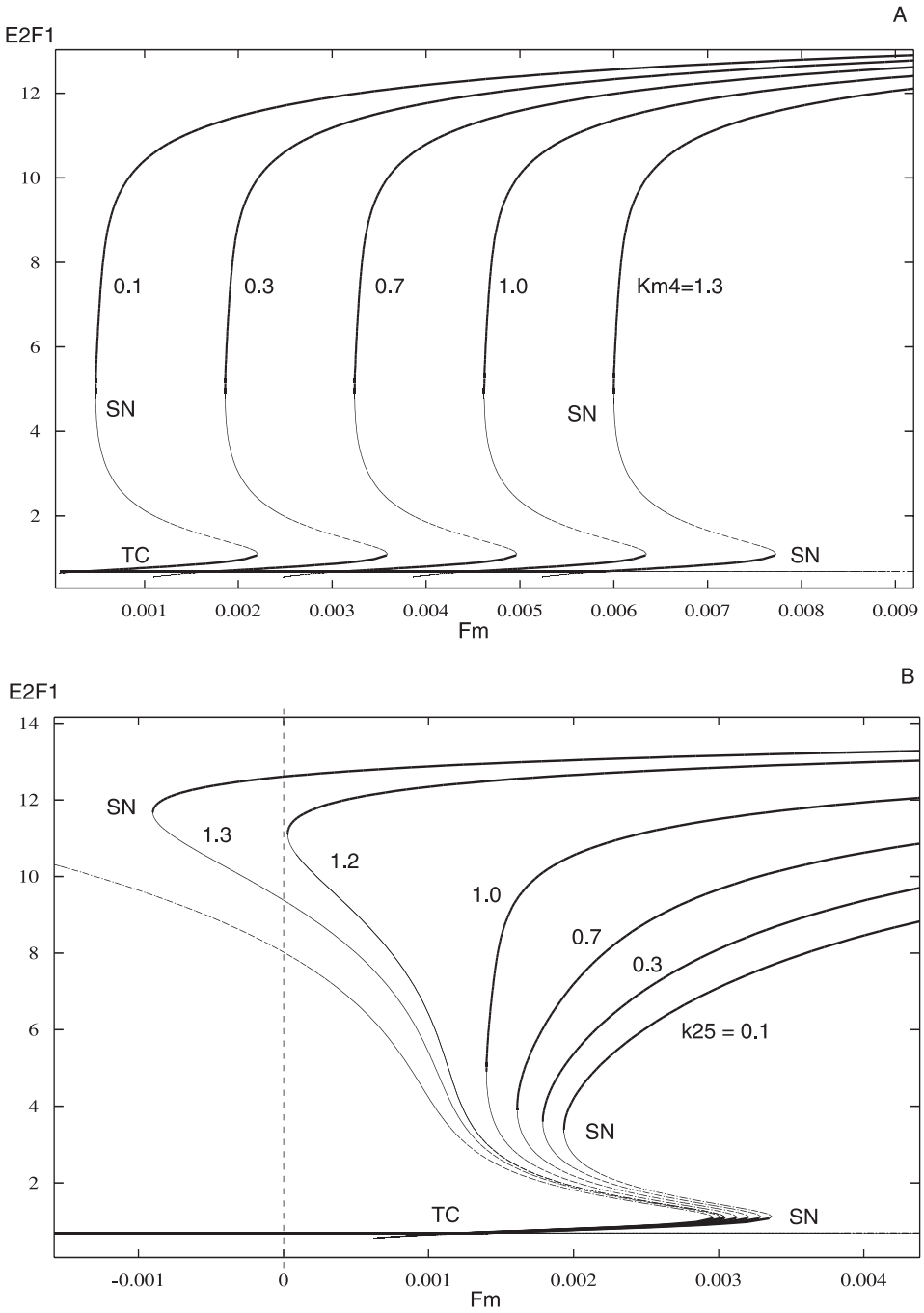

Figure 6.10: Bifurcation diagrams illustrating the role of the feedbacks via Cyclin D auto-activation (A) and AP-1 stimulation via E2F1(B).

6.6 Comparison with experimental data

The aim of models in systems biology is a possibly detailed description of an regulatory system. In order to verify or falsify a model a comparison with experimental data is necessary. Despite the fact that the understanding of the mammalian cell cycle is of eminent importance for modern medicine, only a few detailed models concerning this topic have been published [Novak and Tyson, 2004, Kohn, 1998, Hatzimanikatis et al., 1999, Obeyesekere et al., 1995, 1997, Thron, 1997, Aguda and Tang, 1999, Qu et al., 2003]. The reasons for this situation is the lack of experimental data in form of time series of synchronized cell cultures and the complexity of the process [Kohn, 1999]. None of the publications cited above verified their results with time resolved data from synchronized cell cultures.

Luckily, we entered recently into a collaboration with an experimental group (Kitano Systems Biology Group, Tokyo, Japan). Ongoing experiments will provide us a set of time series measurements on rat 3Y1 fibroblast cells. The synchronization of this cell culture is achieved by contact inhibition and serum starvation with incubation for 48 hr at 37°C. So far, we can use only the results from a single test run done for a few proteins, Fig.6.11. They allow us only a qualitative analysis and comparison with simulated time courses, Fig.6.8. Due to the fact that no replicas of the measurements have been done, no quantitative statements can be drawn.

Measurements after inhibition release have been done every 30 minutes. The cells enter the S phase short after the E2F peak, i.e. ca 2 1/2 hours after block release. After only 4 hours first cells pass the G2/M transition and after it enter a new cell cycle. The decrease in concentration of the hypophosphorylated form of pRB is in accordance with the simulated time course.

More precise statements will be possible in near future due to running experiments which will provide further quantitative results. Time courses with replicas for Cyclin D,E,A, cdk2,4,6, E2F1, total, hypo-, hyperphosphorylated pRB and p27 concentrations will give us the possibility for parameter estimation and model improvement. With measurements of Cyclin A and cdk2 an extension of the described network will be possible. This complex is responsible for the deactivation of E2F1, which happens via phosphorylation of the subunit DP1. After this the phase transition is completed and the cell starts to duplicate its chromosome set.

Another very interesting and unresolved question can be perhaps approached with the ongoing experiments. At least three theories exist regarding the time delay in the expression of Cyclin E and Cyclin A. Although they both are transcriptional targets of E2F1, Cyclin E becomes active ear-

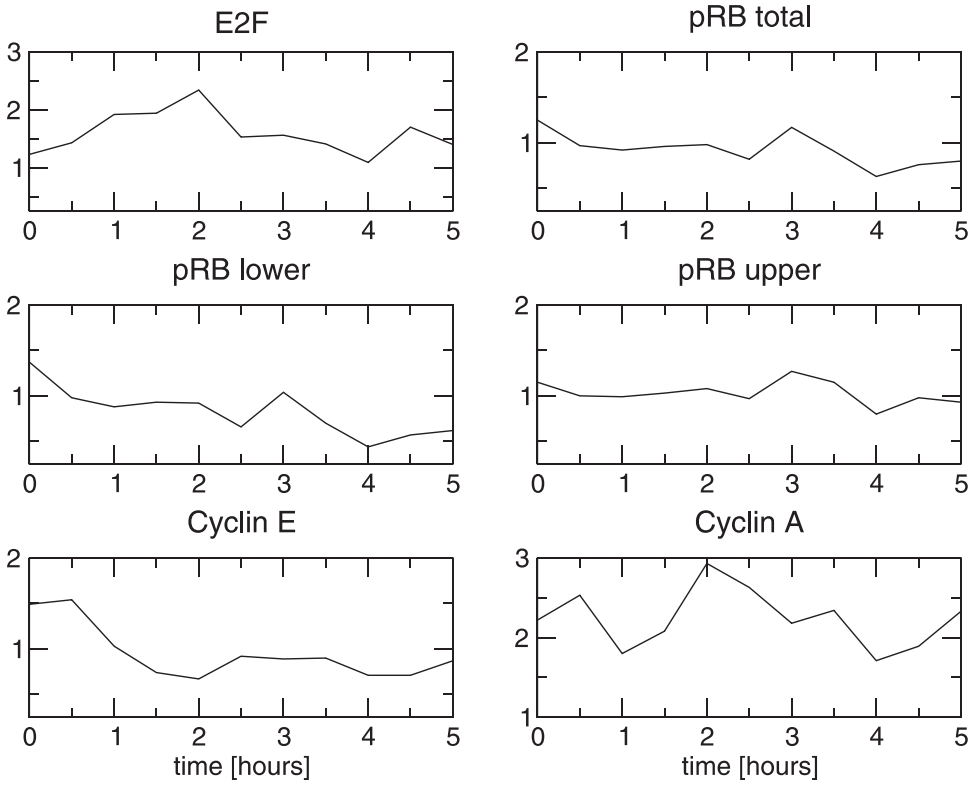

Figure 6.11: Time courses of measured protein levels for the G1/S model as result of a experimental test run without replicas. The phase transition takes place short after the E2F peak, ca. 2 1/2 hours after block release (see discussion in text).

lier than Cyclin A. Zerfass-Thome et al. [1997] showed that Cyclin E/cdk2 in complex with p107/E2F4 dimer is needed for the transcription of Cyclin A what automatically would explain the delay. Another theory is that after first step of phosphorylation of pRB by Cyclin D/cdk4,6 already small amounts of E2F1 are sufficient for Cyclin E expression in contrast to Cyclin A which needs stronger E2F1 signal [Zhang et al., 2000]. The last possibility is that the phosphatase CDC25A, also a transcriptional target of E2F1, which is required for activation of Cyclin A is responsible for the delay [Jinno et al., 1994]. This explanation is supported by the fact that the active complex Cyclin E/cdk2 activates CDC25A [Liu and Greene, 2001].

6.7 Conclusions

We developed a mathematical model describing the G1/S transition of mammalian cells. We show that threshold phenomena (restriction point R) and the G1/S transition can be traced back to core modules. The double activator inhibitor module of the antagonistic players E2F/DP and pRB make up the key unit of this phase transition. It turns out that the dynamics found in this basic system remains preserved in enlarged systems as well. This leads to the conclusion that some crucial elements in a network have a decision taking function. The second main result is a characterization of specific points of the cell cycle.

The Cyclin D/cdk4,6 activation point is associated with a transcritical bifurcation commonly used to describe threshold phenomena. The G1/S transition point is in turn described by a saddle-node bifurcation leading to bistability. Even though most of the parameters are not available yet, basic phenomena such as the described bifurcations are robust features of positive feedback loops [Aguda, 1999, Blüthgen and Herzel, 2003, Novak and Tyson, 2004]. Bifurcation theory can help to identify basic modules in large networks even if kinetic parameters are missing.

Chapter 7

Model of Vav Truncation and Caspase Activation

Summary

The formerly distinct fields of lymphocyte signal transduction and cytoskeletal remodeling have recently become linked, as proteins involved in transducing signals downstream of lymphocyte antigen receptors have also been implicated in actin cytoskeleton remodeling, microtubule dynamics and regulation of cell polarity. These discoveries have fueled interest in understanding the role of the actin cytoskeleton as an integral component of lymphocyte activation. To understand how these complex regulatory networks are wired, we reproduce and simulate this signaling circuits *i*n silico.

It turns out, that crucial features of the system are encoded in small modules, based on the balance interplay between inhibition and positive feedback. The activation threshold is defined by transcritical bifurcation. From the theoretical point of view, there is even more structure in this reduced model, there exist two independent branches of one steady states. Moreover, for certain parameter and initial values subspace, Hopf bifurcation and limit cycle occur.

Finally, due to the similarities with other regulatory systems, new way of classification of biological systems is suggested.

7.1 Introduction

The activation process of T cells constitutes the core of the immunological system response. The recognition of antigenic peptides bound to the major histocompatibility complex (MHC) molecules by the T cell receptor (TCR)

complex is the primary signal for T cell activation. This step is followed by the formation of a tight interface between the T cell and the antigen-presenting cell (APC), referred to as the immunological synapse (IS); [Miletic et al., 2003, Monks et al., 1998, Grakoui et al., 1999]. Studies in a variety of experimental systems have led to the identification of the components of the IS and an understanding of the order of their recruitment and assembly.

During IS formation, surface molecule redistribution and cytoskeletal rearrangement at the T cell APC interface occur in distinct stages: TCR pMHC complexes initially form a ring around a cluster of leukocyte function-associated antigen (LFA)-1 in contact with the integrin inter-cellular adhesion molecule (ICAM)-1, followed by the inversion of this pattern, during which the TCR pMHC relocates to the center and is surrounded by an LFA-1 ICAM-1 ring, in the mature IS.

The onset of signaling triggered by ligand TCR p-SMAC (for peripheral supra-molecular activation complex) formation involves the activation of several protein tyrosine kinases (PTKs), like Lck, and the assembly of the LAT signalosome (Fig.7.2), the mechanism of which is relatively well understood [Tomlinson et al., 2000, Clements et al., 1999, Hornstein et al., 2004].

The actin cytoskeleton is a key component for the organization of the IS and subsequent proper T cell activity. The cytoskeleton is involved both in the molecular movements on the surface of the T cell required for formation of the IS and in the scaffolding of the signaling complexes which promote early receptor-mediated signaling. Because of that, signal transducer proteins that are involved in the control of actin organization, such as Vav1, are expected to participate in such events.

Vav1 can be seen therefore as a pivotal integrator of the complex relationship between IS formation, T cell signaling and the actin cytoskeleton [Hornstein et al., 2004].

7.2 Vav protein family

Rearrangement of the actin cytoskeleton is highly influenced by the activity of Rho family GTPases. Rho GTPases are molecular switches that cycle between two conformational states: a GTP-bound 'active' state and a GDP-bound 'inactive' state. The transition between these two conformations is tightly regulated by three classes of proteins:

- GTPase activating proteins (GAPs) stimulate the intrinsic GTPase activity, thereby pushing the switch towards the inactive state,

- guanine nucleotide dissociation inhibitors (GDIs) keep the GTPase in the GDPbound inactive conformation,
- guanine nucleotide exchange factors (GEFs) facilitate the exchange of GDP for GTP, thus activating Rho GTPases.

The Vav family of proteins is one well-studied family of GEFs for Rho GTPases and includes three conserved members:

- Vav1 – a cell-specific signal transducer has been originally identified as a transforming gene in fibroblasts, expressed exclusively in hematopoietic cells (i.e. cells that give rise to all mature blood cells).
- Vav2, Vav3 – two other Vav-family guanine-nucleotide exchange factors which are widely expressed.

The functional importance of Vav1 was demonstrated in $Vav1^{-/-}$ mice, which show activation defects in T and B lymphocytes, NK cells and T cells, all of which probably result from defects in actin polymerization and impaired phospholipase C (PLC)-g1 regulation.

7.2.1 Vav1 protein domains

Vav proteins are modular and contain the Dbl-homology (DH) domain which is typical of all known Rho-GEFs, in addition to several other structural domains characteristic of proteins involved in signal transduction (Fig.7.1, [Bustelo, 2002, Turner and Billadeau, 2002, Hornstein et al., 2004]). The catalytic specificity of various Vav DH domains has been the subject of intense study. However, the exact specificity towards individual Rho-GTPases in vivo conditions remains elusive. Although the exact mode of regulation of Vav1 in lymphocytes is still unknown, it is thought that the accessibility of its DH domain for the Rho substrates is regulated by tyrosine phosphorylation and involves conformational changes of the amino-terminal auto-inhibitory extension [Aghazadeh et al., 2000].

7.2.2 Vav1 features

Recent experiments uncovered a number of interesting features pointing out the importance of Vav proteins and especially of Vav1. It turned out that the family element Vav1 exists in a long/wild type (p95 Vav1) and short/truncated (p75 Vav1) form. Each of them shows different behavior:

1. the level of Vav1 protein is significantly reduced in extracts from thymocytes undergoing apoptosis,

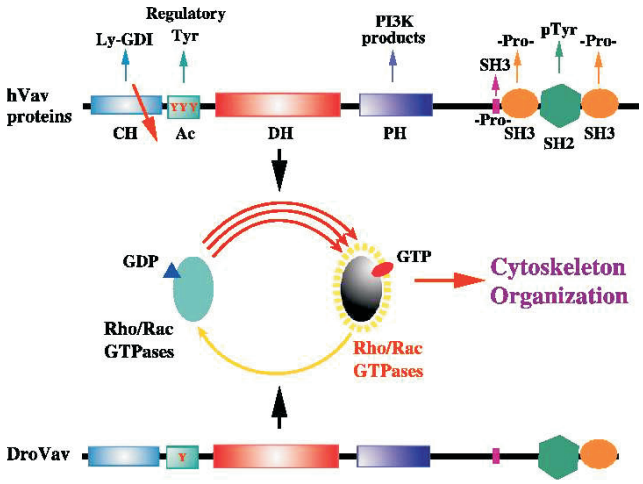

Figure 7.1: Vav1 domains and their role in the reorganization of the cytoskeleton: CH – NFAT stimulation and transforming activity of Vav; Ac – contains three regulatory tyrosines; DH – DBL-homology domain promotes the exchange of GDP for GTP on Rac/Rho GTPases – promotes the cytoskeleton reorganization; PH – binds PI3K enabling it to move to the inner face of the plasma membrane; Pro – enables the binding of Vav proteins to SH3 containing proteins; SH2, SH3 – this region interacts with proteins that contain proline-rich sequences. [Hornstein et al., 2004]

2. the generation of p75 Vav1 was completely eliminated by treatment of cells with a caspase inhibitor,

3. p75 Vav1 has been localized in a different sub-cellular compartment than p95 Vav1,

4. p75 Vav1 was found with the cytoskeleton rather than plasma membrane in thymocytes,

5. the lost N-terminal region of Vav1 – Vav1-D – is essential for normal signaling and distribution inside a cell,

6. expression of Vav1-D effects dramatic changes in the actin cytoskeleton, micro-tubular network and cell morphology.

There are several consequences and conclusions out of these experimental observations which stimulated a hypothetical mathematical model presented in the following.

7.3 Mathematical model of Vav1 truncation and actin remodeling

The aim of the mathematical model was to reproduce the T-cell activation process from the point of view of the signal transducer protein Vav1. Different processes take place during this time (Fig.7.2, I and II) like T-cell receptor reorganization, (see arrow from the peripheral TCR_{p-SMAC} to the central form TCR_{c-SMAC}), activation of Lck and the Signalosome. These active units are indispensable for phosphorylation and subsequently activation of Vav1.

As explained in the previous section, actin reorganization and possibly its

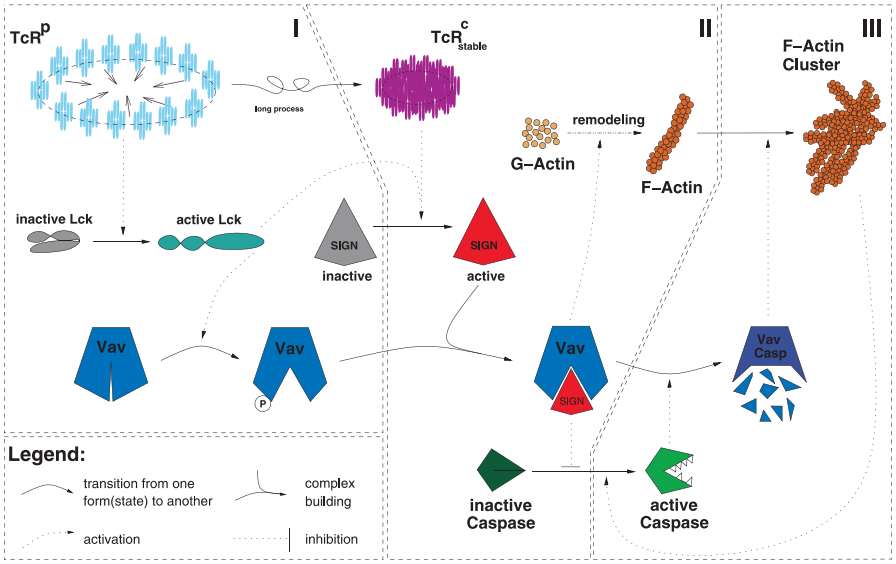

Figure 7.2: The full model of T-cell activation, Vav truncation and caspase activation. Due to long time activation and stabilization of T-cell receptor and presence or absence of extrinsic signals, three stages are separable: I – T-cell activation upon MHC recognition and onset of interface relocation, Lck activation and Vav phosphorylation; II – formation of stable TCR, Signalosome activation; III – Vav remodeling and F-actin clustering in case of an extrinsic caspase activation.

clustering may occur as consequence of extrinsic caspase activation. It is known that caspase activation pathway is a multi-step process [Zheng and Flavell, 2000, Fussenegger et al., 2000] including a number of pro-caspases and caspases. We reduce here the caspase activation for simplicity to Caspase 3,

denoted in their inactive and active states as Casp_I and Casp_A, respectively (Fig.7.2 II and III).

The following set of differential equations describes the behavior of our network, Table7.2. Each equation shows the rate-of-concentration change for each state variable involved in it: T-cell receptor immature (peripheral) form $\text{TCR}_{p\text{–}SMAC}$ and T-cell receptor mature (central) form $\text{TCR}_{c\text{–}SMAC}$, four states of Vav, the active form of tyrosine kinase, Lck_A, and Signalosome *Sign*. *F−actin* stands for the filamentous actin, *Cluster* for its clustered aggregates.

Constant		**V**alue
Stimulus	F_{APC}	0.1
TCR remodeling	$k_{p\rightarrow c}$	0.004
$TCR_{p\text{–}SMAC}$ degradation	ϕ_p	0.1
$TCR_{c\text{–}SMAC}$ degradation	ϕ_c	1×10^{-4}
Lck activation	k_{Lck}	0.05
Lck degradation	ϕ_{Lck_A}	0.05
Signalosome activation	k_{Sign}	0.12
Signalosome degradation	ϕ_{Sign}	0.01
Vav_{+P} activation	$k_{Vav_{+P}}$	0.45
Vav_{Sign} complex building	$k_{Vav_{Sign}}$	0.4
Vav_{Casp} production	$k_{Vav_{Casp}}$	0.25
F–actin production	k_{Act}	0.06
F–actin degradation	$\phi_{F\text{–}actin}$	0.01
F–actin cluster synthesis	$k_{Cluster}$	0.5
F–actin cluster synthesis	$J_{F\text{–}actin}$	0.1
F–actin cluster degradation	$\phi_{Cluster}$	1×10^{-5}
$Casp_I$ production	k_{Pcasp_I}	0.025
$Casp_I$ degradation	ϕ_{Casp_I}	0.04
$Casp_A$ activation	k_{Casp}	0.28
$Casp_A$ inhibition	$J_{Vav_{Sign}}$	1
$Casp_A$ degradation	ϕ_{Casp_A}	0.01

Table 7.1: Parameter used for the simulations of the full Vav1 model defined by equations in Tab.7.2.

All equations with one exception contain simple linear and bilinear kinetics. The clustering is formulated as the Michael-Menten rate law. The stimulation signal has a constant value and a certain duration (t_{TCR}) defined as follows:

$$F_{APC}(t) = \begin{cases} F_{APC} & \text{if} \quad t < t_{TCR} \\ 0 & \text{else} \end{cases} \tag{7.1}$$

$$
\begin{aligned}
\frac{d[TCR_{p\text{–}SMAC}]}{dt} &= F_{APC}(t) - k_{p\to c}\,[TCR_{p\text{–}SMAC}]\,(1+[F\text{–}actin]) \\
&\quad -\phi_p\,[TCR_{p\text{–}SMAC}] \\
\frac{d[TCR_{c\text{–}SMAC}]}{dt} &= k_{p\to c}\,[TCR_{p\text{–}SMAC}]\,(1+[F\text{–}actin]) - \phi_c\,[TCR_{c\text{–}SMAC}] \\
\frac{d[Lck_A]}{dt} &= k_{Lck}\,[TCR_{p\text{–}SMAC}]\; - \phi_{Lck_A}[Lck_A] \\
\frac{d[Sign]}{dt} &= k_{Sign}\,[Lck_A]\,[TCR_{c\text{–}SMAC}]\; - k_{Vav_{+P}}\,[Vav_{-P}]\,[Lck_A] \\
&\quad -\phi_{Sign}[Sign] \\
\frac{d[Vav_{-P}]}{dt} &= -k_{Vav_{+P}}\,[Vav_{-P}]\,[Lck_A] \\
\frac{d[Vav_{+P}]}{dt} &= k_{Vav_{+P}}\,[Vav_{-P}]\,[Lck_A] - k_{Vav_{Sign}}\,[Vav_{+P}]\,[Sign] \\
\frac{d[Vav_{Sign}]}{dt} &= k_{Vav_{Sign}}\,[Vav_{+P}]\,[Sign] - k_{Vav_{Casp}}\,[Casp_A]\,[Vav_{Sign}] \\
\frac{d[Vav_{Casp}]}{dt} &= k_{Vav_{Casp}}\,[Casp_A]\,[Vav_{Sign}] \\
\frac{d[F\text{–}actin]}{dt} &= k_{Act}\,[Vav_{Sign}] - k_{Cluster}\,[Vav_{Casp}]\,\frac{[F\text{–}actin]}{J_{F\text{–}actin}+[F\text{–}actin]} \\
&\quad -\phi_{F\text{–}actin}\,[F\text{–}actin] \\
\frac{d[Cluster]}{dt} &= k_{Cluster}\,[Vav_{Casp}]\,\frac{[F\text{–}actin]}{J_{F\text{–}actin}+[F\text{–}actin]} - \phi_{Cluster}\,[Cluster] \\
\frac{d[Casp_I]}{dt} &= k_{Pcasp_I} - \frac{k_{Casp}\,[Cluster]\,[Casp_I]}{J_{Vav_{Sign}}+[Vav_{Sign}]} - \phi_{Casp_I}\,[Casp_I] \\
\frac{d[Casp_A]}{dt} &= \frac{k_{Casp}\,[Cluster]\,[Casp_I]}{J_{Vav_{Sign}}+[Vav_{Sign}]} - \phi_{Casp_A}\,[Casp_A]
\end{aligned}
$$

Table 7.2: Equations for the full system

The total concentration of Vav is assumed to be constant, i.e.:

$$[Vav_{-P}] + [Vav_{+P}] + [Vav_{Sign}] + [Vav_{Casp}] = 1.$$

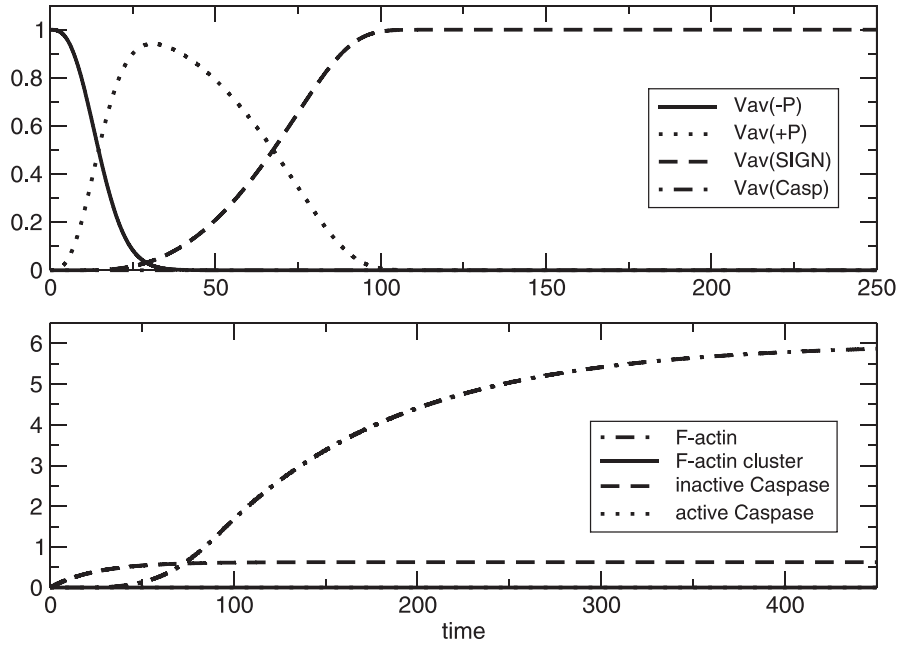

Figure 7.3: Vav1 complete model time course without extrinsic caspase activation defined by the equations set from Tab.7.2 using the parameters in Tab.7.1.

The actin cytoskeleton is a key component for the proper T cell activity. Therefore, signal transducer proteins that are involved in the control of actin organization, such as Vav1, are expected to participate in events like remodeling of actin. The model shown in Fig.7.2 represents the main features of the Vav1 regulation in the process of actin remodeling. In the default situation and after the activation of full length Vav1, this protein works as a signal transducer in some signaling pathways like activation of lymphocytes T and proliferation. Although a small amount of activated caspase and actin aggregates is present in the cell, the inhibitory influence of full length Vav1 is strong enough to keep it under control. Full length protein Vav1 prevails the competition, Fig.7.3. The balance remains on the site of full length Vav, Vav_{Sign}, F-actin unclustered form, *F–actin*, and deactivated Caspase, $Casp_I$.

However, under some special conditions like apoptotic events or extrinsic signals, the caspase pathway gets activated, Fig.7.4. The balance is now on

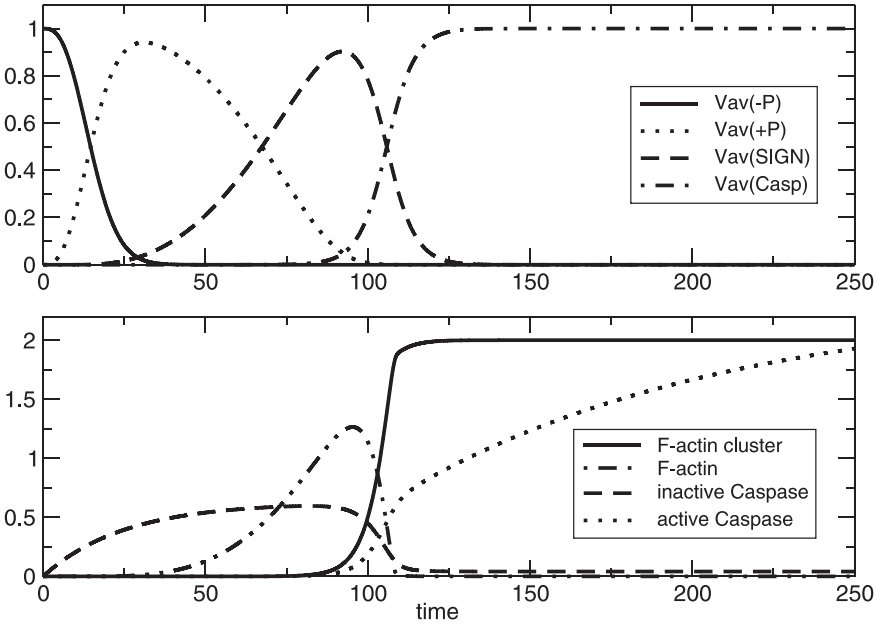

Figure 7.4: The time courses for the complete Vav1 model with extrinsic caspase activation defined by the equations set from Tab.7.2 using the parameters in Tab.7.1.

the side of truncated Vav1 form, Vav_{Casp}, clusters of F-actin, $Cluster$, and activated Caspase, $Casp_A$.

The simulation of a reduced model of Vav1 truncation (Sec.7.4) shows that beyond a certain critical value of caspase activation the balance is shifted toward truncated Vav1 form and active caspase. Former experimental results indicate a close relation between the process of Vav1 truncation and enhanced caspase activation [Miletic et al., 2003]. A possible scenario for the form of the positive feedback is that cytoskeleton remodeling is positively effected by truncated form of Vav1. This results in actin aggregation.

7.3.1 Similarities with other biological systems

The aggregation of F-actin in the presented model surprisingly resembles the Huntingtin aggregation observed in the neuro-degenerative disease Huntington (HT) [Wanker, 2000, Sieradzan and Mann, 2001, Temussi et al., 2003]. A mutated Huntington gene coding for the Huntingtin protein (Htt) contains 40 or more glutamine repeats, which are characteristic for polyglutamine expansion disorders. Because glutamine is polar, Htt molecules stick to one

another and form strands called protein aggregates (clusters). As in our case, the Huntingtin protein clusters activate eventually a caspase pathway. Due to the fact that Htt is cleaved by a number of different proteases, including some caspases, and the fact that cleaved Htt accelerates the clustering process, a positive feedback evolves. Although the clustering mechanism of F-actin is still unclear, major precesses involved in Vav1 and Huntingtin truncation are analog.

Another example including truncation of a functional protein in connection with caspase pathway activation is found in B-cells. The effector caspase 3 appears in a full and a truncated from. The emergence of the short form, caused by caspase 8, is a marker for the all-or-non response toward germinal center B-cell apoptosis. Short form of the effector caspase 3 stimulates activation of caspase 8, closing the positive feedback loop [Hennino et al., 2001, van Eijk et al., 2001].

All together, it seems that one simple mathematical model explaining the main features of an underlying biological network can be applied with minor changes to different systems. Such modules like the present one and the autocatalytical circuits shown in chapter 4, constitute an opportunity for a classification of biological systems. This approach could be a powerful systems biology tool towards understanding biological problems from the point of view of network structure.

7.4 Minimal Vav1 model

We have seen in many examples that main system features are often encoded in small modules. This is also the case for the model of Vav1 truncation. Therefore, a detailed analysis has been performed for a reduced network (Fig.7.5) modeled by three differential equations 7.2. We drop the assumption of constant total Vav concentration and define linear degradation of all three module components. This has important consequences.

In the following we will use a simplified notation, as in Fig.7.5: y_1, y_2 and y_3 for $[Casp_A]$, $[Vav_{Sign}]$ and $[Vav_{Casp}]$ respectively.

$$\begin{aligned} \frac{y_1}{dt} &= k_C \frac{y_3}{J + y_2} - \phi_{Casp}\, y_1 \\ \frac{y_2}{dt} &= k_V - k_{SC}\, y_1\, y_2 - \phi_S\, y_2 \\ \frac{y_3}{dt} &= k_{SC}\, y_1\, y_2 - \phi_C\, y_3 \end{aligned} \tag{7.2}$$

In this form one can convince oneself, how simple the minimal system

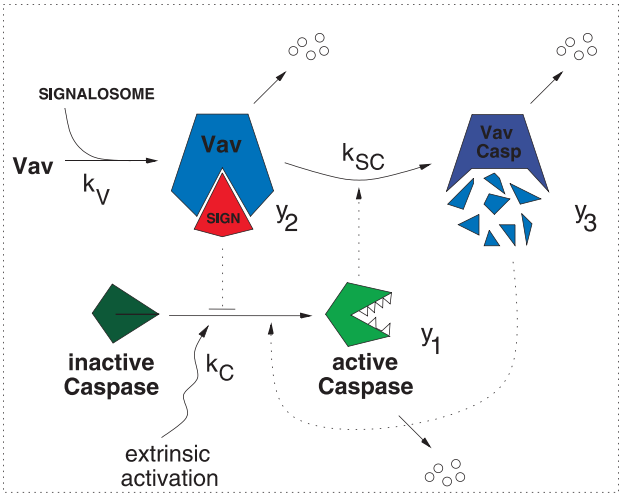

Figure 7.5: The minimal model of Vav truncation and caspase activation. Instead of F-actin clusters, the truncated Vav form Vav_{Casp} stimulates the caspase activation. Beside Vav activation the extrinsic caspase activation k_V is an important input variable. Now, linear degradation of all three proteins is assumed.

is. This observation will even more meaningful, at the sight of the complex solution structure. The simulations were done with following parameters: $k_C = 0.01, k_V = 0.04, k_{SC} = 0.02, J = 3, \phi_{Casp} = 2\phi_S = 2\phi_C = 0.04$.

The behavior of the minimal system is determined mainly by the positive feedback from the truncated Vav1 form Vav_{Casp} and its cytoskeleton remodeling ability. We omit the processes of F-actin clustering and the possible activation of caspase pathway by these clusters. Beside Vav1 activation, expressed now by production term k_V, the caspase activation k_C is the second important input variable, it can be regulated with good precision as ongoing experiments show. Its value will serve as the control parameter in the detailed bifurcation analysis.

Assuming steady state, we eliminate variables y_2 and y_3 from the equation system (7.2) and obtain an equation for y_1. The result is the normal form for the transcritical bifurcation, i.e. the equation reads

$$\frac{J\phi_{Casp}\phi_S\phi_C - k_V(k_C k_{SC} - \phi_{Casp}\phi_C)}{Jk_{SC}\phi_{Casp}\phi_C}\, y_1 - y_1^2 = 0. \tag{7.3}$$

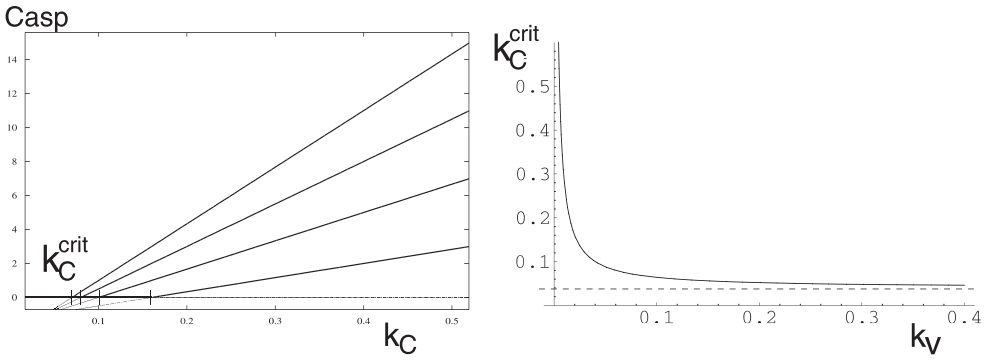

Figure 7.6: A) Different k_V values result in change of the transcritical bifurcation point k_C^{crit}. B) There exists a lower bound of the bifurcation point as function of k_V, Eq.7.4.

The transcritical bifurcation occurs at $y_{1_{crit}}$ (Fig.7.6)

$$k_C^{crit} = \frac{\phi_{Casp}\phi_C(J\phi_S + k_V)}{k_V k_{SC}}$$

Since we assume degradation of the two Vav1 forms, nonzero values for caspase activation do not lead to immediate and irreversible Vav1 truncation in contrast to the full Vav model. There is a lower bound of the bifurcation point as function of k_V, Eq.7.4. Once the caspase activation is increased over a certain threshold the truncation of Vav1 happens much faster moving the balance to the short Vav1 form. The lower bound of caspase activation is plotted in Fig.7.6B.

7.5 Stability analysis for the minimal model

Independent of the context, our model, 7.2, can be regarded as case model for processes involving aggregation stimulated caspase activation, see Section7.3.1. Thus, it is of theoretical interest to explore the complete range of dynamical behavior even though variables might be negative. Of particular interest is the coexistence of transcritical and Hopf bifurcation in such a relatively simple model.

Dependent on the initial conditions we observed oscillations in our simulations. Stimulated by this observation we performed a detailed stability analysis, leading to some unexpected findings. There exist two unconnected branches of the second steady state, y_{S_2}.

The steady states of the system read

$$y_{S_1} = \Big(0, \frac{k_V}{\phi_2}, 0\Big) \quad and \quad y_{S_2} = \Big(\frac{D}{k_{SC}F}, \frac{F}{E}, \frac{D}{\phi_C E}\Big) \tag{7.4}$$

were

$$\begin{aligned} D &= k_C k_V k_{SC} - \phi_{Casp}\phi_C k_V - \phi_{Casp}\phi_S\phi_C J, \\ E &= k_C k_{SC} - \phi_{Casp}\phi_C, \qquad F = \phi_{Casp}\phi_C J. \end{aligned}$$

The steady state y_{S_1} is always positive or zero. The steady state y_{S_2} is positive if following component-wise inequalities hold

$$\begin{aligned} y_{S_{1,1}} > 0 \qquad & \text{if} \quad k_C > \frac{\phi_{Casp}\phi_C}{k_{SC}k_V}(J\phi_S + k_V) =: k_{C_1} \\ y_{S_{1,2}} > 0 \qquad & \text{if} \quad k_C > \frac{\phi_{Casp}\phi_C}{k_{SC}} =: k_{C_0} \\ y_{S_{1,3}} > 0 \qquad & \text{if} \quad k_C > k_{C_1} \;\&\; k_C > k_{C_0} \end{aligned}$$

These two steady state branches will be analyzed in the following, separately and in more detail.

Steady state y_{S_1}

The Jacobi matrix at the steady state y_{S_1} reads

$$J|_{y_{S_1}} = \begin{pmatrix} -\phi_{Casp} & 0 & \frac{k_C\phi_S}{k_V + J\phi_S} \\ -\frac{k_{SC}k_V}{\phi_S} & -\phi_S & 0 \\ \frac{k_{SC}k_V}{\phi_S} & 0 & -\phi_C \end{pmatrix} \tag{7.5}$$

In order to make statements about the steady state we use the Hurwitz criterion (see Appendix A), which provides sufficient conditions for their stability:

$$\begin{aligned} det(J - \lambda\mathbf{I}) &= \begin{vmatrix} -\phi_{Casp} - \lambda & 0 & \frac{k_C\phi_S}{k_V + J\phi_S} \\ -\frac{k_{SC}k_V}{\phi_S} & -\phi_S - \lambda & 0 \\ \frac{k_{SC}k_V}{\phi_S} & 0 & -\phi_C - \lambda \end{vmatrix} = \\ &= \lambda^3 + (\phi_{Casp} + \phi_S + \phi_C)\lambda^2 \\ &\quad + \Big(\phi_{Casp}\phi_S + \phi_{Casp}\phi_C + \phi_S\phi_C - \frac{k_C k_{SC} k_V}{k_V + J\phi_S}\Big)\lambda \\ &\quad + \Big(\phi_{Casp}\phi_S\phi_C - \frac{k_C k_{SC} k_V}{k_V + J\phi_S}\phi_S\Big) = a_0\lambda^3 + a_1\lambda^2 + a_2\lambda + a_3 \stackrel{!}{=} 0 \end{aligned}$$

Application of the criterion leads to following inequalities:

$$
\begin{aligned}
D_1 &:= a_1 = \phi_{Casp} + \phi_S + \phi_C \overset{!}{>} 0, \\
D_2 &:= \begin{vmatrix} \phi_{Casp} + \phi_S + \phi_C & 1 \\ \phi_{Casp}\phi_S\phi_C - \frac{k_C k_{SC} k_V}{k_V + J\phi_S}\phi_S & \left(\phi_{Casp}\phi_S + \phi_{Casp}\phi_C + \phi_S\phi_C - \frac{k_C k_{SC} k_V}{k_V + J\phi_S}\right) \end{vmatrix} \\
&= \phi_{Casp}^2(\phi_S + \phi_C) + \phi_S^2(\phi_{Casp} + \phi_C) + \phi_C^2(\phi_{Casp} + \phi_S) \\
&\quad + \phi_{Casp}\phi_S\phi_C - \frac{k_C k_{SC} k_V}{k_V + J\phi_S}(\phi_{Casp} + \phi_C) \\
&\quad (with\ \phi_{Casp} = 2\phi_S = 2\phi_C = 2\phi) \\
&\Rightarrow \quad k_C < \frac{6\phi^2(k_V + J\phi)}{k_{SC}k_V}, \\
D_3 &:= \begin{vmatrix} a_1 & 1 & 0 \\ a_3 & a_2 & a_1 \\ 0 & 0 & a_3 \end{vmatrix} \overset{!}{>} 0 \equiv a_3 \overset{!}{>} 0 \ \ since \ \ D_n = D_{n-1}\, a_n \\
&\Rightarrow \quad a_3 = \phi^3 - \frac{k_C k_{SC} k_V}{k_V + J\phi}\phi \overset{!}{>} 0 \Rightarrow k_C < \frac{2\phi^2(k_V + J\phi)}{k_{SC}k_V}.
\end{aligned}
$$

$$
\boxed{\text{The steady state } y_{S_1} \text{ is stable if } k_C < \tfrac{2\phi^2(k_V + J\phi)}{k_{SC}k_V}} \tag{7.6}
$$

Eigenvalues

$$
\begin{aligned}
det(J - \lambda\mathbf{I}) &= \begin{vmatrix} -2\phi - \lambda & 0 & \frac{k_C\phi}{k_V + J\phi} \\ -\frac{k_{SC}k_V}{\phi} & -\phi - \lambda & 0 \\ \frac{k_{SC}k_V}{\phi} & 0 & -\phi - \lambda \end{vmatrix} \overset{!}{=} 0 \\
&\Leftrightarrow \quad -(2\phi + \lambda)(\phi + \lambda)(\phi + \lambda) + \frac{k_C k_{SC} k_V}{k_V + J\phi}(\phi + \lambda) \overset{!}{=} 0 \\
&\Rightarrow \quad \boxed{\lambda_1 = -\phi}, \\
&\quad \lambda^2 + 3\phi\lambda + 2\phi^2 - \frac{k_C k_{SC} k_V}{k_V + J\phi} = 0 \\
&\Rightarrow \quad \boxed{\lambda_{2/3} = -\tfrac{3\phi}{2} \pm \sqrt{\tfrac{9\phi^2}{4} + \tfrac{k_C k_{SC} k_V}{k_V + J\phi}}}.
\end{aligned}
$$

The free term of the quadratic equation is smaller than zero if $k_C > \frac{2\phi^2(k_V + J\phi)}{k_{SC}k_V}$. From the Descarte's rule of signs follows that the quadratic equation has one real negative and one real positive solution[1]. For the opposite case, if

[1]The sign of the coefficients of the equation $\lambda^2 + A\lambda + B = 0$ with $B < 0$, changes once which means that there exist one real positive solution. For $\lambda = -\omega$ the sign of the

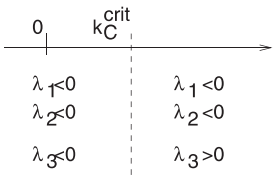

Figure 7.7: Dependence of the eigenvalues with respect to the caspase activation constant k_C (for $\phi_{Casp} = 2\phi_S = 2\phi_C = 2\phi$). All three eigenvalues are negative, i.e. the steady state is stable, when condition (7.6) holds.

$k_C < \frac{2\phi^2(k_V+J\phi)}{k_{SC}k_V}$ the free term of the last equation is bigger than zero. The Descarte's rule of signs says that there are no real positive solutions. However, there exit two or non real negative solutions.

Eigenvectors

$$\lambda_{1_{S_1}} = \{0, 1, 0\}$$
$$\lambda_{2,3_{S_1}} = \Big\{ -\frac{\phi}{2k_{SC}k_V}\Big[\phi \pm \sqrt{4k_c k_{SC} k_v + \phi^2(k_V + J\phi)}\Big], -1, 1\Big\}$$

The eigenvectors of the steady state y_{S_1} are always real.

Steady state y_{S_2}

The steady state y_{S_2} covers more interesting features. Whereas one eigenvalue is always real, two remaining steady states are for certain parameter range complex.

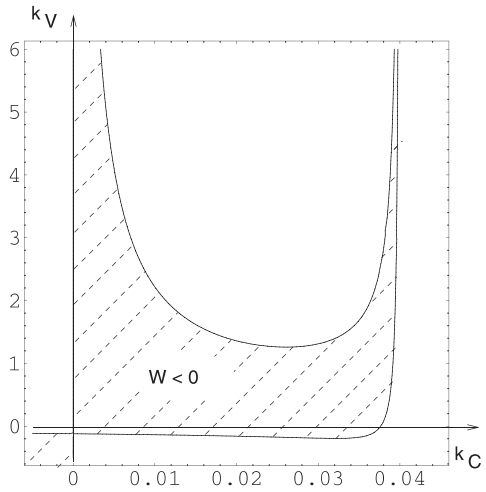

Figure 7.8: In the $k_V - k_C$ – space there exists a region where $W < 0$, i.e. the eigenvalues $\lambda_{2,3_{S_2}}$ are complex.

Eigenvalues

$$det(J-\lambda\mathbf{I}) = \begin{vmatrix} -2\phi-\lambda & -\frac{k_C\, y_3}{(J+y_2)^2} & -\frac{k_C}{J+y_2} \\ -k_{SC}\, y_2 & -k_{SC}\, y_1 - \phi - \lambda & 0 \\ k_{SC}\, y_2 & k_{SC}\, y_1 & -\phi-\lambda \end{vmatrix} \stackrel{!}{=} 0$$

$$\Leftrightarrow \quad -\lambda^3 - \lambda^2 \frac{k_C^2 k_{SC}^2 k_V - 2k_C k_{SC} k_V \phi^2 + 6Jk_C k_{SC}\phi^3}{2Jk_C k_{SC}\phi^2}$$

$$-\lambda \frac{3k_C^2 k_{SC}^2 k_V \phi - 10 k_C k_{SC} k_V \phi^3 + 8\phi^5(k_V + J\phi)}{2Jk_C k_{SC}\phi^2}$$

$$-\frac{2k_C^2 k_{SC}^2 k_V \phi^2 - 8k_C k_{SC} k_V \phi^4 - 4Jk_C k_{SC}\phi^5 + 8\phi^6(k_V + J\phi)}{2Jk_C k_{SC}\phi^2} = 0$$

$$\Rightarrow \quad \lambda_1 = -\phi,$$

$$\lambda_{2/3} = \frac{1}{4Jk_C k_{SC}\,\phi^2}\Big(- k_C^2\, k_{SC}^2\, k_V + 2k_C\, k_{SC}\, k_V\, \phi^2 - 4Jk_C\, k_{SC}\, \phi^3 \pm \sqrt{k_C\, k_{SC}\, W}\Big)$$

with

$$W = k_C k_{SC}\big[k_C k_{SC} k_V + 2\phi^2(k_V - 2J\phi)\big] - 16J\phi^3(k_C k_{SC} - 2\phi^2)\big[k_C k_{SC} k_V - 2\phi^2(k_V - 2J\phi)\big] \qquad (7.7)$$

coefficients of the equation $\omega^2 - A\omega + B = 0, B < 0$, changes once, i.e. there exits one real negative solution for λ.

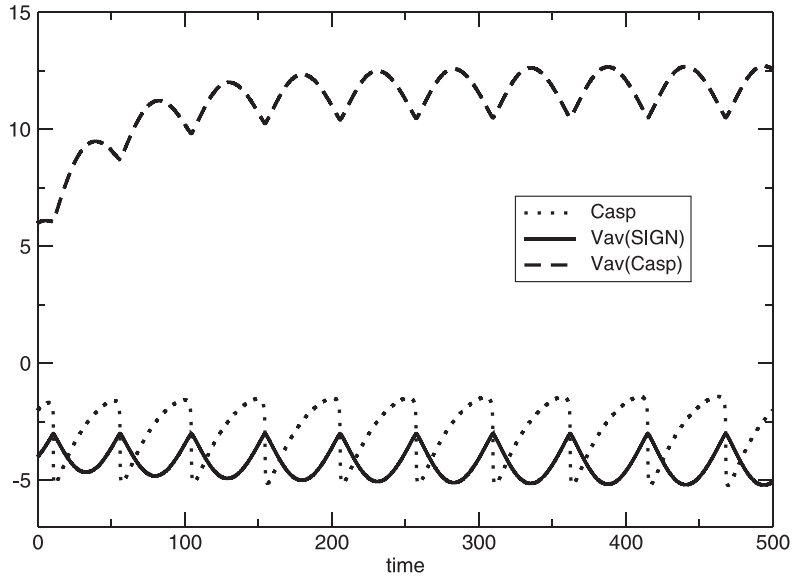

Figure 7.9: Oscillations in the reduced Vav1 model.

The dependence of the sign of W as function of the Vav1 production k_V and the caspase activation k_C, $W = W(k_V, k_C)$, is shown in Fig. 7.8. There is a region where $W(k_V, k_C) < 0$, i.e. the eigenvalues are complex. For fixed value of k_V decreasing k_C leads to a new bifurcation. Assuming parameter values as in the example before one observes at $k_C = 0.04$ the Hopf bifurcation, Fig.7.9. However, this has no consequences for the model since it occurs on the negative steady state branch y_{S_2} (see Fig.7.10).

Eigenvectors

$$\begin{aligned}
\lambda_{1_{S_2}} &= \left\{ \frac{k_C^2 k_{SC} - 2k_C\phi^2}{Jk_Ck_{SC}\phi - 4J\phi^3}, -\frac{4Jk_Ck_{SC}\phi^3}{(k_Ck_{SC} - 4\phi^2)(k_Ck_{SC}k_V - 2\phi^2(k_V + J\phi))}, 1 \right\} \\
\lambda_{2,3_{S_2}} &= \left\{ \frac{1}{8J^2k_Ck_{SC}^2\,\phi^4}\left[(k_Ck_{SC} - 2\phi^2)\left(V \pm \sqrt{k_C\,k_{SC}\,W}\right)\right], -1, 1 \right\}
\end{aligned}$$

with

$$V = -k_C^2\,k_{SC}^2\,k_V + 2k_C\,k_{SC}\,k_V\,\phi^2 - 4Jk_C\,k_{SC}\,\phi^2$$

and W as defined by equation (7.7).

Figure 7.10 shows the resulting bifurcation diagram uncovering the highly complex dynamical behavior of the minimal Vav model 7.5 described by 7.2. The separated solution branches of y_{S_2} are now visible. The first one crosses

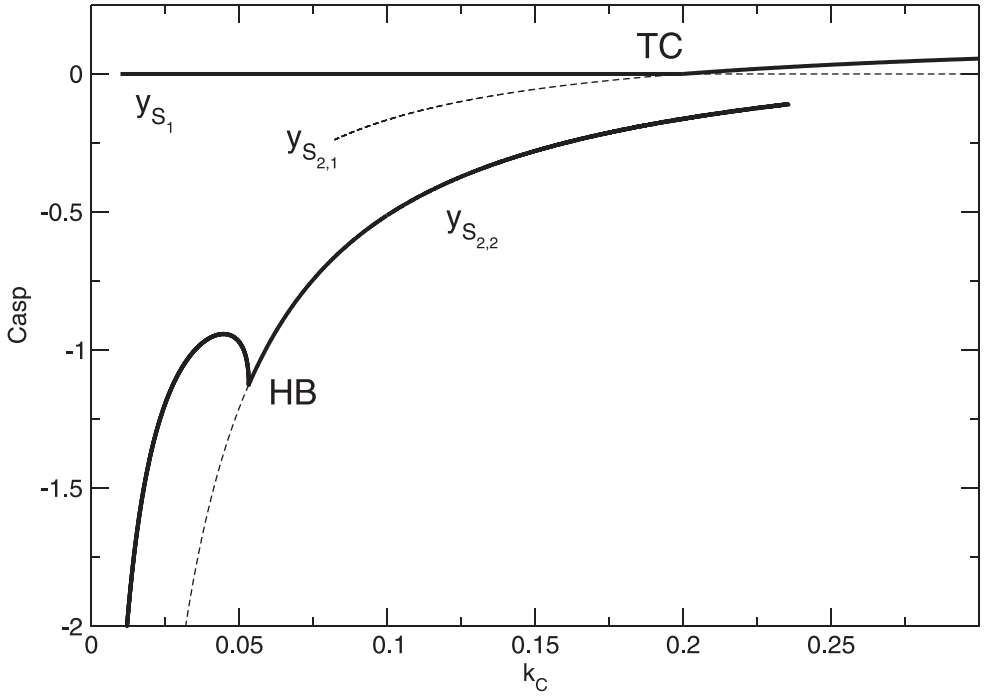

Figure 7.10: Bifurcation diagram for the active Caspase in the reduced Vav1 model. Two branches of the steady state are shown, $y_{S_{2,1}}$ and $y_{S_{2,2}}$. The first one crosses the steady state y_{S_1} at the transcritical bifurcation point (TC). Behind the Hopf bifurcation point (HB) only the upper branch of the limit cycle is shown.

with the steady state y_{S_1} at the transcritical bifurcation point (TC). This point is related to the threshold in the caspase activation needed for the initialization of the truncation process.

The separated branch $y_{S_{2,2}}$ contains a Hopf bifurcation point. In the figure 7.10 only the upper part of the limit cycle is shown.

7.6 Conclusions

Besides interesting mathematical details, we emphasize once more the importance and consequences of the existence of autocatalytical circuits. Transcritical or saddle node bifurcations due to this kind of feedback define biological thresholds in slightly different way [Aguda, 1999].

Moreover, even if, in current stage, no exact experimental proofs of hy-

potheses made on the base of the presented mathematical model are possible, there is one important observation. The presence of common structures and mechanisms found in different biological systems, mentioned in section 7.3.1, might not be just coincidence. It seems like they converged to this one stable and efficient system.

There is no common theoretical framework in biology so far in contrast to mathematics or physics. A classification of biological networks based on their architecture could be a step towards such a systematics.

Chapter 8

Discussion and Outlook

The underlying idea of this thesis was to identify small regulatory modules in cell biological systems and to perform their steady-state analysis. For this purpose we have chosen two networks. The first one is related to the mammalian cell cycle. It has been analyzed in the past using different approaches: via deterministic modeling [Obeyesekere et al., 1995, Aguda and Tang, 1999, Novak and Tyson, 2004] and via microarray gene expression studies on synchronized HeLa cell line [Whitfield et al., 2002]. However, two aspects have not been taken into consideration so far: the dissection of the underlying gene-protein network into subunits and identification of crucial decision-talking modules. We proposed a simple G1/S phase transition module based on the interaction of two proteins: the tumor suppressor Retinoblastoma, pRB, and the transcription factor, E2F-1. It is shown that the transition between G1 and S phase works like a toggle switch, due to the autocatalysis and cooperativity of E2F-1. Interestingly, this behavior remains preserved if we add new components indispensable to mimic known behavior at this cell cycle stage. Another identified module, the Cyclin D/cdk4,6 auto-activation unit, completes the picture. The outcome of a steady-state analysis can be easily illustrated in a bifurcation diagram. We used this tool from nonlinear dynamics to depict the results for this system. Its transcritical bifurcation is followed by a bistability corresponding to the Cyclin D/cdk4,6 activation and phase transition, respectively.

The second analyzed system plays an important role during T-cells activation and it is the first attempt to build a mathematical model for this signal transduction pathway. It is involved in actin remodeling, Vav1 truncation and activation of the cascade pathway. Besides new insights into the dynamics of this specific system, we discovered similarities to other systems. Especially Huntingtin aggregation in the neuro-degenerative disease Huntington resembles the F-actin aggregation in the Vav1 model. The striking

likeness between these systems suggests that efficient mechanisms evolved in nature to preform certain tasks in a well defined way. Such similarities offer an opportunity to classify biological systems with regard to their network structure.

The common observation after the analysis of these two models is that small modules determine, under certain circumstances, the behavior of big networks whose part they are. This decision-taking on the level of modules observed in different systems means shifts in our perception of cell biology. There is a chance in the transition 'from molecular to modular biology', as the new approach offers us new insights and suggests fresh ideas [Hartwell et al., 1999].

Stimulated by the cell cycle model we analyzed the intriguing features of coupled autocatalytical modules. Already in simple systems an almost arbitrary number of stable steady-states is achievable and offers wide opportunities for modern bioengineering architectures. Moreover, in coupled systems the realization of very efficient switches is possible. In comparison to single feedback loop modules they offer high robustness against perturbations and noise.

We hope that our results are a solid base for further investigations. Primarily the cell cycle model extension and its validation with the aid of the ongoing experiments will be in focus of future work. There are several possibilities how to bring our model closer to the biological reality. It is known, for example, that the tumor suppressor pRB exerts its growth suppressive effect through its ability to binding and interacting with a variety of proteins. The activity control of pRB is carried out by different kinases and phosphatases by adding or removing phosphate groups. However, it is not known how the phosphatase PP1, needed to dephosphorylation of pRB in early G1, is displaced from its target [Tamrakar et al., 2000] and how differences in PP1 activity towards various pRB phosphorylation sites can be explained.

Recently, a new cyclin/cdk complex involved in inactivation of pRB has been characterized. Cyclin C/cdk3 dimer phosphorylates pRB to allow cells to exit G0 efficiently [Ren and Rollins, 2004]. G1 entry is thus regulated in an analogous fashion to S phase entry. These findings suggest an additional step in the cascade of events which accompany cell exit from a quiescent state. Obviously, if further experiments confirm the importance of Cyclin C/cdk3, taking this complex into account would be very desirable. These possible model extensions were related so far to the G1/S transition of a wild-type cell. From the therapeutic point of view models of checkpoints are of interest, as many cancers target checkpoint related proteins, Tab.2.3. There is a number of checkpoints (e.g., G1/S-, S-, G2/M-phase or spindel checkpoint) which

still wait for mathematical models.

Recently, new theoretical approaches, belonging to the class of formal methods, have been developed. A tool developed by Fages et al. [2004] provides a system for automated reasoning tools for querying the temporal properties of the system under all its possible behaviors. Especially, biological systems described by ordinary differential equations can be treated in this framework using time discretization methods, and can be then combined with Boolean models. In some cases the systems properties can be checked by computing a fewer number of states then by traditional simulations. This would constitute a big advantage when working with networks with hundreds of components, as the mammalian cell cycle which is based of more than 850 periodically expressed genes [Whitfield et al., 2002].

From the experimental point of view, during the last three years, a new technology has revolutionized functional genomics. Transfection of small interfering RNA (siRNA) molecules into mammalian cells induces post - transcriptional gene silencing via sequence-specific mRNA degradation (RNA interference) [Elbashir et al., 2001, Yu et al., 2002]. SiRNAs have become a standard tool in functional genomics. Once incorporated into the RNA-induced silencing complex (RISC), siRNAs mediate the specific recognition of corresponding target mRNAs and their cleavage. A recently created database, provides sequences of published functional siRNA molecules targeting human genes and important technical details of the corresponding gene silencing experiments [Truss et al., 2005]. These technique has been used successfully to analyze the role of E2F family in cell proliferation and apoptosis [Crosby and Almasan, 2004] and the redundant functions of histons deacetylases in regulation of cell cycle [Zhu et al., 2004].

As stated before, many tumors have mutations or gene silencing that results in inactivation of pRB and others checkpoint related proteins [Sherr, 1996]. The development of detailed cell cycle models is indispensable for further progress. Only the combination of theoretical and experimental methods ensures successful endeavor in modern medicine.

Bibliography

B. Aghazadeh, W.E. Lowry, X.Y. Huang, and M.K. Rosen. Structural basis for relief of autoinhibition of the Dbl homology domain of proto-oncogene Vav by tyrosine phosphorylation. *Cell*, 102(5):625–33, 2000.

B.D. Aguda. Kick-starting the cell cycle: From growth-factor stimulation to initiation of DNA replication. *Chaos*, 11(1):269–276, 2001.

B.D. Aguda. Instabilities in phosphorylation-dephosphorylation cascades and cell cycle checkpoints. *Oncogene*, 18(18):2846–51, 1999.

B.D. Aguda and Y. Tang. The kinetic origins of the restriction point in the mammalian cell cycle. *Cell Prolif*, 32(5):321–35, 1999.

D. Angeli, J.E. Ferrell, Jr, and E.D. Sontag. Detection of multistability, bifurcations, and hysteresis in a large class of biological positive-feedback systems. *Proc Natl Acad Sci U S A*, 101(7):1822–7, 2004.

C.P. Bagowski and J.E. Ferrell, Jr. Bistability in the JNK cascade. *Curr Biol*, 11(15):1176–82, 2001.

S. Becker-Weimann, J. Wolf, H. Herzel, and A. Kramer. Modeling feedback loops of the Mammalian circadian oscillator. *Biophys J*, 87(5):3023–34, 2004.

A. Becskei and L. Serrano. Engineering stability in gene networks by autoregulation. *Nature*, 405(6786):590–3, 2000.

A.K. Bielinsky and S.A. Gerbi. Where it all starts: eukaryotic origins of DNA replication. *J Cell Sci*, 114(Pt 4):643–51, 2001.

M.V. Blagosklonny and A.B. Pardee. The restriction point of the cell cycle. *Cell Cycle*, 1(2):103–10, 2002.

N. Blüthgen and H. Herzel. How robust are switches in intracellular signaling cascades? *J Theor Biol*, 225(3):293–300, 2003.

A.P. Bracken, M. Ciro, A. Cocito, and K. Helin. E2F target genes: unraveling the biology. *Trends Biochem Sci*, 29(8):409–17, 2004.

X.R. Bustelo. Regulation of Vav proteins by intramolecular events. *Front Biosci*, 7:d24–30, 2002.

F. Chang, L.S. Steelman, J.T. Lee, J.G. Shelton, P.M. Navolanic, W.L. Blalock, R.A. Franklin, and J.A. McCubrey. Signal transduction mediated by the Ras/Raf/MEK/ERK pathway from cytokine receptors to transcription factors: potential targeting for therapeutic intervention. *Leukemia*, 17 (7):1263–93, 2003.

J.L. Cherry and F.R. Adler. How to make a biological switch. *J Theor Biol*, 203(2):117–33, 2000.

K.N. Chow and D.C. Dean. Domains A and B in the Rb pocket interact to form a transcriptional repressor motif. *Mol Cell Biol*, 16(9):4862–8, 1996.

O. Cinquin and J. Demongeot. Roles of positive and negative feedback in biological systems. *C R Biol*, 325(11):1085–95, 2002.

J.L. Clements, N.J. Boerth, J.R. Lee, and G.A. Koretzky. Integration of T cell receptor-dependent signaling pathways by adapter proteins. *Annu Rev Immunol*, 17:89–108, 1999.

I. Conlon and M. Raff. Differences in the way a mammalian cell and yeast cells coordinate cell growth and cell-cycle progression. *J Biol*, 2(1):7, 2003.

S. Cooper. Rethinking synchronization of mammalian cells for cell cycle analysis. *Cell Mol Life Sci*, 60(6):1099–106, 2003.

S. Cooper. Is whole-culture synchronization biology's 'perpetual-motion machine'? *Trends Biotechnol*, 22(6):266–9, 2004.

O. Coqueret. Linking cyclins to transcriptional control. *Gene*, 299(1-2): 35–55, 2002.

M. Costanzo, J.L. Nishikawa, X. Tang, J.S. Millman, O. Schub, K. Breitkreuz, D. Dewar, I. Rupes, B. Andrews, and M. Tyers. CDK activity antagonizes Whi5, an inhibitor of G1/S transcription in yeast. *Cell*, 117 (7):899–913, 2004.

M.E. Crosby and A. Almasan. Opposing Roles of E2Fs in Cell Proliferation and Death. *Cancer Biol Ther*, 3(12), 2004.

A. de Bruin, B. Maiti, L. Jakoi, C. Timmers, R. Buerki, and G. Leone. Identification and characterization of E2F7, a novel mammalian E2F family member capable of blocking cellular proliferation. *J Biol Chem*, 278(43): 42041–9, 2003.

R.A. de Bruin, W.H. McDonald, T.I. Kalashnikova, J. Yates, 3rd, and C. Wittenberg. Cln3 activates G1-specific transcription via phosphorylation of the SBF bound repressor Whi5. *Cell*, 117(7):887–98, 2004.

H. de Jong. Modeling and simulation of genetic regulatory systems: a literature review. *J Comput Biol*, 9(1):67–103, 2002.

J. DeGregori. The genetics of the E2F family of transcription factors: shared functions and unique roles. *Biochim Biophys Acta*, 1602(2):131–50, 2002.

J. Demongeot, M. Kaufman, and R. Thomas. Positive feedback circuits and memory. *C R Acad Sci III*, 323(1):69–79, 2000.

R.J. Deshaies and J.E. Ferrell, Jr. Multisite phosphorylation and the countdown to S phase. *Cell*, 107(7):819–22, 2001.

L. Di Stefano, M.R. Jensen, and K. Helin. E2F7, a novel E2F featuring DP-independent repression of a subset of E2F-regulated genes. *EMBO J*, 22 (23):6289–98, 2003.

B.D. Dynlacht. Regulation of transcription by proteins that control the cell cycle. *Nature*, 389(6647):149–52, 1997.

N. Dyson. The regulation of E2F by pRB-family proteins. *Genes Dev*, 12 (15):2245–62, 1998.

Leah Edelstein-Keshet. *Mathematical Models in Biology*. Birkhauser Mathematics Series, 1988.

S. Ekholm-Reed. *The role of Cyclin E in cell cycle regulation and genomic instability*. PhD thesis, Department of Pathology-Oncology, Cancer Center Karolinska, Karolinska Intitutet, Stockholm, 2004.

S.M. Elbashir, J. Harborth, W. Lendeckel, A. Yalcin, K. Weber, and T. Tuschl. Duplexes of 21-nucleotide RNAs mediate RNA interference in cultured mammalian cells. *Nature*, 411(6836):494–8, 2001.

B. Ermentrout. XPPAUT5.85 The differential equations tool. Technical report, University of Pittsburgh, 1998. http://www.math.pitt.edu/ bard/xpp/xpp.html.

M.E. Ewen, Y.G. Xing, J.B. Lawrence, and D.M. Livingston. Molecular cloning, chromosomal mapping, and expression of the cDNA for p107, a retinoblastoma gene product-related protein. *Cell*, 66(6):1155–64, 1991.

F. Fages, S. Soliman, and N. Chabrier-Rivier. Modeling and querying interaction networks in the biochemical abstract machine BIOCHAM. *Journal of Biological Physics and Chemistry*, 4:64–73, 2004.

C. Fall, E. Marland, J. Wagner, and J. Tyson. *Computational Cell Biology*. Springer-Verlag Telos, 2002.

J.E. Ferrell and W. Xiong. Bistability in cell signaling: How to make continuous processes discontinuous, and reversible processes irreversible. *Chaos*, 11(1):227–236, 2001.

J.E. Ferrell, Jr. Six steps to destruction. *Nature*, 414(6863):498–9, 2001.

J.E. Ferrell, Jr. Self-perpetuating states in signal transduction: positive feedback, double-negative feedback and bistability. *Curr Opin Cell Biol*, 14(2):140–8, 2002.

J.E. Ferrell, Jr. How regulated protein translocation can produce switch-like responses. *Trends Biochem Sci*, 23(12):461–5, 1998.

S.E. Fraser and R.M. Harland. The molecular metamorphosis of experimental embryology. *Cell*, 100(1):41–55, 2000.

N. Fujita, D.L. Jaye, C. Geigerman, A. Akyildiz, M.R. Mooney, J.M. Boss, and P.A. Wade. MTA3 and the Mi-2/NuRD complex regulate cell fate during B lymphocyte differentiation. *Cell*, 119(1):75–86, 2004.

Y. Furukawa, S. Iwase, J. Kikuchi, M. Nakamura, H. Yamada, and M. Matsuda. Transcriptional repression of the E2F-1 gene by interferon-alpha is mediated through induction of E2F-4/pRB and E2F-4/p130 complexes. *Oncogene*, 18(11):2003–14, 1999.

M. Fussenegger, J.E. Bailey, and J. Varner. A mathematical model of caspase function in apoptosis. *Nat Biotechnol*, 18(7):768–74, 2000.

T.S. Gardner and J.J. Collins. Neutralizing noise in gene networks. *Nature*, 405(6786):520–1, 2000.

T.S. Gardner, C.R. Cantor, and J.J. Collins. Construction of a genetic toggle switch in Escherichia coli. *Nature*, 403(6767):339–42, 2000.

A. Goldbeter. *Biochemical Oscillations and Cellular Rhythms*. Cambridge University Press, Cambridge, 1996.

D. Gonze, J. Halloy, and A. Goldbeter. Robustness of circadian rhythms with respect to molecular noise. *Proc Natl Acad Sci U S A*, 99(2):673–8, 2002.

A. Grakoui, S.K. Bromley, C. Sumen, M.M. Davis, A.S. Shaw, P.M. Allen, and M.L. Dustin. The immunological synapse: a molecular machine controlling T cell activation. *Science*, 285(5425):221–7, 1999.

J.S. Griffith. Mathematics of cellular control processes. II. Positive feedback to one gene. *J Theor Biol*, 20(2):209–16, 1968a.

J.S. Griffith. Mathematics of cellular control processes. I. Negative feedback to one gene. *J Theor Biol*, 20(2):202–8, 1968b.

G.J. Hannon, D. Demetrick, and D. Beach. Isolation of the Rb-related p130 through its interaction with CDK2 and cyclins. *Genes Dev*, 7(12A):2378–91, 1993.

J.W. Harbour and D.C. Dean. The Rb/E2F pathway: expanding roles and emerging paradigms. *Genes Dev*, 14(19):2393–409, 2000a.

J.W. Harbour and D.C. Dean. Rb function in cell-cycle regulation and apoptosis. *Nat Cell Biol*, 2(4):E65–7, 2000b.

L.H. Hartwell, J.J. Hopfield, S. Leibler, and A.W. Murray. From molecular to modular cell biology. *Nature*, 402(6761 Suppl):C47–52, 1999.

J. Hasty, J. Pradines, M. Dolnik, and J.J. Collins. Noise-based switches and amplifiers for gene expression. *Proc Natl Acad Sci U S A*, 97(5):2075–80, 2000.

J. Hasty, F. Isaacs, M. Dolnik, D. McMillen, and J.J. Collins. Designer gene networks: Towards fundamental cellular control. *Chaos*, 11(1):207–220, 2001.

G. Hateboer, A. Wobst, B.O. Petersen, L. Le Cam, E. Vigo, C. Sardet, and K. Helin. Cell cycle-regulated expression of mammalian CDC6 is dependent on E2F. *Mol Cell Biol*, 18(11):6679–97, 1998.

V. Hatzimanikatis, K.H. Lee, and J.E. Bailey. A mathematical description of regulation of the G1-S transition of the mammalian cell cycle. *Biotechnol Bioeng*, 65(6):631–7, 1999.

R. Heinrich and S. Schuster. *The Regulation of Cellular Systems*. Chapman and Hall, New York, 1996.

A. Hennino, M. Berard, P.H. Krammer, and T. Defrance. FLICE-inhibitory protein is a key regulator of germinal center B cell apoptosis. *J Exp Med*, 193(4):447–58, 2001.

T. Hofer, H. Nathansen, M. Lohning, A. Radbruch, and R. Heinrich. GATA-3 transcriptional imprinting in Th2 lymphocytes: a mathematical model. *Proc Natl Acad Sci U S A*, 99(14):9364–8, 2002.

I. Hornstein, A. Alcover, and S. Katzav. Vav proteins, masters of the world of cytoskeleton organization. *Cell Signal*, 16(1):1–11, 2004.

K.M. Hsiao, S.L. McMahon, and P.J. Farnham. Multiple DNA elements are required for the growth regulation of the mouse E2F1 promoter. *Genes Dev*, 8(13):1526–37, 1994.

P.A. Iglesias and A. Levchenko. Modeling the cell's guidance system. *Sci STKE*, 2002(148):RE12, 2002.

F.J. Isaacs, J. Hasty, C.R. Cantor, and J.J. Collins. Prediction and measurement of an autoregulatory genetic module. *Proc Natl Acad Sci U S A*, 100 (13):7714–9, 2003.

G. Jetschke. *Mathematik der Selbstorganisation*. Verlag Harri Deutch, Berlin, 1989.

S. Jinno, K. Suto, A. Nagata, M. Igarashi, Y. Kanaoka, H. Nojima, and H. Okayama. Cdc25A is a novel phosphatase functioning early in the cell cycle. *EMBO J*, 13(7):1549–56, 1994.

D.G. Johnson and C.L. Walker. Cyclins and cell cycle checkpoints. *Annu Rev Pharmacol Toxicol*, 39:295–312, 1999.

D.G. Johnson, K. Ohtani, and J.R. Nevins. Autoregulatory control of E2F1 expression in response to positive and negative regulators of cell cycle progression. *Genes Dev*, 8(13):1514–25, 1994.

R.W. Johnstone. Histone-deacetylase inhibitors: novel drugs for the treatment of cancer. *Nat Rev Drug Discov*, 1(4):287–99, 2002.

S.M. Jones and A. Kazlauskas. Growth factor-dependent signaling and cell cycle progression. *FEBS Lett*, 490(3):110–6, 2001a.

S.M. Jones and A. Kazlauskas. Growth factor-dependent signaling and cell cycle progression. *Chem Rev*, 101(8):2413–23, 2001b.

M.B. Kastan and J. Bartek. Cell-cycle checkpoints and cancer. *Nature*, 432 (7015):316–23, 2004.

A. Kel. Modeling of gene regulatory network of cell cycle control. Role of E2F feedback loops. In U. Bornberg-Bauer.E., Rost, editor, *Proceedings of the German Conference in Bioinformatics, Heidelberg*, pages 107–114, Heidelberg, 2000. Logos Verlag Berlin.

B.N. Kholodenko. Negative feedback and ultrasensitivity can bring about oscillations in the mitogen-activated protein kinase cascades. *Eur J Biochem*, 267(6):1583–8, 2000.

H. Kobayashi, M. Kaern, M. Araki, K. Chung, T.S. Gardner, C.R. Cantor, and J.J. Collins. Programmable cells: interfacing natural and engineered gene networks. *Proc Natl Acad Sci U S A*, 101(22):8414–9, 2004.

K.W. Kohn. Functional capabilities of molecular network components controlling the mammalian G1/S cell cycle phase transition. *Oncogene*, 16(8): 1065–75, 1998.

K.W. Kohn. Molecular interaction map of the mammalian cell cycle control and DNA repair systems. *Mol Biol Cell*, 10(8):2703–34, 1999.

I. Kovesdi, R. Reichel, and J.R. Nevins. Identification of a cellular transcription factor involved in E1A trans-activation. *Cell*, 45(2):219–28, 1986.

B.P. Kramer, W. Weber, and M. Fussenegger. Artificial regulatory networks and cascades for discrete multilevel transgene control in mammalian cells. *Biotechnol Bioeng*, 83(7):810–20, 2003.

G. Lahav, N. Rosenfeld, A. Sigal, N. Geva-Zatorsky, A.J. Levine, M.B. Elowitz, and U. Alon. Dynamics of the p53-Mdm2 feedback loop in individual cells. *Nat Genet*, 36(2):147–50, 2004.

P. Lavia and P. Jansen-Durr. E2F target genes and cell-cycle checkpoint control. *Bioessays*, 21(3):221–30, 1999.

T.I. Lee, N.J. Rinaldi, F. Robert, D.T. Odom, Z. Bar-Joseph, G.K. Gerber, N.M. Hannett, C.T. Harbison, C.M. Thompson, I. Simon, J. Zeitlinger, E.G. Jennings, H.L. Murray, D.B. Gordon, B. Ren, J.J. Wyrick, J.B.

Tagne, T.L. Volkert, E. Fraenkel, D.K. Gifford, and R.A. Young. Transcriptional regulatory networks in Saccharomyces cerevisiae. *Science*, 298 (5594):799–804, 2002.

Y. Li, C. Graham, S. Lacy, A.M. Duncan, and P. Whyte. The adenovirus E1A-associated 130-kD protein is encoded by a member of the retinoblastoma gene family and physically interacts with cyclins A and E. *Genes Dev*, 7(12A):2366–77, 1993.

Y. Li, J.E. Slansky, D.J. Myers, N.R. Drinkwater, W.G. Kaelin, and P.J. Farnham. Cloning, chromosomal location, and characterization of mouse E2F1. *Mol Cell Biol*, 14(3):1861–9, 1994.

D.X. Liu and L.A. Greene. Neuronal apoptosis at the G1/S cell cycle checkpoint. *Cell Tissue Res*, 305(2):217–28, 2001.

M.A. Martinez-Balbas, U.M. Bauer, S.J. Nielsen, A. Brehm, and T. Kouzarides. Regulation of E2F1 activity by acetylation. *EMBO J*, 19(4):662–71, 2000.

J. Massague. G1 cell-cycle control and cancer. *Nature*, 432(7015):298–306, 2004.

A.V. Miletic, M. Swat, K. Fujikawa, and W. Swat. Cytoskeletal remodeling in lymphocyte activation. *Curr Opin Immunol*, 15(3):261–8, 2003.

C.R. Monks, B.A. Freiberg, H. Kupfer, N. Sciaky, and A. Kupfer. Three-dimensional segregation of supramolecular activation clusters in T cells. *Nature*, 395(6697):82–6, 1998.

J. Monod and F. Jacob. Teleonomic mechanisms in cellular metabolism, growth, and differentiation. *Cold Spring Harb Symp Quant Biol*, 26:389–401, 1961.

S.D. Mundle and G. Saberwal. Evolving intricacies and implications of E2F1 regulation. *FASEB J*, 17(6):569–74, 2003.

J. D. Murray. *Mathematical Biology*, volume 19 of *Biomathematics*. Springer-Verlag, Berlin Heidelberg, 1993.

E. Neuman, E.K. Flemington, W.R. Sellers, and W.G. Kaelin, Jr. Transcription of the E2F-1 gene is rendered cell cycle dependent by E2F DNA-binding sites within its promoter. *Mol Cell Biol*, 14(10):6607–15, 1994.

B. Novak and J.J. Tyson. A model for restriction point control of the mammalian cell cycle. *J Theor Biol*, 230(4):563–79, 2004.

M.N. Obeyesekere, J.R. Herbert, and S.O. Zimmerman. A model of the G1 phase of the cell cycle incorporating cyclin E/cdk2 complex and retinoblastoma protein. *Oncogene*, 11(6):1199–205, 1995.

M.N. Obeyesekere, E.S. Knudsen, J.Y. Wang, and S.O. Zimmerman. A mathematical model of the regulation of the G1 phase of Rb+/+ and Rb-/- mouse embryonic fibroblasts and an osteosarcoma cell line. *Cell Prolif*, 30 (3-4):171–94, 1997.

M. Pagano and P.K. Jackson. Wagging the dogma; tissue-specific cell cycle control in the mouse embryo. *Cell*, 118(5):535–8, 2004.

L. Perko. *Differential equations and dynamical systems.* Texts in Applied Mathematics. Springer, 2nd. edition, 1993.

J. Pines and T. Hunter. Isolation of a human cyclin cDNA: evidence for cyclin mRNA and protein regulation in the cell cycle and for interaction with p34cdc2. *Cell*, 58(5):833–46, 1989.

T. Poston and I. Stewart. *Catastrophe theory and its applications.* Pitman Publishing, London, 1978.

Z. Qu, J.N. Weiss, and W.R. MacLellan. Regulation of the mammalian cell cycle: a model of the G1-to-S transition. *Am J Physiol Cell Physiol*, 284 (2):C349–64, 2003.

Z. Qu, J.N. Weiss, and W.R. MacLellan. Coordination of cell growth and cell division: a mathematical modeling study. *J Cell Sci*, 117(Pt 18):4199–207, 2004.

S. Ren and B.J. Rollins. Cyclin C/cdk3 promotes Rb-dependent G0 exit. *Cell*, 117(2):239–51, 2004.

J. Sage. Cyclin C makes an entry into the cell cycle. *Dev Cell*, 6(5):607–8, 2004.

H.M. Sauro and B.N. Kholodenko. Quantitative analysis of signaling networks. *Prog Biophys Mol Biol*, 86(1):5–43, 2004.

J.B. Schaefer and L.L. Breeden. RB from a bud's eye view. *Cell*, 117(7): 849–50, 2004.

S.S. Shen-Orr, R. Milo, S. Mangan, and U. Alon. Network motifs in the transcriptional regulation network of Escherichia coli. *Nat Genet*, 31(1): 64–8, 2002.

C.J. Sherr. Cancer cell cycles. *Science*, 274(5293):1672–7, 1996.

C.J. Sherr and J.M. Roberts. Living with or without cyclins and cyclin-dependent kinases. *Genes Dev*, 18(22):2699–711, 2004.

C.J. Sherr and J.M. Roberts. Inhibitors of mammalian G1 cyclin-dependent kinases. *Genes Dev*, 9(10):1149–63, 1995.

K.A. Sieradzan and D.M. Mann. The selective vulnerability of nerve cells in Huntington's disease. *Neuropathol Appl Neurobiol*, 27(1):1–21, 2001.

J.E. Slansky, Y. Li, W.G. Kaelin, and P.J. Farnham. A protein synthesis-dependent increase in E2F1 mRNA correlates with growth regulation of the dihydrofolate reductase promoter. *Mol Cell Biol*, 13(3):1610–8, 1993.

P. Smolen, D.A. Baxter, and J.H. Byrne. Frequency selectivity, multistability, and oscillations emerge from models of genetic regulatory systems. *Am J Physiol*, 274(2 Pt 1):C531–42, 1998.

L.M. Staudt. Cancer: negative feedback for B cells. *Nature*, 431(7011): 919–20, 2004.

Steven H. Strogatz. *Nonlinear Dynamics and Chaos: With Applications to Physics, Biology, Chemistry and Engineering*. Perseus Books Group; 1st edition, 2001.

M. Swat, A. Kel, and H. Herzel. Bifurcation analysis of the regulatory modules of the mammalian G1/S transition. *Bioinformatics*, 20(10):1506–11, 2004.

S. Tamrakar, E. Rubin, and J.W. Ludlow. Role of pRB dephosphorylation in cell cycle regulation. *Front Biosci*, 5:D121–37, 2000.

P.A. Temussi, L. Masino, and A. Pastore. From Alzheimer to Huntington: why is a structural understanding so difficult? *EMBO J*, 22(3):355–61, 2003.

D. Thieffry, A.M. Huerta, E. Perez-Rueda, and J. Collado-Vides. From specific gene regulation to genomic networks: a global analysis of transcriptional regulation in Escherichia coli. *Bioessays*, 20(5):433–40, 1998.

R. Thomas. Laws for the dynamics of regulatory networks. *Int J Dev Biol*, 42(3):479–85, 1998.

C.D. Thron. Bistable biochemical switching and the control of the events of the cell cycle. *Oncogene*, 15(3):317–25, 1997.

M.G. Tomlinson, J. Lin, and A. Weiss. Lymphocytes with a complex: adapter proteins in antigen receptor signaling. *Immunol Today*, 21(11):584–91, 2000.

M. Truss, M. Swat, S.M. Kielbasa, R. Schafer, H. Herzel, and C. Hagemeier. HuSiDa–the human siRNA database: an open-access database for published functional siRNA sequences and technical details of efficient transfer into recipient cells. *Nucleic Acids Res*, 33 Database Issue:D108–11, 2005.

M. Turner and D.D. Billadeau. VAV proteins as signal integrators for multisubunit immune-recognition receptors. *Nat Rev Immunol*, 2(7):476–86, 2002.

J.J. Tyson, K. Chen, and B. Novak. Network dynamics and cell physiology. *Nat Rev Mol Cell Biol*, 2(12):908–16, 2001.

M. van Eijk, J.P. Medema, and C. de Groot. Cutting edge: cellular Fas-associated death domain-like IL-1-converting enzyme-inhibitory protein protects germinal center B cells from apoptosis during germinal center reactions. *J Immunol*, 166(11):6473–6, 2001.

A.M. Walczak, M. Sasai, and P.G. Wolynes. Self Consistent Proteomic Field Theory of Stochastic Gene Switches. *Biophys J*, 88(2):828–50, 2005.

E.E. Wanker. Protein aggregation and pathogenesis of Huntington's disease: mechanisms and correlations. *Biol Chem*, 381(9-10):937–42, 2000.

W. Weber and M. Fussenegger. Artificial mammalian gene regulation networks-novel approaches for gene therapy and bioengineering. *J Biotechnol*, 98(2-3):161–87, 2002.

S.J. Weintraub, C.A. Prater, and D.C. Dean. Retinoblastoma protein switches the E2F site from positive to negative element. *Nature*, 358(6383): 259–61, 1992.

M.L. Whitfield, G. Sherlock, A.J. Saldanha, J.I. Murray, C.A. Ball, K.E. Alexander, J.C. Matese, C.M. Perou, M.M. Hurt, P.O. Brown, and D. Botstein. Identification of genes periodically expressed in the human cell cycle and their expression in tumors. *Mol Biol Cell*, 13(6):1977–2000, 2002.

L. Wu, C. Timmers, B. Maiti, H.I. Saavedra, L. Sang, G.T. Chong, F. Nuckolls, P. Giangrande, F.A. Wright, S.J. Field, M.E. Greenberg, S. Orkin, J.R. Nevins, M.L. Robinson, and G. Leone. The E2F1-3 transcription factors are essential for cellular proliferation. *Nature*, 414(6862):457–62, 2001.

J.Y. Yu, S.L. DeRuiter, and D.L. Turner. RNA interference by expression of short-interfering RNAs and hairpin RNAs in mammalian cells. *Proc Natl Acad Sci U S A*, 99(9):6047–52, 2002.

K. Zerfass-Thome, A. Schulze, W. Zwerschke, B. Vogt, K. Helin, J. Bartek, B. Henglein, and P. Jansen-Durr. p27KIP1 blocks cyclin E-dependent transactivation of cyclin A gene expression. *Mol Cell Biol*, 17(1):407–15, 1997.

A. Zetterberg, O. Larsson, and K.G. Wiman. What is the restriction point? *Curr Opin Cell Biol*, 7(6):835–42, 1995.

H.S. Zhang and D.C. Dean. Rb-mediated chromatin structure regulation and transcriptional repression. *Oncogene*, 20(24):3134–8, 2001.

H.S. Zhang, M. Gavin, A. Dahiya, A.A. Postigo, D. Ma, R.X. Luo, J.W. Harbour, and D.C. Dean. Exit from G1 and S phase of the cell cycle is regulated by repressor complexes containing HDAC-Rb-hSWI/SNF and Rb-hSWI/SNF. *Cell*, 101(1):79–89, 2000.

T.S. Zheng and R.A. Flavell. Death by numbers. *Nat Biotechnol*, 18(7): 717–8, 2000.

P. Zhu, E. Huber, F. Kiefer, and M. Gottlicher. Specific and redundant functions of histone deacetylases in regulation of cell cycle and apoptosis. *Cell Cycle*, 3(10):1240–2, 2004.

Appendix A

Hurwitz criterion

All eigenvalues $\lambda_1, \ldots, \lambda_n$ of the Matrix A have negative real part if and only if for the coefficients $a_1, \ldots, a_n$ of the characteristic polynom $\sum_{k=0}^{n} a_{n-k}\lambda^k = 0, a_0 \stackrel{!}{=} 1$ following inequalities are true ($a_k \equiv 0 \; for \; k > n$):

$$D_1 := a_1 > 0, \; D_2 := \begin{vmatrix} a_1 & 1 \\ a_3 & a_2 \end{vmatrix} > 0, \ldots, D_n := \begin{vmatrix} a_1 & 1 & 0 & \ldots & 0 \\ a_3 & a_2 & a_1 & 1 & 0 \ldots 0 \\ a_5 & a_4 & a_3 & a_2 & \ldots 0 \\ \vdots & \vdots & & & \vdots \\ a_{2n-1} & a_{2n-2} & & \ldots & a_n \end{vmatrix} > 0$$

Appendix B

Descartes' rule of signs

We consider the polynomial

$$P(y) = A_0 + A_1 y + \cdots + A_{n-1} y^{n-1} + A_n y^n, \quad A_i \in \mathbb{R}^+, i = 1, \ldots, n. \quad \text{(B.1)}$$

Let N be the number of sign changes in the sequence of the coefficients $\{A_0, A_1, \ldots, A_{n-1}, A_n\}$, ignoring any which are zero. *D*escartes' Rule of Signs says that there are at most N roots λ of (B.1), which are real and positive, and further, that there are either N or $N-2$ or $N-4$, ... real positive roots.

By setting $\omega = -\lambda$ and again applying the rule, information is obtained about the possible real negative roots.

Appendix C

Steady state polynomial of 27th degree

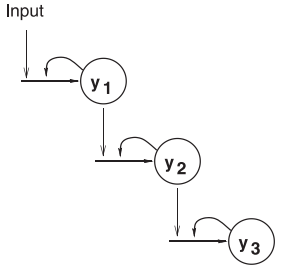

$$\begin{aligned}
\frac{dy_1}{dt} &= k_1 \frac{a_1 + y_1^2}{b_1 + y_1^2} - \phi_1 y_1 \\
\frac{dy_2}{dt} &= y_1 k_2 \frac{a_2 + y_2^2}{b_2 + y_2^2} - \phi_2 y_2 \\
\frac{dy_3}{dt} &= y_2 k_3 \frac{a_3 + y_3^2}{b_3 + y_3^2} - \phi_3 y_3
\end{aligned}$$

The steady-state polynomial of y_3 with the alternating coefficient signs, chapter 4, equation (5.5),

$$P_{StSt}^{[27]}(y_3) = A_0 + A_1 y_3 + A_2 y_3^2 + \cdots + A_{26} y_3^{26} + A_{27} y_3^{27}, \quad A_i \in R,$$

reads in its full form:
$P_{StSt}^{[27]}(y_3) = a_1 a_2^3 a_3^9 k_1 k_2^3 k_3^9 \; - \; a_2^2 a_3^8 b_1 b_2 b_3 k_2^2 k_3^8 \phi_1 \phi_2 \phi_3 \; y_3 \; +$
$(9 a_1 a_2^3 a_3^8 k_1 k_2^3 k_3^9 \; + \; 3 a_1 a_2^2 a_3^7 b_3^2 k_1 k_2^3 k_3^7 \phi_3^2 \; + \; a_2 a_3^7 b_2^2 b_3^2 k_1 k_2 k_3^7 \phi_2^2 \phi_3^2) \; y_3^2$
$+ \; (-a_2^2 a_3^8 b_1 b_2 k_2^2 k_3^8 \phi_1 \phi_2 \phi_3 \; - \; 8 a_2^2 a_3^7 b_1 b_2 b_3 k_2^2 k_3^8 \phi_1 \phi_2 \phi_3 \; - \; a_2^2 a_3^6 b_1 b_3^3 k_2^2 k_3^6 \phi_1 \phi_2 \phi_3^3 \; -$
$2 a_2 a_3^6 b_1 b_2 b_3^3 k_2^2 k_3^6 \phi_1 \phi_2 \phi_3^3 \; - \; a_3^6 b_2^3 b_3^3 k_3^6 \phi_1 \phi_2^3 \phi_3^3) \; y_3^3 \; +$
$(36 a_1 a_2^3 a_3^7 k_1 k_2^3 k_3^9 \; + \; 6 a_1 a_2^2 a_3^7 b_3 k_1 k_2^3 k_3^7 \phi_3^2 \; + \; 21 a_1 a_2^2 a_3^6 b_3^2 k_1 k_2^3 k_3^7 \phi_3^2 \; +$
$2 a_2 a_3^7 b_2^2 b_3 k_1 k_2 k_3^7 \phi_2^2 \phi_3^2 \; + \; 7 a_2 a_3^6 b_2^2 b_3^2 k_1 k_2 k_3^7 \phi_2^2 \phi_3^2 \; + \; 3 a_1 a_2 a_3^5 b_3^4 k_1 k_2^3 k_3^5 \phi_3^4 \; +$
$2 a_2 a_3^5 b_2 b_3^4 k_1 k_2 k_3^5 \phi_2^2 \phi_3^4 \; + \; a_3^5 b_2^2 b_3^4 k_1 k_2 k_3^5 \phi_2^2 \phi_3^4) \; y_3^4 \; +$
$(-8 a_2^2 a_3^7 b_1 b_2 k_2^2 k_3^8 \phi_1 \phi_2 \phi_3 \; - \; 28 a_2^2 a_3^6 b_1 b_2 b_3 k_2^2 k_3^8 \phi_1 \phi_2 \phi_3 \; - \; 3 a_2^2 a_3^6 b_1 b_3^2 k_2^2 k_3^6 \phi_1 \phi_2 \phi_3^3 \; -$
$6 a_2 a_3^6 b_1 b_2 b_3^2 k_2^2 k_3^6 \phi_1 \phi_2 \phi_3^3 \; - \; 6 a_2^2 a_3^5 b_1 b_3^3 k_2^2 k_3^6 \phi_1 \phi_2 \phi_3^3 \; - \; 12 a_2 a_3^5 b_1 b_2 b_3^3 k_2^2 k_3^6 \phi_1 \phi_2 \phi_3^3 \; -$
$3 a_3^6 b_2^3 b_3^2 k_3^6 \phi_1 \phi_2^3 \phi_3^3 \; - \; 6 a_3^5 b_2^3 b_3^3 k_3^6 \phi_1 \phi_2^3 \phi_3^3 \; - \; 2 a_2 a_3^4 b_1 b_3^5 k_2^2 k_3^4 \phi_1 \phi_2 \phi_3^5 \; -$
$a_3^4 b_1 b_2 b_3^5 k_2^2 k_3^4 \phi_1 \phi_2 \phi_3^5 \; - \; 3 a_3^4 b_2^2 b_3^5 k_3^4 \phi_1 \phi_2^3 \phi_3^5) \; y_3^5 \; +$
$(84 a_1 a_2^3 a_3^6 k_1 k_2^3 k_3^9 \; + \; 3 a_1 a_2^2 a_3^7 k_1 k_2^3 k_3^7 \phi_3^2 \; + \; 42 a_1 a_2^2 a_3^6 b_3 k_1 k_2^3 k_3^7 \phi_3^2 \; +$

$$63a_1a_2^2a_3^5b_3^2k_1k_2^3k_3^7\phi_3^2 + a_2a_3^7b_2^2k_1k_2k_3^7\phi_2^2\phi_3^2 + 14a_2a_3^6b_2^2b_3k_1k_2k_3^7\phi_2^2\phi_3^2 + 21a_2a_3^5b_2^2b_3^2k_1k_2k_3^7\phi_2^2\phi_3^2 + 12a_1a_2a_3^5b_3^3k_1k_2^3k_3^5\phi_3^4 + 15a_1a_2a_3^4b_3^4k_1k_2^3k_3^5\phi_3^4 + 8a_2a_3^5b_2b_3^3k_1k_2k_3^5\phi_2^2\phi_3^4 + 4a_3^5b_2^2b_3^3k_1k_2k_3^5\phi_2^2\phi_3^4 + 10a_2a_3^4b_2b_3^4k_1k_2k_3^5\phi_2^2\phi_3^4 + 5a_3^4b_2^2b_3^4k_1k_2k_3^5\phi_2^2\phi_3^4 + a_1a_3^3b_3^6k_1k_2^3k_3^3\phi_3^6 + a_2a_3^3b_3^6k_1k_2k_3^3\phi_2^2\phi_3^6 + 2a_3^3b_2b_3^6k_1k_2k_3^3\phi_2^2\phi_3^6)\ y_3^6 +$$

$$(-28a_2^2a_3^6b_1b_2k_2^2k_3^8\phi_1\phi_2\phi_3 - 56a_2^2a_3^5b_1b_2b_3k_2^2k_3^8\phi_1\phi_2\phi_3 - 3a_2^2a_3^6b_1b_3k_2^2k_3^6\phi_1\phi_2\phi_3^2 - 6a_2a_3^6b_1b_2b_3k_2^2k_3^6\phi_1\phi_2\phi_3^2 - 18a_2^2a_3^5b_1b_3^2k_2^2k_3^6\phi_1\phi_2\phi_3^2 - 36a_2a_3^5b_1b_2b_3^2k_2^2k_3^6\phi_1\phi_2\phi_3^2 - 15a_2^2a_3^4b_1b_3^3k_2^2k_3^6\phi_1\phi_2\phi_3^2 - 30a_2a_3^4b_1b_2b_3^3k_2^2k_3^6\phi_1\phi_2\phi_3^2 - 3a_3^6b_2^3b_3k_3^6\phi_1\phi_2^3\phi_3^2 - 18a_3^5b_2^3b_3^2k_3^6\phi_1\phi_2^3\phi_3^2 - 15a_3^4b_2^3b_3^3k_3^6\phi_1\phi_2^3\phi_3^2 - 10a_2a_3^4b_1b_3^4k_2^2k_3^4\phi_1\phi_2\phi_3^5 - 5a_3^4b_1b_2b_3^4k_2^2k_3^4\phi_1\phi_2\phi_3^5 - 8a_2a_3^3b_1b_3^5k_2^2k_3^4\phi_1\phi_2\phi_3^5 - 4a_3^3b_1b_2b_3^5k_2^2k_3^4\phi_1\phi_2\phi_3^5 - 15a_3^4b_2^2b_3^4k_3^4\phi_1\phi_2^3\phi_3^5 - 12a_3^3b_2^2b_3^5k_3^4\phi_1\phi_2^3\phi_3^5 - a_3^2b_1b_3^7k_2^2k_3^2\phi_1\phi_2\phi_3^7 - 3a_3^2b_2b_3^7k_3^2\phi_1\phi_2^3\phi_3^7)\ y_3^7 +$$

$$(126a_1a_2^3a_3^5k_1k_2^3k_3^9 + 21a_1a_2^2a_3^6k_1k_2^3k_3^7\phi_3^2 + 126a_1a_2^2a_3^5b_3k_1k_2^3k_3^7\phi_3^2 + 105a_1a_2^2a_3^4b_3^2k_1k_2^3k_3^7\phi_3^2 + 7a_2a_3^6b_2^2k_1k_2k_3^7\phi_2^2\phi_3^2 + 42a_2a_3^5b_2^2b_3k_1k_2k_3^7\phi_2^2\phi_3^2 + 35a_2a_3^4b_2^2b_3^2k_1k_2k_3^7\phi_2^2\phi_3^2 + 18a_1a_2a_3^5b_3^2k_1k_2^3k_3^5\phi_3^4 + 60a_1a_2a_3^4b_3^3k_1k_2^3k_3^5\phi_3^4 + 30a_1a_2a_3^3b_3^4k_1k_2^3k_3^5\phi_3^4 + 12a_2a_3^5b_2b_3^2k_1k_2k_3^5\phi_2^2\phi_3^4 + 6a_3^5b_2^2b_3^2k_1k_2k_3^5\phi_2^2\phi_3^4 + 40a_2a_3^4b_2b_3^3k_1k_2k_3^5\phi_2^2\phi_3^4 + 20a_3^4b_2^2b_3^3k_1k_2k_3^5\phi_2^2\phi_3^4 + 20a_2a_3^3b_2b_3^4k_1k_2k_3^5\phi_2^2\phi_3^4 + 10a_3^3b_2^2b_3^4k_1k_2k_3^5\phi_2^2\phi_3^4 + 6a_1a_3^3b_3^5k_1k_2^3k_3^3\phi_3^6 + 3a_1a_3^2b_3^6k_1k_2^3k_3^3\phi_3^6 + 6a_2a_3^3b_3^5k_1k_2k_3^3\phi_2^2\phi_3^6 + 12a_3^3b_2b_3^5k_1k_2k_3^3\phi_2^2\phi_3^6 + 3a_2a_3^2b_3^6k_1k_2k_3^3\phi_2^2\phi_3^6 + 6a_3^2b_2b_3^6k_1k_2k_3^3\phi_2^2\phi_3^6 + a_3b_3^8k_1k_2k_3\phi_2^2\phi_3^8)\ y_3^8 +$$

$$(-56a_2^2a_3^5b_1b_2k_2^2k_3^8\phi_1\phi_2\phi_3 - 70a_2^2a_3^4b_1b_2b_3k_2^2k_3^8\phi_1\phi_2\phi_3 - a_2^2a_3^6b_1k_2^2k_3^6\phi_1\phi_2\phi_3^2 - 2a_2a_3^6b_1b_2k_2^2k_3^6\phi_1\phi_2\phi_3^2 - 18a_2^2a_3^5b_1b_3k_2^2k_3^6\phi_1\phi_2\phi_3^2 - 36a_2a_3^5b_1b_2b_3k_2^2k_3^6\phi_1\phi_2\phi_3^2 - 45a_2^2a_3^4b_1b_3^2k_2^2k_3^6\phi_1\phi_2\phi_3^2 - 90a_2a_3^4b_1b_2b_3^2k_2^2k_3^6\phi_1\phi_2\phi_3^2 - 20a_2^2a_3^3b_1b_3^3k_2^2k_3^6\phi_1\phi_2\phi_3^2 - 40a_2a_3^3b_1b_2b_3^3k_2^2k_3^6\phi_1\phi_2\phi_3^2 - a_3^6b_2^3k_3^6\phi_1\phi_2^3\phi_3^2 - 18a_3^5b_2^3b_3k_3^6\phi_1\phi_2^3\phi_3^2 - 45a_3^4b_2^3b_3^2k_3^6\phi_1\phi_2^3\phi_3^2 - 20a_3^3b_2^3b_3^3k_3^6\phi_1\phi_2^3\phi_3^2 - 20a_2a_3^4b_1b_3^3k_2^2k_3^4\phi_1\phi_2\phi_3^5 - 10a_3^4b_1b_2b_3^3k_2^2k_3^4\phi_1\phi_2\phi_3^5 - 40a_2a_3^3b_1b_3^4k_2^2k_3^4\phi_1\phi_2\phi_3^5 - 20a_3^3b_1b_2b_3^4k_2^2k_3^4\phi_1\phi_2\phi_3^5 - 12a_2a_3^2b_1b_3^5k_2^2k_3^4\phi_1\phi_2\phi_3^5 - 6a_3^2b_1b_2b_3^5k_2^2k_3^4\phi_1\phi_2\phi_3^5 - 30a_3^4b_2^2b_3^3k_3^4\phi_1\phi_2^3\phi_3^5 - 60a_3^3b_2^2b_3^4k_3^4\phi_1\phi_2^3\phi_3^5 - 18a_3^2b_2^2b_3^5k_3^4\phi_1\phi_2^3\phi_3^5 - 7a_3^2b_1b_3^6k_2^2k_3^2\phi_1\phi_2\phi_3^7 - 2a_3b_1b_3^7k_2^2k_3^2\phi_1\phi_2\phi_3^7 - 21a_3^2b_2b_3^6k_3^2\phi_1\phi_2^3\phi_3^7 - 6a_3b_2b_3^7k_3^2\phi_1\phi_2^3\phi_3^7 - b_3^9\phi_1\phi_2^3\phi_3^9)\ y_3^9 +$$

$$(126a_1a_2^3a_3^4k_1k_2^3k_3^9 + 63a_1a_2^2a_3^5k_1k_2^3k_3^7\phi_3^2 + 210a_1a_2^2a_3^4b_3k_1k_2^3k_3^7\phi_3^2 + 105a_1a_2^2a_3^3b_3^2k_1k_2^3k_3^7\phi_3^2 + 21a_2a_3^5b_2^2k_1k_2k_3^7\phi_2^2\phi_3^2 + 70a_2a_3^4b_2^2b_3k_1k_2k_3^7\phi_2^2\phi_3^2 + 35a_2a_3^3b_2^2b_3^2k_1k_2k_3^7\phi_2^2\phi_3^2 + 12a_1a_2a_3^5b_3k_1k_2^3k_3^5\phi_3^4 + 90a_1a_2a_3^4b_3^2k_1k_2^3k_3^5\phi_3^4 + 120a_1a_2a_3^3b_3^3k_1k_2^3k_3^5\phi_3^4 + 30a_1a_2a_3^2b_3^4k_1k_2^3k_3^5\phi_3^4 + 8a_2a_3^5b_2b_3k_1k_2k_3^5\phi_2^2\phi_3^4 + 4a_3^5b_2^2b_3k_1k_2k_3^5\phi_2^2\phi_3^4 + 60a_2a_3^4b_2b_3^2k_1k_2k_3^5\phi_2^2\phi_3^4 + 30a_3^4b_2^2b_3^2k_1k_2k_3^5\phi_2^2\phi_3^4 + 80a_2a_3^3b_2b_3^3k_1k_2k_3^5\phi_2^2\phi_3^4 + 40a_3^3b_2^2b_3^3k_1k_2k_3^5\phi_2^2\phi_3^4 + 20a_2a_3^2b_2b_3^4k_1k_2k_3^5\phi_2^2\phi_3^4 + 10a_3^2b_2^2b_3^4k_1k_2k_3^5\phi_2^2\phi_3^4 + 15a_1a_3^3b_3^4k_1k_2^3k_3^3\phi_3^6 + 18a_1a_3^2b_3^5k_1k_2^3k_3^3\phi_3^6 + 3a_1a_3b_3^6k_1k_2^3k_3^3\phi_3^6 + 15a_2a_3^3b_3^4k_1k_2k_3^3\phi_2^2\phi_3^6 + 30a_3^3b_2b_3^4k_1k_2k_3^3\phi_2^2\phi_3^6 + 18a_2a_3^2b_3^5k_1k_2k_3^3\phi_2^2\phi_3^6 + 36a_3^2b_2b_3^5k_1k_2k_3^3\phi_2^2\phi_3^6 + 3a_2a_3b_3^6k_1k_2k_3^3\phi_2^2\phi_3^6 + 6a_3b_2b_3^6k_1k_2k_3^3\phi_2^2\phi_3^6 + 8a_3b_3^7k_1k_2k_3\phi_2^2\phi_3^8 + b_3^8k_1k_2k_3\phi_2^2\phi_3^8)\ y_3^{10} +$$

$$(-70a_2^2a_3^4b_1b_2k_2^2k_3^8\phi_1\phi_2\phi_3 - 56a_2^2a_3^3b_1b_2b_3k_2^2k_3^8\phi_1\phi_2\phi_3 - 6a_2^2a_3^5b_1k_2^2k_3^6\phi_1\phi_2\phi_3^2 -$$

$$12a_2a_3^5b_1b_2k_2^2k_3^6\phi_1\phi_2\phi_3^3 - 45a_2^2a_3^4b_1b_3k_2^2k_3^6\phi_1\phi_2\phi_3^3 - 90a_2a_3^4b_1b_2b_3k_2^2k_3^6\phi_1\phi_2\phi_3^3 -$$
$$60a_2^2a_3^3b_1b_3^2k_2^2k_3^6\phi_1\phi_2\phi_3^3 - 120a_2a_3^3b_1b_2b_3^2k_2^2k_3^6\phi_1\phi_2\phi_3^3 - 15a_2^2a_3^2b_1b_3^3k_2^2k_3^6\phi_1\phi_2\phi_3^3 -$$
$$30a_2a_3^2b_1b_2b_3^3k_2^2k_3^6\phi_1\phi_2\phi_3^3 - 6a_3^5b_2^3k_3^6\phi_1\phi_2^3\phi_3^3 - 45a_3^4b_2^3b_3k_3^6\phi_1\phi_2^3\phi_3^3 -$$
$$60a_3^3b_2^3b_3^2k_3^6\phi_1\phi_2^3\phi_3^3 - 15a_3^2b_2^3b_3^3k_3^6\phi_1\phi_2^3\phi_3^3 - 20a_2a_3^4b_1b_3^2k_2^2k_3^4\phi_1\phi_2\phi_3^5 -$$
$$10a_3^4b_1b_2b_3^2k_2^2k_3^4\phi_1\phi_2\phi_3^5 - 80a_2a_3^3b_1b_3^3k_2^2k_3^4\phi_1\phi_2\phi_3^5 - 40a_3^3b_1b_2b_3^3k_2^2k_3^4\phi_1\phi_2\phi_3^5 -$$
$$60a_2a_3^2b_1b_3^4k_2^2k_3^4\phi_1\phi_2\phi_3^5 - 30a_3^2b_1b_2b_3^4k_2^2k_3^4\phi_1\phi_2\phi_3^5 - 8a_2a_3b_1b_3^5k_2^2k_3^4\phi_1\phi_2\phi_3^5 -$$
$$4a_3b_1b_2b_3^5k_2^2k_3^4\phi_1\phi_2\phi_3^5 - 30a_3^4b_2^2b_3^2k_3^4\phi_1\phi_2^3\phi_3^5 - 120a_3^3b_2^2b_3^3k_3^4\phi_1\phi_2^3\phi_3^5 -$$
$$90a_3^2b_2^2b_3^4k_3^4\phi_1\phi_2^3\phi_3^5 - 12a_3b_2^2b_3^5k_3^4\phi_1\phi_2^3\phi_3^5 - 21a_3^2b_1b_3^5k_2^2k_3^2\phi_1\phi_2\phi_3^7 -$$
$$14a_3b_1b_3^6k_2^2k_3^2\phi_1\phi_2\phi_3^7 - b_1b_3^7k_2^2k_3^2\phi_1\phi_2\phi_3^7 - 63a_3^2b_2b_3^5k_3^2\phi_1\phi_2^3\phi_3^7 -$$
$$42a_3b_2b_3^6k_3^2\phi_1\phi_2^3\phi_3^7 - 3b_2b_3^7k_3^2\phi_1\phi_2^3\phi_3^7 - 9b_3^8\phi_1\phi_2^3\phi_3^9)\ y_3^{11} +$$
$$(84a_1a_2^3a_3^3k_1k_2^3k_3^9 + 105a_1a_2^2a_3^4k_1k_2^3k_3^7\phi_3^2 + 210a_1a_2^2a_3^3b_3k_1k_2^3k_3^7\phi_3^2 +$$
$$63a_1a_2^2a_3^2b_3^2k_1k_2^3k_3^7\phi_3^2 + 35a_2a_3^4b_2^2k_1k_2k_3^7\phi_2^2\phi_3^2 + 70a_2a_3^3b_2^2b_3k_1k_2k_3^7\phi_2^2\phi_3^2 +$$
$$21a_2a_3^2b_2^2b_3^2k_1k_2k_3^7\phi_2^2\phi_3^2 + 3a_1a_2a_3^5k_1k_2^3k_3^5\phi_3^4 + 60a_1a_2a_3^4b_3k_1k_2^3k_3^5\phi_3^4 +$$
$$180a_1a_2a_3^3b_3^2k_1k_2^3k_3^5\phi_3^4 + 120a_1a_2a_3^2b_3^3k_1k_2^3k_3^5\phi_3^4 + 15a_1a_2a_3b_3^4k_1k_2^3k_3^5\phi_3^4 +$$
$$2a_2a_3^5b_2k_1k_2k_3^5\phi_2^2\phi_3^4 + a_3^5b_2^2k_1k_2k_3^5\phi_2^2\phi_3^4 + 40a_2a_3^4b_2b_3k_1k_2k_3^5\phi_2^2\phi_3^4 +$$
$$20a_3^4b_2^2b_3k_1k_2k_3^5\phi_2^2\phi_3^4 + 120a_2a_3^3b_2b_3^2k_1k_2k_3^5\phi_2^2\phi_3^4 + 60a_3^3b_2^2b_3^2k_1k_2k_3^5\phi_2^2\phi_3^4 +$$
$$80a_2a_3^2b_2b_3^3k_1k_2k_3^5\phi_2^2\phi_3^4 + 40a_3^2b_2^2b_3^3k_1k_2k_3^5\phi_2^2\phi_3^4 + 10a_2a_3b_2b_3^4k_1k_2k_3^5\phi_2^2\phi_3^4 +$$
$$5a_3b_2^2b_3^4k_1k_2k_3^5\phi_2^2\phi_3^4 + 20a_1a_3^3b_3^3k_1k_2^3k_3^3\phi_3^6 + 45a_1a_3^2b_3^4k_1k_2^3k_3^3\phi_3^6 +$$
$$18a_1a_3b_3^5k_1k_2^3k_3^3\phi_3^6 + a_1b_3^6k_1k_2^3k_3^3\phi_3^6 + 20a_2a_3^3b_3^3k_1k_2k_3^3\phi_2^2\phi_3^6 +$$
$$40a_3^3b_2b_3^3k_1k_2k_3^3\phi_2^2\phi_3^6 + 45a_2a_3^2b_3^4k_1k_2k_3^3\phi_2^2\phi_3^6 + 90a_3^2b_2b_3^4k_1k_2k_3^3\phi_2^2\phi_3^6 +$$
$$18a_2a_3b_3^5k_1k_2k_3^3\phi_2^2\phi_3^6 + 36a_3b_2b_3^5k_1k_2k_3^3\phi_2^2\phi_3^6 + a_2b_3^6k_1k_2k_3^3\phi_2^2\phi_3^6 +$$
$$2b_2b_3^6k_1k_2k_3^3\phi_2^2\phi_3^6 + 28a_3b_3^6k_1k_2k_3\phi_2^2\phi_3^8 + 8b_3^7k_1k_2k_3\phi_2^2\phi_3^8)\ y_3^{12} +$$
$$(-56a_2^2a_3^3b_1b_2k_2^2k_3^8\phi_1\phi_2\phi_3 - 28a_2^2a_3^2b_1b_2b_3k_2^2k_3^8\phi_1\phi_2\phi_3 - 15a_2^2a_3^4b_1k_2^2k_3^6\phi_1\phi_2\phi_3^3 -$$
$$30a_2a_3^4b_1b_2k_2^2k_3^6\phi_1\phi_2\phi_3^3 - 60a_2^2a_3^3b_1b_3k_2^2k_3^6\phi_1\phi_2\phi_3^3 - 120a_2a_3^3b_1b_2b_3k_2^2k_3^6\phi_1\phi_2\phi_3^3 -$$
$$45a_2^2a_3^2b_1b_3^2k_2^2k_3^6\phi_1\phi_2\phi_3^3 - 90a_2a_3^2b_1b_2b_3^2k_2^2k_3^6\phi_1\phi_2\phi_3^3 - 6a_2^2a_3b_1b_3^3k_2^2k_3^6\phi_1\phi_2\phi_3^3 -$$
$$12a_2a_3b_1b_2b_3^3k_2^2k_3^6\phi_1\phi_2\phi_3^3 - 15a_3^4b_2^3k_3^6\phi_1\phi_2^3\phi_3^3 - 60a_3^3b_2^3b_3k_3^6\phi_1\phi_2^3\phi_3^3 -$$
$$45a_3^2b_2^3b_3^2k_3^6\phi_1\phi_2^3\phi_3^3 - 6a_3b_2^3b_3^3k_3^6\phi_1\phi_2^3\phi_3^3 - 10a_2a_3^4b_1b_3k_2^2k_3^4\phi_1\phi_2\phi_3^5 -$$
$$5a_3^4b_1b_2b_3k_2^2k_3^4\phi_1\phi_2\phi_3^5 - 80a_2a_3^3b_1b_3^2k_2^2k_3^4\phi_1\phi_2\phi_3^5 - 40a_3^3b_1b_2b_3^2k_2^2k_3^4\phi_1\phi_2\phi_3^5 -$$
$$120a_2a_3^2b_1b_3^3k_2^2k_3^4\phi_1\phi_2\phi_3^5 - 60a_3^2b_1b_2b_3^3k_2^2k_3^4\phi_1\phi_2\phi_3^5 - 40a_2a_3b_1b_3^4k_2^2k_3^4\phi_1\phi_2\phi_3^5 -$$
$$20a_3b_1b_2b_3^4k_2^2k_3^4\phi_1\phi_2\phi_3^5 - 2a_2b_1b_3^5k_2^2k_3^4\phi_1\phi_2\phi_3^5 - b_1b_2b_3^5k_2^2k_3^4\phi_1\phi_2\phi_3^5 -$$
$$15a_3^4b_2^2b_3k_3^4\phi_1\phi_2^3\phi_3^5 - 120a_3^3b_2^2b_3^2k_3^4\phi_1\phi_2^3\phi_3^5 - 180a_3^2b_2^2b_3^3k_3^4\phi_1\phi_2^3\phi_3^5 -$$
$$60a_3b_2^2b_3^4k_3^4\phi_1\phi_2^3\phi_3^5 - 3b_2^2b_3^5k_3^4\phi_1\phi_2^3\phi_3^5 - 35a_3^2b_1b_3^4k_2^2k_3^2\phi_1\phi_2\phi_3^7 -$$
$$42a_3b_1b_3^5k_2^2k_3^2\phi_1\phi_2\phi_3^7 - 7b_1b_3^6k_2^2k_3^2\phi_1\phi_2\phi_3^7 - 105a_3^2b_2b_3^4k_3^2\phi_1\phi_2^3\phi_3^7 -$$
$$126a_3b_2b_3^5k_3^2\phi_1\phi_2^3\phi_3^7 - 21b_2b_3^6k_3^2\phi_1\phi_2^3\phi_3^7 - 36b_3^7\phi_1\phi_2^3\phi_3^9)\ y_3^{13} +$$
$$(36a_1a_2^3a_3^2k_1k_2^3k_3^9 + 105a_1a_2^2a_3^3k_1k_2^3k_3^7\phi_3^2 + 126a_1a_2^2a_3^2b_3k_1k_2^3k_3^7\phi_3^2 +$$
$$21a_1a_2^2a_3b_3^2k_1k_2^3k_3^7\phi_3^2 + 35a_2a_3^3b_2^2k_1k_2k_3^7\phi_2^2\phi_3^2 + 42a_2a_3^2b_2^2b_3k_1k_2k_3^7\phi_2^2\phi_3^2 +$$
$$7a_2a_3b_2^2b_3^2k_1k_2k_3^7\phi_2^2\phi_3^2 + 15a_1a_2a_3^4k_1k_2^3k_3^5\phi_3^4 + 120a_1a_2a_3^3b_3k_1k_2^3k_3^5\phi_3^4 +$$
$$180a_1a_2a_3^2b_3^2k_1k_2^3k_3^5\phi_3^4 + 60a_1a_2a_3b_3^3k_1k_2^3k_3^5\phi_3^4 + 3a_1a_2b_3^4k_1k_2^3k_3^5\phi_3^4 +$$
$$10a_2a_3^4b_2k_1k_2k_3^5\phi_2^2\phi_3^4 + 5a_3^4b_2^2k_1k_2k_3^5\phi_2^2\phi_3^4 + 80a_2a_3^3b_2b_3k_1k_2k_3^5\phi_2^2\phi_3^4 +$$
$$40a_3^3b_2^2b_3k_1k_2k_3^5\phi_2^2\phi_3^4 + 120a_2a_3^2b_2b_3^2k_1k_2k_3^5\phi_2^2\phi_3^4 + 60a_3^2b_2^2b_3^2k_1k_2k_3^5\phi_2^2\phi_3^4 +$$
$$40a_2a_3b_2b_3^3k_1k_2k_3^5\phi_2^2\phi_3^4 + 20a_3b_2^2b_3^3k_1k_2k_3^5\phi_2^2\phi_3^4 + 2a_2b_2b_3^4k_1k_2k_3^5\phi_2^2\phi_3^4 +$$

$$b_2^2b_3^4k_1k_2k_3^5\phi_2^2\phi_3^4 + 15a_1a_3^3b_2^2k_1k_2^3k_3^3\phi_3^6 + 60a_1a_2^2b_3^3k_1k_2^3k_3^3\phi_3^6 +$$
$$45a_1a_3b_3^4k_1k_2^3k_3^3\phi_3^6 + 6a_1b_3^5k_1k_2^3k_3^3\phi_3^6 + 15a_2a_3^3b_2^2k_1k_2k_3^3\phi_2^2\phi_3^6 +$$
$$30a_3^3b_2b_3^2k_1k_2k_3^3\phi_2^2\phi_3^6 + 60a_2a_3^2b_3^3k_1k_2k_3^3\phi_2^2\phi_3^6 + 120a_3^2b_2b_3^3k_1k_2k_3^3\phi_2^2\phi_3^6 +$$
$$45a_2a_3b_3^4k_1k_2k_3^3\phi_2^2\phi_3^6 + 90a_3b_2b_3^4k_1k_2k_3^3\phi_2^2\phi_3^6 + 6a_2b_3^5k_1k_2k_3^3\phi_2^2\phi_3^6 +$$
$$12b_2b_3^5k_1k_2k_3^3\phi_2^2\phi_3^6 + 56a_3b_3^5k_1k_2k_3\phi_2^2\phi_3^8 + 28b_3^6k_1k_2k_3\phi_2^2\phi_3^8)\ y_3^{14} +$$
$$(-28a_2^2a_3^2b_1b_2k_2^2k_3^8\phi_1\phi_2\phi_3 - 8a_2^2a_3b_1b_2b_3k_2^2k_3^8\phi_1\phi_2\phi_3 - 20a_2^2a_3^3b_1k_2^2k_3^6\phi_1\phi_2\phi_3^3 -$$
$$40a_2a_3^3b_1b_2k_2^2k_3^6\phi_1\phi_2\phi_3^3 - 45a_2^2a_3^2b_1b_3k_2^2k_3^6\phi_1\phi_2\phi_3^3 - 90a_2a_3^2b_1b_2b_3k_2^2k_3^6\phi_1\phi_2\phi_3^3 -$$
$$18a_2^2a_3b_1b_3^2k_2^2k_3^6\phi_1\phi_2\phi_3^3 - 36a_2a_3b_1b_2b_3^2k_2^2k_3^6\phi_1\phi_2\phi_3^3 - a_2^2b_1b_3^3k_2^2k_3^6\phi_1\phi_2\phi_3^3 -$$
$$2a_2b_1b_2b_3^3k_2^2k_3^6\phi_1\phi_2\phi_3^3 - 20a_3^3b_2^3k_3^6\phi_1\phi_2^3\phi_3^3 - 45a_3^2b_2^3b_3k_3^6\phi_1\phi_2^3\phi_3^3 -$$
$$18a_3b_2^3b_3^2k_3^6\phi_1\phi_2^3\phi_3^3 - b_2^3b_3^3k_3^6\phi_1\phi_2^3\phi_3^3 - 2a_2a_3^4b_1k_2^2k_3^4\phi_1\phi_2\phi_3^5 -$$
$$a_3^4b_1b_2k_2^2k_3^4\phi_1\phi_2\phi_3^5 - 40a_2a_3^3b_1b_3k_2^2k_3^4\phi_1\phi_2\phi_3^5 - 20a_3^3b_1b_2b_3k_2^2k_3^4\phi_1\phi_2\phi_3^5 -$$
$$120a_2a_3^2b_1b_3^2k_2^2k_3^4\phi_1\phi_2\phi_3^5 - 60a_3^2b_1b_2b_3^2k_2^2k_3^4\phi_1\phi_2\phi_3^5 - 80a_2a_3b_1b_3^3k_2^2k_3^4\phi_1\phi_2\phi_3^5 -$$
$$40a_3b_1b_2b_3^3k_2^2k_3^4\phi_1\phi_2\phi_3^5 - 10a_2b_1b_3^4k_2^2k_3^4\phi_1\phi_2\phi_3^5 - 5b_1b_2b_3^4k_2^2k_3^4\phi_1\phi_2\phi_3^5 -$$
$$3a_3^4b_2^2k_3^4\phi_1\phi_2^3\phi_3^5 - 60a_3^3b_2^2b_3k_3^4\phi_1\phi_2^3\phi_3^5 - 180a_3^2b_2^2b_3^2k_3^4\phi_1\phi_2^3\phi_3^5 -$$
$$120a_3b_2^2b_3^3k_3^4\phi_1\phi_2^3\phi_3^5 - 15b_2^2b_3^4k_3^4\phi_1\phi_2^3\phi_3^5 - 35a_3^2b_1b_3^3k_2^2k_3^2\phi_1\phi_2\phi_3^7 -$$
$$70a_3b_1b_3^4k_2^2k_3^2\phi_1\phi_2\phi_3^7 - 21b_1b_3^5k_2^2k_3^2\phi_1\phi_2\phi_3^7 - 105a_3^2b_2b_3^3k_3^2\phi_1\phi_2^3\phi_3^7 -$$
$$210a_3b_2b_3^4k_3^2\phi_1\phi_2^3\phi_3^7 - 63b_2b_3^5k_3^2\phi_1\phi_2^3\phi_3^7 - 84b_3^6\phi_1\phi_2^3\phi_3^9)\ y_3^{15} +$$
$$(9a_1a_2^3a_3k_1k_2^3k_3^9 + 63a_1a_2^2a_3^2k_1k_2^3k_3^7\phi_3^2 + 42a_1a_2^2a_3b_3k_1k_2^3k_3^7\phi_3^2 +$$
$$3a_1a_2^2b_3^2k_1k_2^3k_3^7\phi_3^2 + 21a_2a_3^2b_2^2k_1k_2k_3^7\phi_2^2\phi_3^2 + 14a_2a_3b_2^2b_3k_1k_2k_3^7\phi_2^2\phi_3^2 +$$
$$a_2b_2^2b_3^2k_1k_2k_3^7\phi_2^2\phi_3^2 + 30a_1a_2a_3^3k_1k_2^3k_3^5\phi_3^4 + 120a_1a_2a_3^2b_3k_1k_2^3k_3^5\phi_3^4 +$$
$$90a_1a_2a_3b_3^2k_1k_2^3k_3^5\phi_3^4 + 12a_1a_2b_3^3k_1k_2^3k_3^5\phi_3^4 + 20a_2a_3^3b_2k_1k_2k_3^5\phi_2^2\phi_3^4 +$$
$$10a_3^3b_2^2k_1k_2k_3^5\phi_2^2\phi_3^4 + 80a_2a_3^2b_2b_3k_1k_2k_3^5\phi_2^2\phi_3^4 + 40a_3^2b_2^2b_3k_1k_2k_3^5\phi_2^2\phi_3^4 +$$
$$60a_2a_3b_2b_3^2k_1k_2k_3^5\phi_2^2\phi_3^4 + 30a_3b_2^2b_3^2k_1k_2k_3^5\phi_2^2\phi_3^4 + 8a_2b_2b_3^3k_1k_2k_3^5\phi_2^2\phi_3^4 +$$
$$4b_2^2b_3^3k_1k_2k_3^5\phi_2^2\phi_3^4 + 6a_1a_3^3b_3k_1k_2^3k_3^3\phi_3^6 + 45a_1a_3^2b_3^2k_1k_2^3k_3^3\phi_3^6 +$$
$$60a_1a_3b_3^3k_1k_2^3k_3^3\phi_3^6 + 15a_1b_3^4k_1k_2^3k_3^3\phi_3^6 + 6a_2a_3^3b_3k_1k_2k_3^3\phi_2^2\phi_3^6 +$$
$$12a_3^3b_2b_3k_1k_2k_3^3\phi_2^2\phi_3^6 + 45a_2a_3^2b_3^2k_1k_2k_3^3\phi_2^2\phi_3^6 + 90a_3^2b_2b_3^2k_1k_2k_3^3\phi_2^2\phi_3^6 +$$
$$60a_2a_3b_3^3k_1k_2k_3^3\phi_2^2\phi_3^6 + 120a_3b_2b_3^3k_1k_2k_3^3\phi_2^2\phi_3^6 + 15a_2b_3^4k_1k_2k_3^3\phi_2^2\phi_3^6 +$$
$$30b_2b_3^4k_1k_2k_3^3\phi_2^2\phi_3^6 + 70a_3b_3^4k_1k_2k_3\phi_2^2\phi_3^8 + 56b_3^5k_1k_2k_3\phi_2^2\phi_3^8)\ y_3^{16} +$$
$$(-8a_2^2a_3b_1b_2k_2^2k_3^8\phi_1\phi_2\phi_3 - a_2^2b_1b_2b_3k_2^2k_3^8\phi_1\phi_2\phi_3 - 15a_2^2a_3^2b_1k_2^2k_3^6\phi_1\phi_2\phi_3^3 -$$
$$30a_2a_3^2b_1b_2k_2^2k_3^6\phi_1\phi_2\phi_3^3 - 18a_2^2a_3b_1b_3k_2^2k_3^6\phi_1\phi_2\phi_3^3 - 36a_2a_3b_1b_2b_3k_2^2k_3^6\phi_1\phi_2\phi_3^3 -$$
$$3a_2^2b_1b_3^2k_2^2k_3^6\phi_1\phi_2\phi_3^3 - 6a_2b_1b_2b_3^2k_2^2k_3^6\phi_1\phi_2\phi_3^3 - 15a_3^2b_2^3k_3^6\phi_1\phi_2^3\phi_3^3 -$$
$$18a_3b_2^3b_3k_3^6\phi_1\phi_2^3\phi_3^3 - 3b_2^3b_3^2k_3^6\phi_1\phi_2^3\phi_3^3 - 8a_2a_3^3b_1k_2^2k_3^4\phi_1\phi_2\phi_3^5 -$$
$$4a_3^3b_1b_2k_2^2k_3^4\phi_1\phi_2\phi_3^5 - 60a_2a_3^2b_1b_3k_2^2k_3^4\phi_1\phi_2\phi_3^5 - 30a_3^2b_1b_2b_3k_2^2k_3^4\phi_1\phi_2\phi_3^5 -$$
$$80a_2a_3b_1b_3^2k_2^2k_3^4\phi_1\phi_2\phi_3^5 - 40a_3b_1b_2b_3^2k_2^2k_3^4\phi_1\phi_2\phi_3^5 - 20a_2b_1b_3^3k_2^2k_3^4\phi_1\phi_2\phi_3^5 -$$
$$10b_1b_2b_3^3k_2^2k_3^4\phi_1\phi_2\phi_3^5 - 12a_3^3b_2^2k_3^4\phi_1\phi_2^3\phi_3^5 - 90a_3^2b_2^2b_3k_3^4\phi_1\phi_2^3\phi_3^5 -$$
$$120a_3b_2^2b_3^2k_3^4\phi_1\phi_2^3\phi_3^5 - 30b_2^2b_3^3k_3^4\phi_1\phi_2^3\phi_3^5 - 21a_3^2b_1b_3^2k_2^2k_3^2\phi_1\phi_2\phi_3^7 -$$
$$70a_3b_1b_3^3k_2^2k_3^2\phi_1\phi_2\phi_3^7 - 35b_1b_3^4k_2^2k_3^2\phi_1\phi_2\phi_3^7 - 63a_3^2b_2b_3^2k_3^2\phi_1\phi_2^3\phi_3^7 -$$
$$210a_3b_2b_3^3k_3^2\phi_1\phi_2^3\phi_3^7 - 105b_2b_3^4k_3^2\phi_1\phi_2^3\phi_3^7 - 126b_3^5\phi_1\phi_2^3\phi_3^9)\ y_3^{17} +$$
$$(a_1a_2^3k_1k_2^3k_3^9 + 21a_1a_2^2a_3k_1k_2^3k_3^7\phi_3^2 + 6a_1a_2^2b_3k_1k_2^3k_3^7\phi_3^2 +$$
$$7a_2a_3b_2^2k_1k_2k_3^7\phi_2^2\phi_3^2 + 2a_2b_2^2b_3k_1k_2k_3^7\phi_2^2\phi_3^2 + 30a_1a_2a_3^2k_1k_2^3k_3^5\phi_3^4 +$$
$$60a_1a_2a_3b_3k_1k_2^3k_3^5\phi_3^4 + 18a_1a_2b_3^2k_1k_2^3k_3^5\phi_3^4 + 20a_2a_3^2b_2k_1k_2k_3^5\phi_2^2\phi_3^4 +$$

$$10a_3^2b_2^2k_1k_2k_3^5\phi_2^2\phi_3^4 + 40a_2a_3b_2b_3k_1k_2k_3^5\phi_2^2\phi_3^4 + 20a_3b_2^2b_3k_1k_2k_3^5\phi_2^2\phi_3^4 + 12a_2b_2b_3^2k_1k_2k_3^5\phi_2^2\phi_3^4 + 6b_2^2b_3^2k_1k_2k_3^5\phi_2^2\phi_3^4 + a_1a_3^3k_1k_2^3k_3^3\phi_3^6 + 18a_1a_3^2b_3k_1k_2^3k_3^3\phi_3^6 + 45a_1a_3b_3^2k_1k_2^3k_3^3\phi_3^6 + 20a_1b_3^3k_1k_2^3k_3^3\phi_3^6 + a_2a_3^3k_1k_2k_3^3\phi_2^2\phi_3^6 + 2a_3^3b_2k_1k_2k_3^3\phi_2^2\phi_3^6 + 18a_2a_3^2b_3k_1k_2k_3^3\phi_2^2\phi_3^6 + 36a_3^2b_2b_3k_1k_2k_3^3\phi_2^2\phi_3^6 + 45a_2a_3b_3^2k_1k_2k_3^3\phi_2^2\phi_3^6 + 90a_3b_2b_3^2k_1k_2k_3^3\phi_2^2\phi_3^6 + 20a_2b_3^3k_1k_2k_3^3\phi_2^2\phi_3^6 + 40b_2b_3^3k_1k_2k_3^3\phi_2^2\phi_3^6 + 56a_3b_3^3k_1k_2k_3\phi_2^2\phi_3^8 + 70b_3^4k_1k_2k_3\phi_2^2\phi_3^8)\ y_3^{18} +$$

$$(-a_2^2b_1b_2k_2^2k_3^8\phi_1\phi_2\phi_3 - 6a_2^2a_3b_1k_2^2k_3^6\phi_1\phi_2\phi_3^3 - 12a_2a_3b_1b_2k_2^2k_3^6\phi_1\phi_2\phi_3^3 - 3a_2^2b_1b_3k_2^2k_3^6\phi_1\phi_2\phi_3^3 - 6a_2b_1b_2b_3k_2^2k_3^6\phi_1\phi_2\phi_3^3 - 6a_3b_2^3k_3^6\phi_1\phi_2^3\phi_3^3 - 3b_2^3b_3k_3^6\phi_1\phi_2^3\phi_3^3 - 12a_2a_3^2b_1k_2^2k_3^4\phi_1\phi_2\phi_3^5 - 6a_3^2b_1b_2k_2^2k_3^4\phi_1\phi_2\phi_3^5 - 40a_2a_3b_1b_3k_2^2k_3^4\phi_1\phi_2\phi_3^5 - 20a_3b_1b_2b_3k_2^2k_3^4\phi_1\phi_2\phi_3^5 - 20a_2b_1b_3^2k_2^2k_3^4\phi_1\phi_2\phi_3^5 - 10b_1b_2b_3^2k_2^2k_3^4\phi_1\phi_2\phi_3^5 - 18a_3^2b_2^2k_3^4\phi_1\phi_2^3\phi_3^5 - 60a_3b_2^2b_3k_3^4\phi_1\phi_2^3\phi_3^5 - 30b_2^2b_3^2k_3^4\phi_1\phi_2^3\phi_3^5 - 7a_3^2b_1b_3k_2^2k_3^2\phi_1\phi_2\phi_3^7 - 42a_3b_1b_3^2k_2^2k_3^2\phi_1\phi_2\phi_3^7 - 35b_1b_3^3k_2^2k_3^2\phi_1\phi_2\phi_3^7 - 21a_3^2b_2b_3k_3^2\phi_1\phi_2^3\phi_3^7 - 126a_3b_2b_3^2k_3^2\phi_1\phi_2^3\phi_3^7 - 105b_2b_3^3k_3^2\phi_1\phi_2^3\phi_3^7 - 126b_3^4\phi_1\phi_2^3\phi_3^9)\ y_3^{19} +$$

$$(3a_1a_2^2k_1k_2^3k_3^7\phi_3^2 + a_2b_2^2k_1k_2k_3^7\phi_2^2\phi_3^2 + 15a_1a_2a_3k_1k_2^3k_3^5\phi_3^4 + 12a_1a_2b_3k_1k_2^3k_3^5\phi_3^4 + 10a_2a_3b_2k_1k_2k_3^5\phi_2^2\phi_3^4 + 5a_3b_2^2k_1k_2k_3^5\phi_2^2\phi_3^4 + 8a_2b_2b_3k_1k_2k_3^5\phi_2^2\phi_3^4 + 4b_2^2b_3k_1k_2k_3^5\phi_2^2\phi_3^4 + 3a_1a_3^2k_1k_2^3k_3^3\phi_3^6 + 18a_1a_3b_3k_1k_2^3k_3^3\phi_3^6 + 15a_1b_3^2k_1k_2^3k_3^3\phi_3^6 + 3a_2a_3^2k_1k_2k_3^3\phi_2^2\phi_3^6 + 6a_3^2b_2k_1k_2k_3^3\phi_2^2\phi_3^6 + 18a_2a_3b_3k_1k_2k_3^3\phi_2^2\phi_3^6 + 36a_3b_2b_3k_1k_2k_3^3\phi_2^2\phi_3^6 + 15a_2b_3^2k_1k_2k_3^3\phi_2^2\phi_3^6 + 30b_2b_3^2k_1k_2k_3^3\phi_2^2\phi_3^6 + 28a_3b_3^2k_1k_2k_3\phi_2^2\phi_3^8 + 56b_3^3k_1k_2k_3\phi_2^2\phi_3^8)\ y_3^{20} +$$

$$(-a_2^2b_1k_2^2k_3^6\phi_1\phi_2\phi_3^3 - 2a_2b_1b_2k_2^2k_3^6\phi_1\phi_2\phi_3^3 - b_2^3k_3^6\phi_1\phi_2^3\phi_3^3 - 8a_2a_3b_1k_2^2k_3^4\phi_1\phi_2\phi_3^5 - 4a_3b_1b_2k_2^2k_3^4\phi_1\phi_2\phi_3^5 - 10a_2b_1b_3k_2^2k_3^4\phi_1\phi_2\phi_3^5 - 5b_1b_2b_3k_2^2k_3^4\phi_1\phi_2\phi_3^5 - 12a_3b_2^2k_3^4\phi_1\phi_2^3\phi_3^5 - 15b_2^2b_3k_3^4\phi_1\phi_2^3\phi_3^5 - a_3^2b_1k_2^2k_3^2\phi_1\phi_2\phi_3^7 - 14a_3b_1b_3k_2^2k_3^2\phi_1\phi_2\phi_3^7 - 21b_1b_3^2k_2^2k_3^2\phi_1\phi_2\phi_3^7 - 3a_3^2b_2k_3^2\phi_1\phi_2^3\phi_3^7 - 42a_3b_2b_3k_3^2\phi_1\phi_2^3\phi_3^7 - 63b_2b_3^2k_3^2\phi_1\phi_2^3\phi_3^7 - 84b_3^3\phi_1\phi_2^3\phi_3^9)\ y_3^{21} +$$

$$(3a_1a_2k_1k_2^3k_3^5\phi_3^4 + 2a_2b_2k_1k_2k_3^5\phi_2^2\phi_3^4 + b_2^2k_1k_2k_3^5\phi_2^2\phi_3^4 + 3a_1a_3k_1k_2^3k_3^3\phi_3^6 + 6a_1b_3k_1k_2^3k_3^3\phi_3^6 + 3a_2a_3k_1k_2k_3^3\phi_2^2\phi_3^6 + 6a_3b_2k_1k_2k_3^3\phi_2^2\phi_3^6 + 6a_2b_3k_1k_2k_3^3\phi_2^2\phi_3^6 + 12b_2b_3k_1k_2k_3^3\phi_2^2\phi_3^6 + 8a_3b_3k_1k_2k_3\phi_2^2\phi_3^8 + 28b_3^2k_1k_2k_3\phi_2^2\phi_3^8)\ y_3^{22} +$$

$$(-2a_2b_1k_2^2k_3^4\phi_1\phi_2\phi_3^5 - b_1b_2k_2^2k_3^4\phi_1\phi_2\phi_3^5 - 3b_2^2k_3^4\phi_1\phi_2^3\phi_3^5 - 2a_3b_1k_2^2k_3^2\phi_1\phi_2\phi_3^7 - 7b_1b_3k_2^2k_3^2\phi_1\phi_2\phi_3^7 - 6a_3b_2k_3^2\phi_1\phi_2^3\phi_3^7 - 21b_2b_3k_3^2\phi_1\phi_2^3\phi_3^7 - 36b_3^2\phi_1\phi_2^3\phi_3^9)\ y_3^{23} +$$

$$(a_1k_1k_2^3k_3^3\phi_3^6 + a_2k_1k_2k_3^3\phi_2^2\phi_3^6 + 2b_2k_1k_2k_3^3\phi_2^2\phi_3^6 + a_3k_1k_2k_3\phi_2^2\phi_3^8 + 8b_3k_1k_2k_3\phi_2^2\phi_3^8)\ y_3^{24} +$$

$$(-b_1k_2^2k_3^2\phi_1\phi_2\phi_3^7 - 3b_2k_3^2\phi_1\phi_2^3\phi_3^7 - 9b_3\phi_1\phi_2^3\phi_3^9)\ y_3^{25} +$$

$$k_1k_2k_3\phi_2^2\phi_3^8\ y_3^{26} - \phi_1\phi_2^3\phi_3^9\ y_3^{27}$$

Acknowledgments

This thesis was done in the Institute for Theoretical Biology at the Humboldt University in Berlin. My work there, in the time of 2001 – 2004, was supported by the Bundesministerium für Bildung und Forschung (BMBF).

Particularly, I would like to thank **H**anspeter Herzel my scientific supervisor for his encouragement, support and guidance during my entire PhD study in his group. Professor Herzel gave me the freedom to follow some questions which were not necessarily related to the on-going projects.

Special gratitudes go to **M**arta for her trust in successful finishing of this thesis and her inspiring confidence during the last years. I also very much appreciate **K**ate's time-consuming proof reading. She suggested various corrections which made the text much more readable. Furthermore, my brother **W**ojtek supported me in many respects. His encouragement and motivation were always very stimulating and inspiring.

My great gratitude belongs to **S**amuel Bernard with whom I worked quite intense during the last year. His guidance and advise helped me to make progress on the chapters on module coupling and Vav1 truncation.

Best acknowledgments to **S**zymon Kiełbasa my roommate at ITB and a great company for discussions on several scientific areas. His sense of humor helped me over some difficult periods and long conferences.

I would also like to thank my colleagues **B**ranka Čajavec, **N**ils Blüthgen and **S**tefan Legewie for their comments on my thesis and discussions on different topics. I had great time in Berlin working and traveling with you. Appreciation is also extended to **D**ieter Beule, **J**ohannes Schuchhardt, **A**ndreas Hantschmann, **C**hristian Waltermann and other members of the "HPH" group.

I would like to thank **N**oriko Hiroi and **A**kira Funahashi from the Kitano Systems Biology Group in Tokyo for the past and ongoing collaboration on the cell cycle project.

Selbständigkeitserklärung

Hiermit erkläre ich, dass alle verwendeten Hilfsmittel und Hilfen in dieser Arbeit angegeben worden sind. Ich versichere, dass die Dissertation auf dieser Grundlage von mir selbständig erarbeitet und verfasst wurde.